2021-03-12

Evaluation of Concrete Bridge Decks Comprising Twisted Steel Micro Rebar

Aubrey Lynne Hebdon
Brigham Young University

Evaluation of Concrete Bridge Decks Comprising Twisted Steel Micro Rebar

Aubrey Lynne Hebdon

A thesis submitted to the faculty of
Brigham Young University
in partial fulfillment of the requirements for the degree of

Master of Science

W. Spencer Guthrie, Chair
Norman L. Jones
Kyle M. Rollins

Department of Civil and Environmental Engineering

Brigham Young University

ABSTRACT

Evaluation of Concrete Bridge Decks Comprising Twisted Steel Micro Rebar

Aubrey Lynne Hebdon
Department of Civil and Environmental Engineering, BYU
Master of Science

The objective of this research was to investigate the effects of twisted steel micro rebar (TSMR) fibers on 1) the mechanical properties of concrete used in bridge deck construction and 2) the early cracking behavior of concrete bridge decks. This research involved the evaluation of four newly constructed bridge decks through a series of laboratory and field tests. At each location, one deck was constructed using a conventional concrete mixture without TSMR, and one was constructed using the same conventional concrete mixture with an addition of 40 lb of TSMR per cubic yard of concrete.

Regarding laboratory testing, the conventional and TSMR beam specimens exhibited similar average changes in height after 4 months of shrinkage testing. The electrical impedance measurements did not indicate a notable difference between specimens comprising concrete with TSMR and those comprising conventional concrete. Although no notable difference in behavior between conventional and TSMR specimens was apparent before initial cracking, the toughness of the TSMR specimens was substantially greater than that of the conventional concrete specimens.

Regarding field testing, sensors installed in the bridge decks indicated that the addition of TSMR does not affect internal concrete temperature, moisture content, or electrical conductivity. The average Schmidt rebound number varied little between the TSMR decks and conventional decks; therefore, the stiffness of the TSMR concrete was very similar to that of conventional concrete. Distress surveys showed that the conventional decks exhibited notably more cracking than the TSMR decks. The TSMR fibers exhibited the ability to limit both crack density and crack width.

For all of the decks, chloride concentrations increased every year as a result of the use of deicing salts on the bridge decks during winter. However, the chloride concentrations for samples collected over cracked concrete increased more rapidly than those for samples collected over non-cracked concrete. Although TSMR fibers themselves do not directly affect the rate at which chloride ions penetrated cracked or non-cracked concrete, the fibers do prevent cracking, which, in turn, limits the penetration of chloride ions into the decks. Therefore, the use of TSMR would be expected to decrease the area of a bridge deck affected by cracking and subsequent chloride-induced corrosion damage and thereby increase the service life of the bridge deck.

Key words: chloride concentration, concrete bridge deck, cracking, fiber-reinforced concrete, twisted steel micro rebar

ACKNOWLEDGEMENTS

This research was supported and funded by the Utah Department of Transportation. Recognition is given to personnel at Ralph L. Wadsworth Construction for assisting with project logistics, HDR for their help with technical reviews, and METER Group for donating the sensors used in this research. Many members of the Materials and Pavements Research Group assisted with drafting, field, and laboratory work. I specifically thank Elizabeth Smith, Jared Baxter, Brindalynn Darby, and Hannah Polanco for their assistance with this project, and I also acknowledge Tenli Waters Emery and Robert Stevens for their constant assistance through the years. Finally, I give special thanks to the graduate committee, Dr. Spencer Guthrie, Dr. Norman Jones, and Dr. Kyle Rollins, for their roles in reviewing this report.

TABLE OF CONTENTS

LIST OF TABLES

LIST OF FIGURES

1 INTRODUCTION

1.1 Problem Statement

Design of durable concrete has become an increasingly important engineering objective as the need for sustainable infrastructure has become more prominent. More than 235,000 bridge decks in the United States are constructed with conventional reinforced concrete, and most of these were built with the intention of providing a 50-year lifespan (NACE International undated, NACE International 2012). The majority of bridge decks, however, experience some degree of premature deterioration before the intended service life is complete. Such deterioration can be caused by a variety of mechanisms, such as concrete shrinkage and degradation, fluctuating temperatures, settlement, overloading, creep, and corrosion of the reinforcing steel (Gucunski et al. 2013, Hema et al. 2004). Among these mechanisms, corrosion of the reinforcing steel is often cited as the leading cause of premature bridge deck deterioration (Balakumaran et al. 2017). Of the $90.9 billion that is needed to rehabilitate and repair structurally deficient bridge decks, as estimated by the United States Department of Transportation, approximately 40 percent is directly attributable to corrosion of reinforcing steel in concrete bridge decks (Zatar 2014).

Corrosion products can be up to 10 times larger in volume than the original steel, thereby causing internal tensile stresses that lead to deck cracking when the induced stresses exceed the tensile strength of the concrete (Ghetasi and Harris 2014, Hema et al. 2004). The formation of cracks allows penetration of additional corrosion agents, such as chloride ions, which accelerate the corrosion process upon reaching the reinforcing steel (Guthrie and Yaede 2014). During this

process, the reinforcing steel loses some of its cross-sectional area, further compromising the structural integrity of the bridge deck. Therefore, the service life of a bridge deck is largely associated with the time required for corrosive agents to penetrate the concrete to the depth of the reinforcing steel (Bentz et al. 2014, Birdsall et al. 2007, Guthrie et al. 2011).

Unfortunately, the ingress of corrosive agents is often accelerated through the occurrence of bridge deck cracking very early after construction, even before a bridge deck is open to normal trafficking (Schmitt and Darwin 1995). With time, these cracks can propagate and widen, creating a direct path for chloride ions to penetrate the deck (Bioubakhsh 2011, Hema et al. 2004). Although efforts to mitigate cracking beginning as early as the 1960s have been documented (Schmitt and Darwin 1995), concrete cracking has continued to reduce the service life of bridge decks through the present time.

Many methods to reduce concrete cracking have been implemented over the past several decades, including the use of shrinkage-reducing admixtures, internal curing agents (Guthrie and Yaede 2013), selected aggregates, and fiber additives. While many types of fiber additives exist, the use of steel fibers in a concrete matrix has become a common solution to mitigate cracking. Steel fibers enhance the post-cracking behavior of a structure by bridging across cracks, thereby minimizing crack widening. The effectiveness of such fibers depends on the tensile strength of the fiber itself and the ability of the fiber to bond with the surrounding concrete matrix (Banthia and Trottier 1991, Naaman 1976, Shannag et al. 1997). Increased anchorage in the concrete has been achieved through the use of hooked-end fibers, for example, but the hooked ends can cause burling of the fibers during mixing (Lee et al. 2019). Consequently, research to develop improved steel fibers continues, with the goal of achieving sufficient crack mitigation to significantly extend the service life of bridge decks.

Twisted steel micro rebar (TSMR) is a recently introduced steel fiber that has already been used in several applications worldwide. In theory, TSMR fibers, which are formed with a minimum of a 360-degree twist, should provide the needed bond between the fiber and the concrete matrix to stop cracks even before they become visible (Marsh 2015). The unique properties of TSMR could have substantial benefits for not only crack mitigation, but also for improvement of basic mechanical properties of bridge decks. While the use of TSMR in concrete bridge decks could significantly improve the behavior of the decks, thereby leading to an increased lifespan, physical data have not yet been published regarding these fibers in bridge decks.

1.2 Research Objective and Scope

The objective of this research was to investigate the effects of TSMR fibers on 1) the mechanical properties of concrete used in bridge deck construction and 2) the early cracking behavior of concrete bridge decks. This research involved the evaluation of four newly constructed bridge decks through a series of laboratory and field tests. Two of the bridge decks were constructed using conventional concrete, and two were constructed using TSMR fibers. The scope of this research included installation and monitoring of sensors in the bridge decks to measure temperature, electrical conductivity, and moisture content; evaluation of cylinder and beam specimens cast in the field at the time of construction of the bridge decks through shrinkage, electrical impedance, compressive strength, flexural strength, and splitting tensile strength tests; preparation and comparison of crack maps; and analysis of chloride concentration data collected before the decks experienced winter conditions and after the first and second winter seasons.

1.3 Report Outline

This report contains five chapters. This chapter introduces the research, defines the problem statement, and states the research objective and scope. Chapter 2 provides background information obtained from a literature review about the cracking behavior of concrete and the use of steel fibers in concrete applications. Chapter 3 describes the experimental methodology, including both laboratory and field testing procedures, and Chapter 4 presents the results of the testing. Chapter 5 concludes the report, providing a summary with findings and recommendations resulting from this research.

2 BACKGROUND

2.1 Overview

This chapter provides background information obtained from a literature review about causes of concrete cracking, steel fibers in concrete, and twisted steel micro rebar.

2.2 Causes of Concrete Cracking

Deterioration of concrete bridge decks is largely associated with cracking. Cracking can be caused by a variety of means such as shrinkage, settlement, environmental conditions, and corrosion of steel reinforcement (Hema et al. 2004). Cracking can begin as soon as the deck has been constructed and can continue throughout the service life of the bridge deck. Cracking through any means has the potential to accelerate chloride ion ingress into bridge decks and ultimately lead to corrosion of the reinforcing steel (Hema et al. 2004).

Shrinkage is one of the most common causes of cracking in bridge decks at early ages. The two main types of shrinkage include plastic shrinkage and drying shrinkage. Plastic shrinkage occurs before the concrete has hardened and is caused when moisture at the surface of the deck evaporates faster than it can be replaced by bleed water (Mindess et al. 2003). The resulting uneven moisture content within the cement paste causes differential volume change, leading to tensile stresses and potential map cracking (Mindess et al. 2003, Safiuddin 2018, Schmitt and Darwin 1995). Drying shrinkage occurs when water is lost from the cement paste after the concrete has hardened (Mindess et al. 2003, Safiuddin 2018, Schmitt and Darwin 1995).

As water evaporates from the capillary pores, curved menisci form, and the surface tension of the water creates negative pore pressures (Master Builders Solutions 2016). The resulting compressive force from the negative pore pressures leads to shrinkage and corresponding cracking (Master Builders Solutions 2016).

Settlement cracking can occur during both the construction and service life of concrete bridge decks. During construction, concrete continues to settle even after placement and finishing (Schmitt and Darwin 1995). Settlement over reinforcing steel is restrained while areas between the reinforcing steel can settle without restraint, thereby causing differential settlement in the structure (Schmitt and Darwin 1995). The tensile stresses caused by this type of settlement often lead to cracking above and parallel to reinforcing bars (Mindess et al. 2003, Schmitt and Darwin 1995).

Environmental conditions play a critical role in the cracking behavior of a bridge deck. Temperature, humidity, and precipitation not only affect the rate of shrinkage of concrete, but they can also introduce strains due to differential contraction. Research has shown that cracking is likely to occur if the surface of concrete experiences a sudden drop in temperature exceeding 15°F (Voigt 2002). The sudden change in temperature causes thermally-induced strains between the exterior and interior of the concrete that often lead to transverse cracking (Safiuddin 2018). Freeze-thaw cycles are often recognized as another mechanism that initiates and exacerbates cracking in concrete. When excessive or sustained precipitation causes high water contents in concrete, temperature fluctuations below freezing cause water in capillary pores to freeze and expand, thereby leading to tensile stresses and cracking.

Corrosion of the reinforcing steel is a common cause of cracking, especially in older bridge decks. The initiation of such cracking is dependent on many factors, including exposure

of the deck to corrosive agents such as chloride-based deicing salts, the rate at which the corrosive agents penetrate the concrete, concrete cover depth, and the type of reinforcing steel used (Hansson et al. 2012). Concrete naturally protects steel by providing an alkaline environment that facilitates development of a passive iron oxide film around the steel bars (Bateman 2018). This passive film, however, is not stable in chloride solutions and is readily compromised when the chloride concentration reaches about 0.2 percent by weight of the cement (Hansson et al. 2012). Once the passive film has been disrupted, an anode and cathode form on the bar, and the chlorides react with the steel to form an oxide. The final product of corrosion can be up to 10 times larger in volume than the original steel, thereby causing excessive tensile stresses that can lead to cracking, delamination, and an overall decrease in the structural integrity of the bridge deck (Getasi and Harris 2014, Hema et al. 2004).

2.3 Steel Fibers in Concrete

Steel fibers are produced worldwide, with over 100 types available (Katzer 2006). The effect of steel fibers on the properties of concrete depends almost completely on the pullout resistance of the fiber; as pullout resistance increases, the overall durability of the concrete increases. Pullout behavior is affected by the fiber slip, elongation, and strength, which can be directly associated with the bond mechanisms of adhesion, friction, and mechanical anchorage (Singh 2017). Beyond straight fibers, which do not provide adequate anchorage in a concrete matrix to develop the tensile strength of the steel (Katzer 2006), many fibers of various shapes and sizes have been introduced in an attempt to increase bonding. As of 2006, over 90% of steel fibers were shaped fibers (Katzer 2006). The most common fibers include straight, hooked, crimped, coned, and toothed, as shown in Figure 2-1 (Katzer 2006). Other types of fibers are rarely used and have not been studied as extensively.

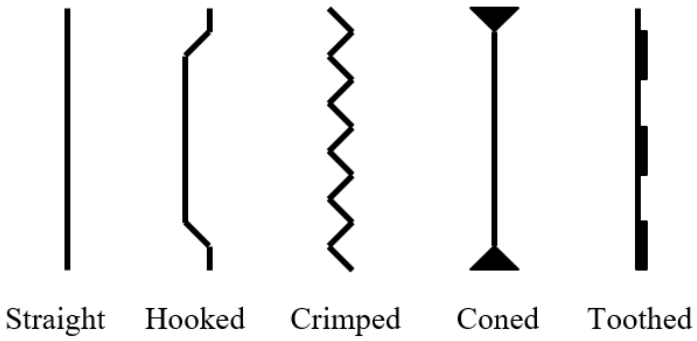

Figure 2-1: Common types of steel fibers.

The principal role of fibers in concrete is controlling cracking. Fibers are ideally distributed randomly throughout the concrete matrix, forming a web-like system around the aggregates (Singh 2017). As micro-cracks form in the concrete, steel fibers act as bridges across the cracks by distributing stresses more evenly throughout the matrix, thereby delaying or preventing formation of larger cracks (Vairagade and Kene 2012, Vondran 1991). Even after macro-cracks have formed, fibers continue to impede crack growth and crack opening (Vairagade and Kene 2012). Indeed, in one study (Grzybowski and Shah 1990), the average crack widths of concrete reinforced with only 0.25 percent steel fibers was 80 percent less than those of conventional concrete without fibers (Vondran 1991). Other studies have also confirmed the advantage of using steel fibers for increasing the crack resistance of concrete.

Studies have also been conducted to investigate the effect of steel fibers on compressive strength, flexural strength, splitting tensile strength, and toughness of concrete. Steel fibers typically have little effect on the compressive strength of concrete. Studies show that an increase in compressive strength ranges from negligible to no more than 25 percent (Nataraja et al. 1999, Vairagade and Kene 2012, Van Chanh 2005). However, significant increases in strain at peak stresses, corresponding to enhanced post-cracking ductility, have been observed (Nataraja et al.

1999, Van Chanh 2005). After initial cracking of the concrete, the fibers dissipate energy as they pull out, causing a relatively ductile failure compared to the brittle failure typically exhibited by conventional concrete (Singh 2017). Steel fibers are reported to have a more substantial effect on improving the ductile behavior of concrete than synthetic fibers (Singh 2017).

In general, concrete has low flexural and tensile strain capacity. Cracks propagate rapidly under tension and often cause a rapid, brittle failure. Under flexural and tensile loadings, steel-fiber-reinforced concrete initially cracks at around the same stress as that of conventional concrete but is able to withstand substantial deformation and cracking before failure, thereby increasing its toughness compared to conventional concrete (Singh 2017).

Toughness, which is the ability of a material to absorb energy during deformation and is a function of the area under a stress-strain or load-deflection curve, for example, can be greatly enhanced through the use of steel fibers (Vondran 1991). However, the increase in toughness occurs mostly in the post-cracking portion of the curve, demonstrating the ability of the fibers to inhibit expansion of cracks after they have already formed on the micro and macro levels (Mindess et al. 2003).

2.4 Twisted Steel Micro Rebar

TSMR is a steel fiber that has been recently promoted for use in concrete bridge decks. TSMR fibers are 1-in.-long strands manufactured using 245-carbon steel and electroplated with zinc to provide corrosion resistance (Wilson 2013). Each fiber has a minimum of one 360-degree twist, as shown in Figure 2-2, which provides enhanced pullout resistance (Helix Steel undated). In particular, when a crack intercepts a TSMR fiber, the crack can widen only by untwisting or straining the fiber, which requires a high level of energy. The fibers were engineered with the intent of preventing cracks on the micro level before they become visible (Marsh 2015). The

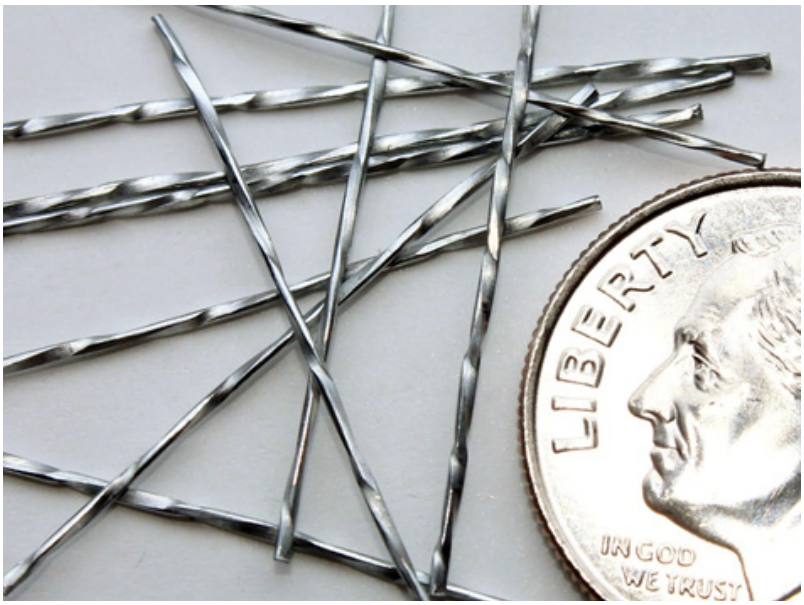

Figure 2-2: Twisted steel micro rebar fibers.

manufacturer indicates that the fibers specifically increase the shear capacity and modulus of rupture of concrete (Concrete News 2015). In general, the fibers are also reported to provide improved strength, durability, and ductility (Concrete News 2015, Helix Steel undated). Therefore, these fibers have the potential to greatly reduce concrete cracking and, in turn, slow the infiltration of corrosive agents.

TSMR was first developed for use in blast-resistant concrete in the late 1990s through university research commissioned by the Army Corp of Engineers (Marsh 2015). Since 2003, when the fibers were licensed for commercial use, they have been used in various concrete projects in over 99 countries worldwide (Helix Steel undated, Pinkerton et al. 2013). These projects include structural footings, slabs, structural foundations, walls, pavements, precast applications, tornado/hurricane-resistant structures, and blast-resistant structures (Pinkerton et al. 2013). However, no studies regarding the application or potential benefits of TSMR in concrete bridge decks were available prior to the start date of the present research.

2.5 Summary

Deterioration of concrete bridge decks is largely associated with cracking. Cracking can be caused by a variety of means such as shrinkage, settlement, environmental conditions, and corrosion of the steel reinforcement. Cracking through any means has the potential to accelerate chloride ion ingress into bridge decks and ultimately lead to corrosion of the reinforcing steel.

The principal role of fibers in concrete is controlling cracking. The effect of steel fibers on the properties of concrete depends almost completely on the pullout resistance of the fiber; as pullout resistance increases, the overall durability of the concrete increases. As micro-cracks form in the concrete, steel fibers act as bridges across the cracks by distributing stresses more evenly throughout the matrix, thereby delaying or preventing formation of larger cracks. After initial cracking of the concrete, the fibers dissipate energy as they pull out, causing a relatively ductile failure compared to the brittle failure typically exhibited by conventional concrete.

TSMR is a steel fiber that has been recently promoted for use in concrete bridge decks. The fibers were engineered with the intent of preventing cracks on the micro level before they become visible. In general, the fibers are also reported to provide improved strength, durability, and ductility. Therefore, these fibers have the potential to greatly reduce concrete cracking and, in turn, slow the infiltration of corrosive agents. However, no studies regarding the application or potential benefits of TSMR in concrete bridge decks were available prior to the start date of the present research.

3 PROCEDURES

3.1 Overview

The objective of this research was met through the comparison of two bridge decks constructed using conventional concrete and two bridge decks constructed using TSMR. Each deck was analyzed through a series of field and laboratory tests that were conducted during the first 2 years following construction of the bridge decks. Data collected from sensors installed in the bridge decks at the time of construction were also analyzed in this research. The following sections provide a site description and discuss deck instrumentation, deck construction, specimen casting and curing, laboratory testing, field testing, and statistical analyses.

3.2 Site Description

In the spring and summer of 2017, the Utah Department of Transportation (UDOT) constructed four new bridge decks along the Mountain View Corridor in West Valley City, Utah, two at Upper Ridge Road and two at Wolverine Way. The bridge decks at Upper Ridge Road were constructed in July 2017 using prestressed concrete girders, while the bridge decks at Wolverine Way were constructed in April 2017 using steel girders. As measured in the field during this research, the lengths of the bridge decks were 91 to 95 ft at Upper Ridge Road and 62 ft at Wolverine Way. Both bridge decks constructed at Upper Ridge Road were comprised of precast half-deck panels with a cast-in-place surface, while both bridge decks constructed at Wolverine Way were comprised of cast-in-place full-depth monolithic concrete. All four bridge

decks were constructed less than 2 miles from each other. At each location, one deck served northbound (NB) traffic, and one deck served southbound (SB) traffic. Two of the bridge decks were constructed using a conventional concrete mixture, to serve as control decks, while the two other bridge decks were constructed using the same conventional concrete mixture but with an addition of TSMR fibers. Figure 3-1 shows an aerial image of the location of each bridge and indicates the type of concrete utilized at each site.

Figure 3-1: Bridge locations and concrete types.

3.3 Deck Instrumentation

Prior to concrete placement, each of the four bridge decks was instrumented with a sensor connected to a data logger. Prior to installation, all sensors were checked in a uniform, moist sand to ensure consistent readings. The sensor was placed in each deck in the wheel path of the right lane; the specific sensor locations are shown in Appendix A. (Additional sensors were also installed in the bridge decks for other research purposes, independent of the present study, and their locations are also shown in Appendix A for completeness; however, data from those sensors are not included in this report.) The sensors measured the internal temperature, moisture content, and electrical conductivity of the concrete at hourly intervals. While temperature and moisture measurements reflected the environmental conditions, electrical conductivity was a useful surrogate measure of diffusivity (Guthrie et al. 2015), which is a critical factor that can affect chloride ion ingress and subsequent corrosion of reinforcing steel.

The sensors were installed just below the top mat of reinforcing steel, as displayed in Figure 3-2. The sensor cables were routed out of each deck and through the nearest diaphragm wall to a location where they could be conveniently terminated in a secure junction box. A battery-powered data logger was mounted inside the box, as shown in Figure 3-3, to facilitate automated data collection. Individual sensors were protected with temporary wooden covers through the duration of the construction process. After the concrete was placed and consolidated around a given sensor, the wooden cover was removed to allow deck finishing.

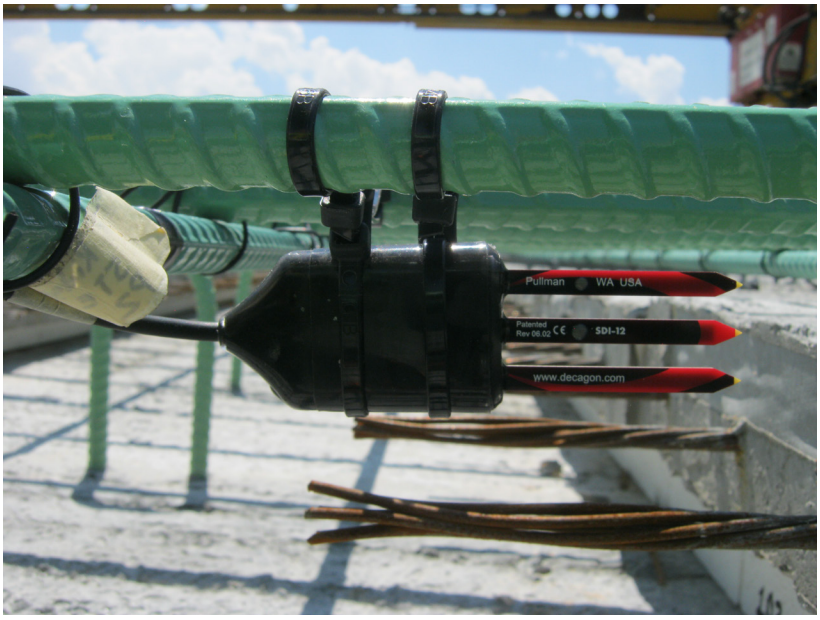

Figure 3-2: Sensor installed just below the top mat of reinforcement.

Figure 3-3: Data logger mounted inside a junction box.

3.4 Deck Construction

The two-lane Wolverine Way SB bridge deck and the Upper Ridge Road NB bridge deck were constructed using a conventional concrete mixture containing portland cement and fly ash as binders with a water-cementitious materials ratio of 0.40 as specified in Table 3-1. The two-lane Wolverine Way NB bridge deck and the Upper Ridge Road SB bridge deck were constructed using the same conventional concrete mixture but with an addition of 40 lb of TSMR per cubic yard of concrete. The concrete bridge deck construction procedures were otherwise consistent for all four bridge decks. The concrete placed on all of the decks was supplied by the same concrete producer and was placed and finished by the same construction crew. Concrete was pumped into place, consolidated using internal vibrators, and uniformly smoothed using a truss-mounted bridge deck paving machine.

A curing agent was sprayed onto each deck following concrete placement. The decks were then covered with plastic, as shown in Figure 3-4, for a specified 14-day curing period, after which the decks were exposed to ambient conditions. After construction, the depth of

Table 3-1: Conventional Concrete Mixture Design

Ingredient	Weight (lb)	SSD Specific Gravity	Volume (yd^3)
Coarse Aggregate	1705	2.67	0.38
Fine Aggregate	1200	2.60	0.27
Water	263	1.00	0.16
Portland Cement (Type II/V)	494	3.15	0.09
Fly Ash (Class F)	164	2.40	0.04
Water Reducer (5.5 fl. oz. cwt)	-	-	-
Shrinkage Reducer (64 fl. oz./yd^3)	-	-	-
Air (2 fl. oz./yd^3)	-	-	0.06
Total	3826	-	1.00

Figure 3-4: Covered bridge deck during curing.

concrete cover above the top mat of rebar was measured using a cover meter at four locations on each deck, as shown in Appendix A. On average, cover depths were 3.0 in. and 3.1 in. at the Upper Ridge Road NB conventional deck and Upper Ridge Road SB TSMR deck, respectively, and 3.0 in. and 3.4 in. at the Wolverine Way NB TSMR deck and Wolverine Way SB conventional deck, respectively.

3.5 Specimen Casting and Curing

During construction of each bridge deck, members of the Brigham Young University (BYU) Materials and Pavements Research Group were present to cast both cylinder and beam specimens of the field-mixed concrete. At each bridge construction site, a designated work area was leveled, and 12 cylinder molds (4 in. x 8 in.), and six beam molds (6 in. x 6 in. x 20 in.) were set up and prepared with a light coating of oil. Buckets were filled with concrete samples from two different locations as shown in Appendix A, one of which corresponded to the location of

the embedded sensor on each deck, and the concrete was immediately consolidated into the molds as shown in Figures 3-5 and 3-6. Cylindrical specimens were prepared in two lifts with 25 rod strokes and 12 mallet strikes per lift. Beam specimens were also prepared in two lifts, with 60 rod strokes per lift. The specimens were then covered with plastic and left undisturbed at the construction site for 24 hours to undergo similar initial curing as the bridge deck. After this period, the specimens were carefully transported back to the BYU Highway Materials Laboratory, where the molds were removed and the specimens were either placed in a fog room to cure or immediately subjected to shrinkage testing. The specimens placed in a fog room were removed after 14 days of curing and were subsequently stored in the laboratory at an average air temperature and relative humidity of 72°F and 48 percent, respectively. The specimens were then subjected to a series of laboratory tests.

Figure 3-5: Casting of cylindrical specimens during construction of bridge decks.

Figure 3-6: Casting of beam specimens during construction of bridge decks.

3.6 Laboratory Testing

Twelve cylinder and six beam specimens collected from each bridge deck at the time of construction were subjected to several laboratory tests over a period of 2 years. Nondestructive tests, including shrinkage and electrical impedance tests, were performed on specimens prior to destructive tests such as compressive strength, flexural strength, and splitting tensile strength tests, as described in the following sections.

3.6.1 Shrinkage Testing

The shrinkage values of two beam specimens from Upper Ridge Road NB and two beam specimens from Upper Ridge Road SB were monitored for a period of 4 months, beginning immediately after removal of the specimens from the molds. Specimens from Wolverine Way NB and Wolverine Way SB decks were not included in this aspect of the research because of a

limited number of available micrometers. Tests were performed in general accordance with American Society for Testing and Materials (ASTM) C157 (Standard Test Method for Length Change of Hardened Hydraulic-Cement Mortar and Concrete), with a modified apparatus to accommodate the larger specimen size used in this study. For the testing, one beam specimen from each sampling location for Upper Ridge Road NB and Upper Ridge Road SB were sealed in plastic wrap to simulate initial field curing conditions and then placed in a vertical orientation on a clean, level concrete surface in a secure area in the BYU Highway Materials Laboratory to ensure they would not be disturbed during the testing period. Micrometers were positioned over the center of the top of each specimen as shown in Figure 3-7, and measurements were recorded

Figure 3-7: Shrinkage testing of beam specimens.

on an approximately daily basis for the 4-month monitoring period. After 14 days, the plastic wrap was removed, and the specimens were exposed to the same room temperature and relative humidity conditions as the other specimens tested in this research.

3.6.2 Electrical Impedance Testing

Electrical impedance testing was performed to evaluate the susceptibility of the decks to chloride ion ingress (Baxter 2019). Developed at BYU, this relatively new test was performed on one cylindrical specimen and one beam specimen from each of the two sampling locations on each of the four decks at 28 days, 3 months, and 1 year from the time of construction of the bridge decks. One cylinder from each sampling location on each of the four decks was also tested at 2 years. For the testing, each cylinder or beam was placed in a horizontal orientation on an electrically insulating base support, as shown in Figure 3-8. Both ends of the specimen were

Figure 3-8: Electrical impedance testing of a cylindrical specimen.

moistened, and a metal mesh, connected to a moist foam pad, was pressed against each end. A peak-to-peak voltage of 3.3 V was then applied at a frequency of 190 Hz across the length of the specimen for 3 minutes while the current was measured using custom circuitry and signal processing software. The electrical resistance of each specimen was then calculated.

3.6.3 Compressive Strength Testing

Compressive strength testing was performed in general accordance with ASTM C39 (Standard Test Methods for Compressive Strength of Cylindrical Concrete Specimens), as illustrated in Figure 3-9. For all four bridge decks, one cylinder from each sampling location was

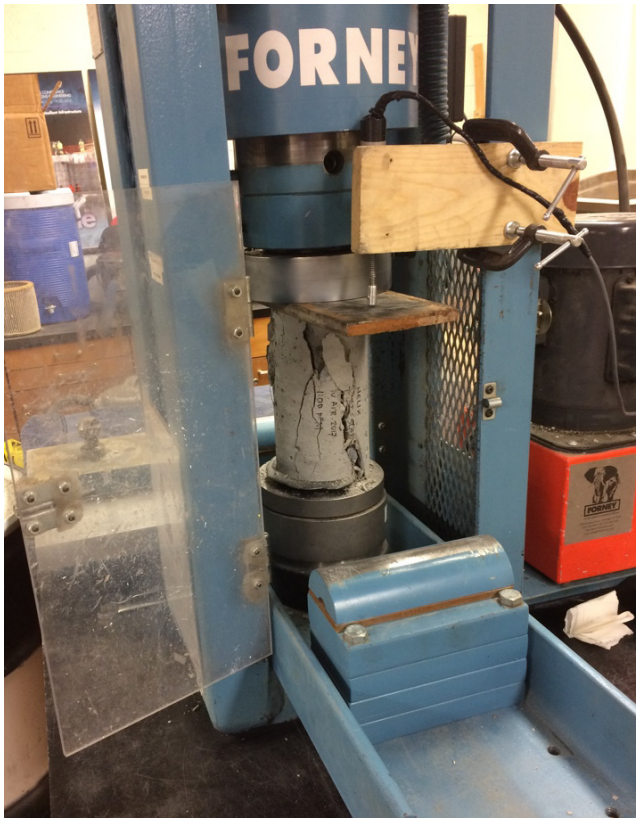

Figure 3-9: Compressive strength testing.

tested at 28 days, 3 months, 1 year, and 2 years from the time of construction of the bridge decks. Prior to the testing, the weight, length, and diameter of each cylinder were recorded. Each specimen was then capped with sulfur and tested at a target strain rate of 0.05 in./minute. Two linear variable differential transducers (LVDTs) were secured to the loading machine to measure average vertical displacement during the compressive strength testing. Load and displacement data were used to create stress-strain curves and calculate toughness. Toughness was calculated by determining the area under the respective stress-strain curve using Riemann sums. For each testing period, the toughness values for the specimens corresponding to both sampling locations on a given bridge deck were then averaged to determine an overall toughness value for each bridge deck.

3.6.4 Flexural Strength Testing

Flexural strength testing was performed in general accordance with ASTM C78 (Standard Test Method for Flexural Strength of Concrete (Using Simple Beam with Third-Point Loading)). For all four bridge decks, one beam from each sampling location was tested at 28 days, 3 months, and 1 year from the time of construction of the bridge decks. Prior to the testing, the weight, length, width, and height of each beam were recorded. Each specimen was centered horizontally between and simply supported on two end supports that were 18 in. apart and loaded at two locations that were each 6 in. from an end support and 6 in. from each other. Each beam was tested at a target strain rate of 0.05 in./minute. Two LVDTs were secured to the loading machine as shown in Figure 3-10 to measure the average vertical deflection during the flexural strength testing. Load and deflection data were used to create load-deflection curves. The energy absorption was determined for beam specimens and used as a measure of flexural toughness,

Figure 3-10: Flexural strength testing.

which was calculated by determining the area under the respective load-deflection curves using Riemann sums. For each testing period, the energy absorption values for the specimens corresponding to both sampling locations on a given bridge deck were then averaged to determine an overall flexural toughness value for each bridge deck.

3.6.5 Splitting Tensile Strength Testing

Splitting tensile strength tests were performed in general accordance with ASTM C496 (Standard Test Method for Splitting Tensile Strength of Cylindrical Concrete Specimens) at 28 days, 3 months, 1 year, and 2 years from the time of construction of the bridge decks. For all four bridge decks, two cylinders from each sampling location were cut into thirds, making each

specimen approximately 2.5 in. in length. Only one of the three cut pieces from each sampling location was used for each testing period, for a total of two tests per bridge deck per testing period. Prior to testing, the weight, height, and diameter of each specimen were recorded, and two diametrically opposed locations on the sides with the least amount of apparent defects, such as entrapped air voids, were marked with a line on the specimen face to indicate the desired points of contact with the upper and lower platens. Thin strips of softwood, approximately 0.125 in. thick, were placed between the specimen and the platens, as shown in Figure 3-11. Each specimen was tested at a target strain rate of 0.05 in./minute, and the peak load was recorded.

Figure 3-11: Splitting tensile strength testing.

3.7 Field Testing

Various field tests were performed to evaluate the performance of the bridge decks at different ages of the concrete. Tests were performed at approximately 3 months, 1 year, and 2 years from the time of construction of the bridge decks, thereby providing a comparison of data collected before the decks experienced winter conditions and normal trafficking, after the decks experienced one winter season with normal trafficking, and after the decks experienced two winter seasons with normal trafficking. The following sections provide explanations of sensor monitoring, Schmidt rebound hammer testing, distress surveys, and chloride concentration testing.

3.7.1 Sensor Monitoring

Data from the sensors installed in the bridge decks were downloaded from the data loggers approximately 2 years from the time of construction of the bridge decks. These data were used to analyze the internal temperature, moisture content, and electrical conductivity of the decks over time.

3.7.2 Schmidt Rebound Hammer Testing

Schmidt rebound hammer testing was performed in general accordance with ASTM C805 (Standard Test Method for Rebound Number of Hardened Concrete) to nondestructively estimate the concrete stiffness. In the test, which involves impacting the concrete surface with a spring-loaded hammer as shown in Figure 3-12, higher rebound numbers correspond to higher concrete stiffness. At approximately 3 months and 2 years from the time of construction of the bridge decks, four locations were evaluated on each bridge deck, as shown in Appendix A. As needed, a

Figure 3-12: Schmidt rebound hammer testing.

grinding stone was used to smooth the surface of the concrete at each location before the testing was performed to provide better contact between the hammer and the concrete. A minimum of four values were obtained at each of the four test locations on each deck. The highest and lowest values at each location were excluded in the data analysis to consistently eliminate any outliers and provide more accurate results.

3.7.3 Distress Surveys

Deck distress surveys were conducted to quantify and compare the degree of surface cracking among the bridge decks at approximately 3 months, 1 year, and 2 years from the time of construction of the bridge decks. Each bridge deck was inspected visually, and all noticeable

cracks, which generally had a width greater than 0.005 in., were marked and drawn on a map of the deck. The extent and severity of the observed deck surface cracking were also documented in terms of crack length and width, respectively. The data were used to create maps showing the progression of cracking over time, and crack density was calculated for each bridge deck in terms of total crack length per deck area. Crack densities calculated from distress surveys were used to determine the percent difference in cracking between bridge decks containing conventional concrete and those containing concrete with TSMR. In addition, differences in crack densities associated with deck construction type were also evaluated to compare the use of precast half-deck panels with a cast-in-place surface at Upper Ridge Road and the use of cast-in-place full-depth monolithic concrete at Wolverine Way.

3.7.4 Chloride Concentration Testing

Chloride concentrations were measured at approximately 3 months, 1 year, and 2 years from the time of construction of the bridge decks. At 3 months, before the decks experienced winter conditions and normal trafficking, four samples over non-cracked concrete were collected per deck. At 1 year, after the bridge decks had experienced one winter season with normal trafficking, two samples were collected over cracked concrete, and two samples were collected over non-cracked concrete on each bridge deck. At 2 years, after the bridge decks had experienced two winter seasons with normal trafficking, four samples were collected over cracked concrete, and four samples were collected over non-cracked concrete on each bridge deck. At each location, holes were drilled in lifts to depths of 0.5 in. and 1.0 in. using a rotary hammer with 1.5-in. and 1.0-in. diameter bits, respectively, as shown in Figure 3-13. Use of a smaller bit for the deeper lift prevented inadvertent scraping of near-surface concrete that may have otherwise contaminated the deeper sample. Pulverized concrete powder from each lift was

Figure 3-13: Concrete sampling for chloride concentration testing.

collected in bags and transported to the BYU Highway Materials Laboratory. Samples were then titrated in general accordance with ASTM C1152 (Standard Test Method for Acid-Soluble Chloride in Mortar and Concrete) to determine chloride concentrations. Chloride concentrations were reported in terms of pounds of chloride per cubic yard of concrete, with an assumed concrete unit weight of 150 lb/ft^3.

3.8 Statistical Analyses

Statistical analyses were performed to determine the significance of the addition of TSMR in the concrete bridge decks. Two-sample *t*-tests were performed on final shrinkage values; electrical impedance values; peak stress, corresponding strain, and toughness values from compressive strength tests; peak stress, corresponding deflection, and toughness values from flexural strength tests; and peak loads from splitting tensile strength tests. *T*-tests were also

performed on Schmidt rebound numbers, crack densities, crack widths, and average chloride concentrations measured over cracked and non-cracked concrete.

The null hypothesis in each *t*-test was that the given value of the specimens with TSMR was equal to that of the specimens without TSMR, and the alternative hypothesis was that the given value of the specimens with TSMR was different than that of the specimens without TSMR. In the test, *p*-values less than or equal to 0.05 allowed rejection of the null hypothesis and acceptance of the alternative hypothesis. A confidence level of 95 percent was used for all tests.

3.9 Summary

In the spring and summer of 2017, UDOT constructed four new bridge decks along the Mountain View Corridor in West Valley City, Utah, two at Upper Ridge Road and two at Wolverine Way. Both bridge decks constructed at Upper Ridge Road were comprised of precast half-deck panels with a cast-in-place surface, while both bridge decks constructed at Wolverine Way were comprised of cast-in-place full-depth monolithic concrete. The two-lane Wolverine Way SB bridge deck and the Upper Ridge Road NB bridge deck were constructed using a conventional concrete mixture containing portland cement and fly ash as binders with a water-cementitious materials ratio of 0.40. The two-lane Wolverine Way NB bridge deck and the Upper Ridge Road SB bridge deck were constructed using the same conventional concrete mixture but with an addition of 40 lb of TSMR per cubic yard of concrete. Prior to concrete placement, each of the four bridge decks was instrumented with a sensor connected to a data logger. The sensor was placed in each deck in the wheel path of the right lane. The sensors measured the internal temperature, moisture content, and electrical conductivity of the concrete

at hourly intervals. A battery-powered data logger was mounted inside a secure junction box to facilitate automated data collection.

Twelve cylinder and six beam specimens cast during construction of each bridge deck were subjected to several laboratory tests over a period of 2 years. Nondestructive tests, including shrinkage and electrical impedance tests, were performed on specimens prior to destructive tests such as compressive strength, flexural strength, and splitting tensile strength tests.

Regarding field testing, data from the sensors installed in the bridge decks were downloaded from the data loggers approximately 2 years from the time of construction of the bridge decks. In addition, Schmidt rebound hammer testing, distress surveys, and chloride concentration tests were performed to evaluate the performance of the bridge decks at different ages of the concrete. Tests were performed at approximately 3 months, 1 year, and 2 years from the time of construction of the bridge decks, thereby providing a comparison of data collected before the decks experienced winter conditions and normal trafficking, after the decks experienced one winter season with normal trafficking, and after the decks experienced two winter seasons with normal trafficking.

Statistical analyses were performed to determine the significance of the addition of TSMR in the concrete bridge decks. The null hypothesis in each *t*-test was that the given value of the specimens with TSMR was equal to that of the specimens without TSMR, and the alternative hypothesis was that the given value of the specimens with TSMR was different than that of the specimens without TSMR.

4 RESULTS

4.1 Overview

The following sections present the results of the laboratory and field testing performed for this research, as well as the results of the statistical analyses, where applicable.

4.2 Laboratory Testing Results

The results of shrinkage, electrical impedance, compressive strength, flexural strength, and splitting tensile strength testing are presented in the following sections. Toughness values calculated from compressive strength and flexural strength testing are also presented. Specific dates for the laboratory testing are given in Table 4-1 with the corresponding ages of the concrete specimens. For results for which a statistical analysis was performed to evaluate differences between conventional and TSMR concrete, *p*-values less than or equal to 0.05 allowed rejection of the null hypothesis. Supporting laboratory data are provided in Appendix B. Stress-strain curves for all compressive strength tests are provided in Appendix C. Pictures of typical specimens after compressive strength, flexural strength, and splitting tensile strength testing are provided in Appendix D.

Table 4-1: Laboratory Testing Schedule

Location	Test Date	Concrete Age	Test Performed				
			Shrinkage	Electrical Impedance	Compressive Strength	Flexural Strength	Splitting Tensile Strength
Upper Ridge Road SB	August 2017	28 days	X	X	X	X	X
	October 2017	3 months	X	X	X	X	X
	July 2018	1 year		X	X	X	X
	July 2019	2 years		X	X		X
Upper Ridge Road NB	August 2017	28 days	X	X	X	X	X
	October 2017	3 months	X	X	X	X	X
	July 2018	1 year		X	X	X	X
	July 2019	2 years		X	X		X
Wolverine Way SB	May 2017	28 days		X	X	X	X
	July 2017	3 months		X	X	X	X
	April 2018	1 year		X	X	X	X
	April 2019	2 years		X	X		X
Wolverine Way NB	May 2017	28 days		X	X	X	X
	July 2017	3 months		X	X	X	X
	April 2018	1 year		X	X	X	X
	April 2019	2 years		X	X		X

4.2.1 Shrinkage Testing

The results of shrinkage testing on two beam specimens from Upper Ridge Road NB and two specimens from Upper Ridge Road SB during the first 4 months after construction are shown in Figure 4-1 and summarized in Table 4-2. Negative and positive values indicate a decrease and increase, respectively, in beam height. The conventional and TSMR beam specimens exhibited similar average changes in height of -7.5 and -7.6 mils, respectively, by the end of the testing. However, during the first 48 hours, the TSMR beam specimens expanded an average of 0.128 mils, whereas the conventional beam specimens expanded an average of 0.679 mils, which is 430 percent more expansion. Therefore, although the specimens from both deck

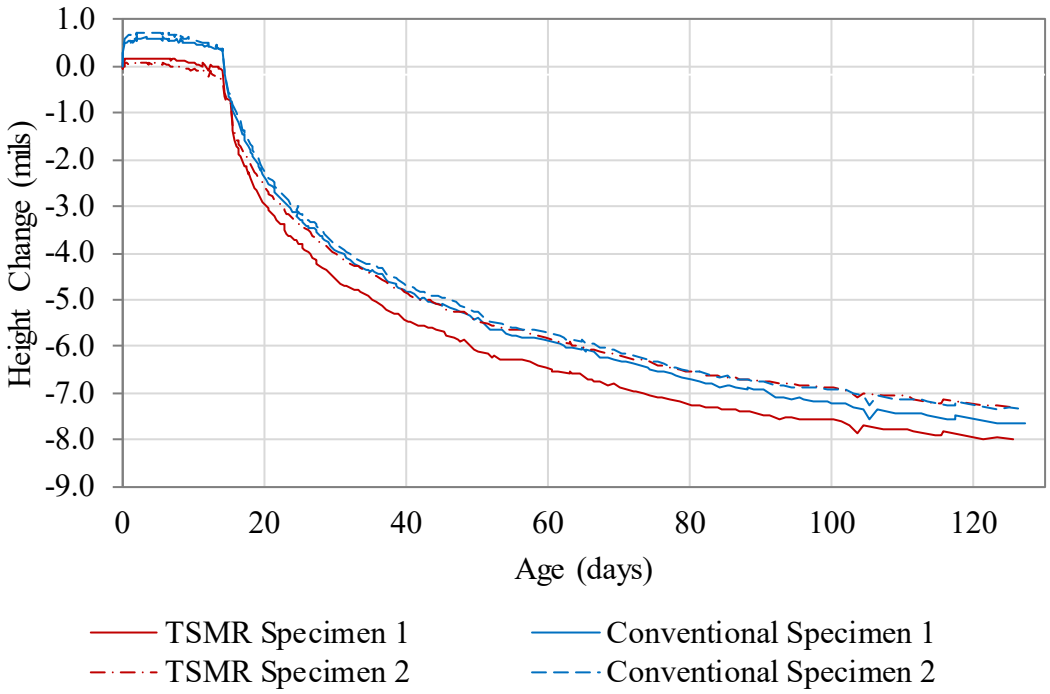

Figure 4-1: Shrinkage values for specimens at Upper Ridge Road.

Table 4-2: Results of Shrinkage Testing

Concrete Type	Height Change at 4 Months		
	Avg. (mils)	St. Dev. (mils)	*p*-value
Conventional	-7.480	0.223	0.735
TSMR	-7.648	0.487	

types converged to roughly the same final shrinkage value, the TSMR specimens experienced less overall change in height during this 4-month period. The small initial expansion for all the specimens is attributable to the increase in temperature experienced by the specimens upon arrival at the BYU Highway Materials Laboratory after having been at a lower temperature in the field. The *t*-test performed to compare the final shrinkage values of TSMR and conventional

concrete resulted in a *p*-value of 0.735, which indicates that insufficient evidence is available to statistically differentiate between the two types of concrete.

4.2.2 Electrical Impedance Testing

The results of electrical impedance testing on the cylinder and beam specimens are presented in Figures 4-2 and 4-3 and summarized in Tables 4-3 and 4-4, respectively. In the figures, the logarithm of the average electrical impedance value is presented in each case. The electrical impedance values exhibited a general trend of increasing with time, which is attributable to the continued hydration of the concrete specimens. Further hydration would not only lead to the subsequent densification of the concrete matrix as additional cementitious products formed, but it would also cause an internal desiccation of the concrete that would also

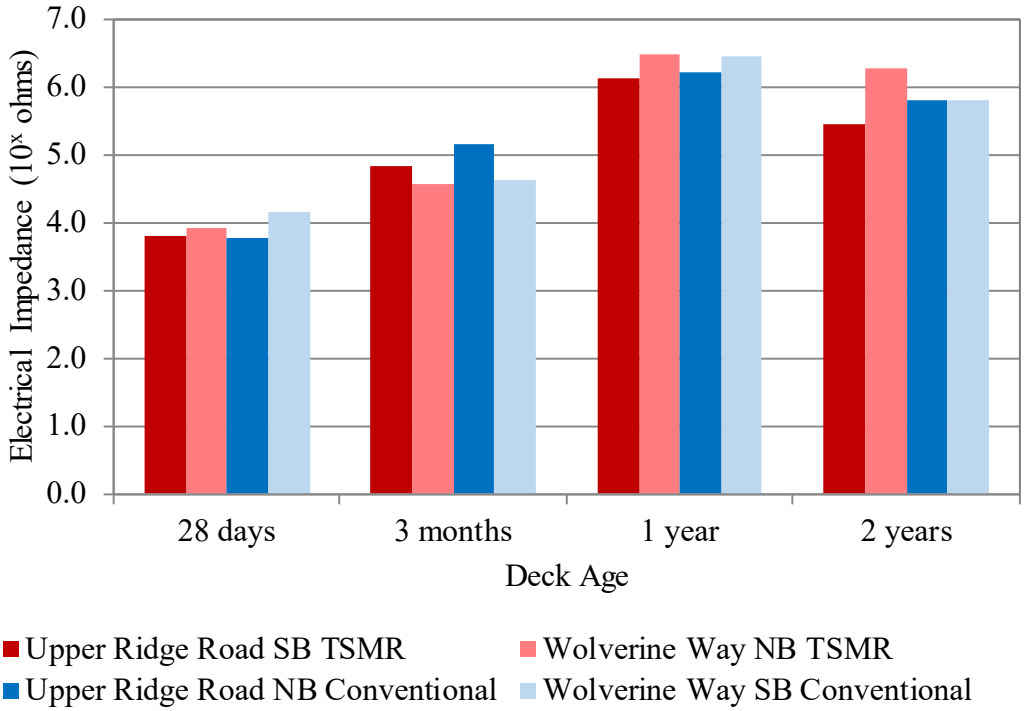

Figure 4-2: Average electrical impedance values for cylindrical specimens.

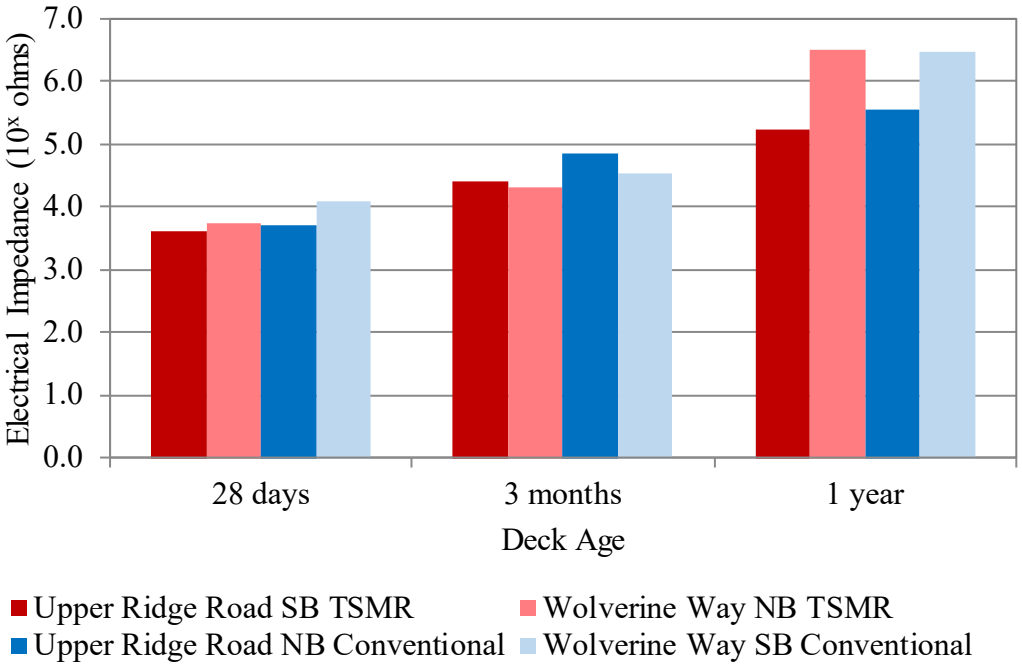

Figure 4-3: Average electrical impedance values for beam specimens.

increase the electrical impedance. Higher electrical impedance values correlate with lower concrete diffusivity and decreased susceptibility to chloride ion ingress.

The electrical impedance measurements did not indicate a notable difference between specimens comprising concrete with TSMR and those comprising conventional concrete. Even with the addition of 40 lb of TSMR per cubic yard of concrete, which was expected to aid in the transfer of electrical current through the concrete matrix due to the conductive nature of the steel fibers, the electrical impedance values of the TSMR specimens were approximately the same as those of the conventional specimens. These results suggest that the fibers did not form a connected conductive path through the concrete matrix. All *p*-values resulting from *t*-tests performed to compare the electrical impedance values of TSMR and conventional concrete, as given in Tables 4-3 and 4-4, are greater than the specified threshold of 0.05, which indicates that insufficient evidence is available to statistically differentiate between the two types of concrete.

Table 4-3: Results of Electrical Impedance Testing on Cylindrical Specimens

Concrete Type	Electrical Impedance (10^x ohms)											
	28 days			3 months			1 year			2 years		
	Avg.	St. Dev.	*p* -value	Avg.	St. Dev.	*p* -value	Avg.	St. Dev.	*p* -value	Avg.	St. Dev.	*p* -value
Conventional	3.954	0.262	0.688	4.878	0.374	0.633	6.318	0.167	0.929	5.805	0.004	0.909
TSMR	3.851	0.080		4.685	0.189		6.294	0.254		5.864	0.587	

Table 4-4: Results of Electrical Impedance Testing on Beam Specimens

Concrete Type	Electrical Impedance (10^x ohms)								
	28 days			3 months			1 year		
	Avg.	St. Dev.	*p* -value	Avg.	St. Dev.	*p* -value	Avg.	St. Dev.	*p* -value
Conventional	3.899	0.263	0.476	4.694	0.214	0.290	6.023	0.646	0.880
TSMR	3.686	0.094		4.369	0.070		5.875	0.892	

4.2.3 Compressive Strength Testing

Typical stress-strain curves from which the compressive strength data were derived are shown in Figures 4-4 and 4-5, and the compressive strength and corresponding strain obtained from compressive strength testing are provided in Tables 4-5 and 4-6, respectively. Stress-strain curves for all compressive strength tests are provided in Appendix C. All specimens containing conventional concrete exhibited a brittle failure, in which the load immediately decreased to zero after reaching the peak stress as demonstrated in Figure 4-4, which shows typical results from the 1-year testing period. In contrast, specimens containing TSMR exhibited an extremely ductile failure. The ductile post-cracking behavior of the TSMR specimens is evident through the extension of the stress-strain curves for the TSMR specimens as demonstrated in Figure 4-5, which shows typical results from the 1-year testing period. TSMR specimens continued to hold loads exceeding 4000 lb even at strains up to 348 percent greater than those corresponding to the peak load. The ability of the TSMR specimens to maintain a substantial amount of load at high strain levels indicates that, after initial cracking, TSMR fibers were able to act as bridges across the cracks, preventing formation of larger cracks that would have led to quicker failure. In fact, after initial cracking, the TSMR specimens never completely broke apart but were held together by the TSMR fibers along the failure plane as shown in Appendix D. Therefore, after initial cracking, TSMR specimens exhibited different behavior than that of conventional specimens; however, before initial cracking, no notable difference in behavior between conventional and TSMR specimens was apparent.

The difference in compressive strength and corresponding strain between specimens containing conventional concrete and specimens containing TSMR was minimal. The *t*-tests performed to compare the peak stress and corresponding strain of TSMR and conventional

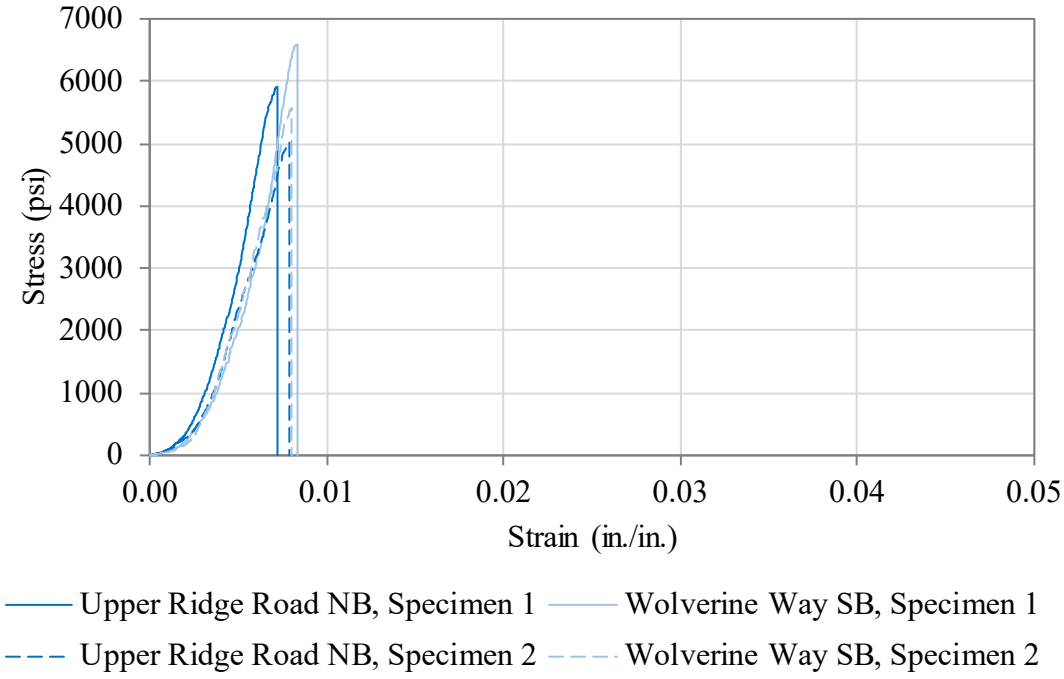

Figure 4-4: Stress-strain curves for conventional concrete specimens.

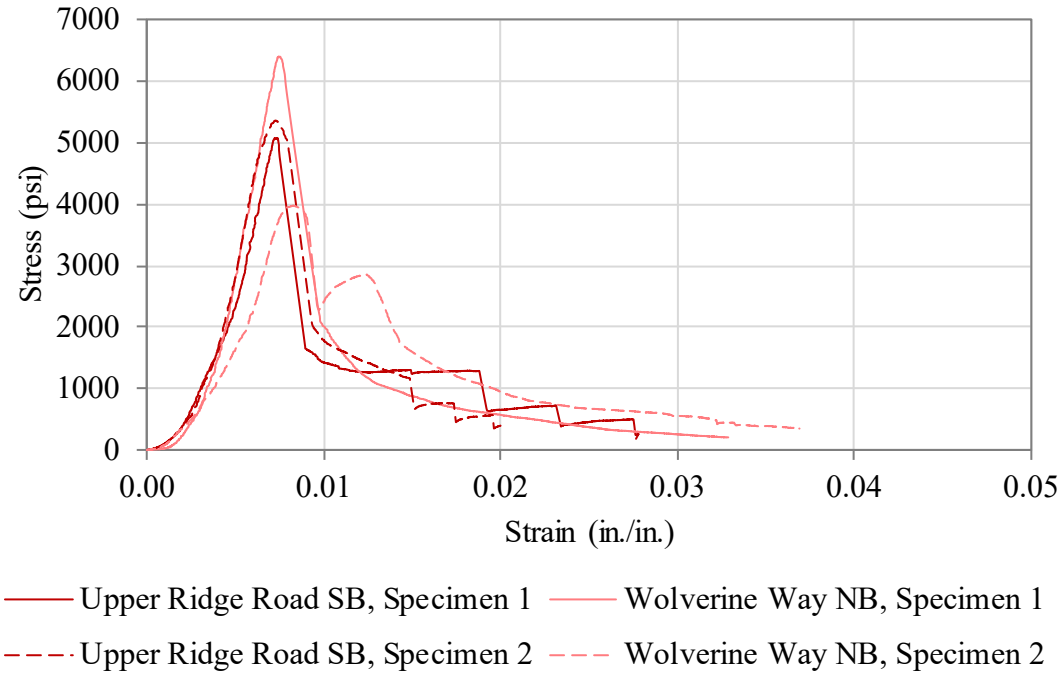

Figure 4-5: Stress-strain curves for specimens containing TSMR.

Table 4-5: Results of Compressive Strength Testing

Concrete Type	Compressive Strength (psi)											
	28 days			3 months			1 year			2 years		
	Avg.	St. Dev.	*p* -value	Avg.	St. Dev.	*p* -value	Avg.	St. Dev.	*p* -value	Avg.	St. Dev.	*p* -value
Conventional	4796	850	0.848	5846	570	0.325	5757	652	0.392	5195	335	0.648
TSMR	4693	570		5477	326		5199	996		5014	654	

Table 4-6: Strain Results Corresponding to Peak Compressive Stress

Concrete Type	Strain (in./in.)											
	28 days			3 months			1 year			2 years		
	Avg.	St. Dev.	*p* -value	Avg.	St. Dev.	*p* -value	Avg.	St. Dev.	*p* -value	Avg.	St. Dev.	*p* -value
Conventional	0.0082	0.0008	0.412	0.0084	0.0012	0.940	0.0078	0.0005	0.419	0.0076	0.0022	0.654
TSMR	0.0078	0.0006		0.0083	0.0014		0.0075	0.0005		0.0083	0.0020	

concrete resulted in *p*-values as high as 0.848 and 0.940, respectively. All *p*-values, as provided in Tables 4-5 and 4-6, are greater than the specified threshold of 0.05, which indicates that insufficient evidence is available to statistically differentiate between the two types of concrete.

4.2.4 Flexural Strength Testing

Typical load-deflection curves from which the flexural strength data were derived are shown in Figures 4-6 and 4-7, and the flexural strength and corresponding deflection obtained from flexural strength testing are provided in Tables 4-7 and 4-8, respectively. Load-deflection curves for all flexural strength tests are provided in Appendix C. The TSMR and conventional specimens all experienced a similar increase in flexural strength during the first year after construction. However, the failure behavior of the TSMR specimens was again different than that of the conventional specimens. All specimens containing conventional concrete exhibited a brittle failure, in which the load immediately decreased to zero after reaching the peak stress as demonstrated in Figure 4-6, which shows typical results from the 3-month testing period. In contrast, specimens containing TSMR exhibited an extremely ductile failure. After initial cracking and an attendant partial decrease in load, specimens containing TSMR continued to hold measurable loads at deflections beyond those corresponding to the peak loads as demonstrated in Figure 4-7, which shows typical results from the 3-month testing period. The fibers again acted as bridges across the cracks, holding the TSMR specimens together during continued testing. As curing time increased, the initial cracking of the TSMR specimens became more brittle, causing a greater decrease in load. At 1 year, TSMR specimens from Wolverine Way NB experienced decreases in loads to as low as 295 lb upon initial cracking. However, under continued loading, the specimens were able to again hold loads exceeding 1000 lb even at displacements of 60 to 350 percent greater than those corresponding to the peak loads. Therefore,

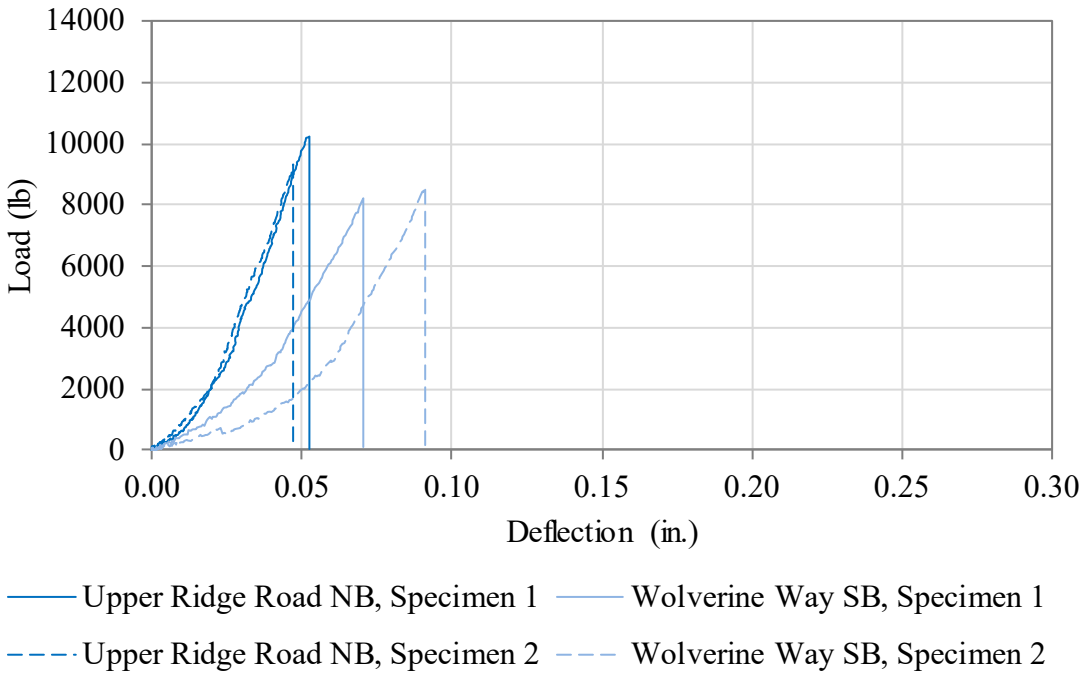

Figure 4-6: Typical load-deflection plot for specimens containing conventional concrete.

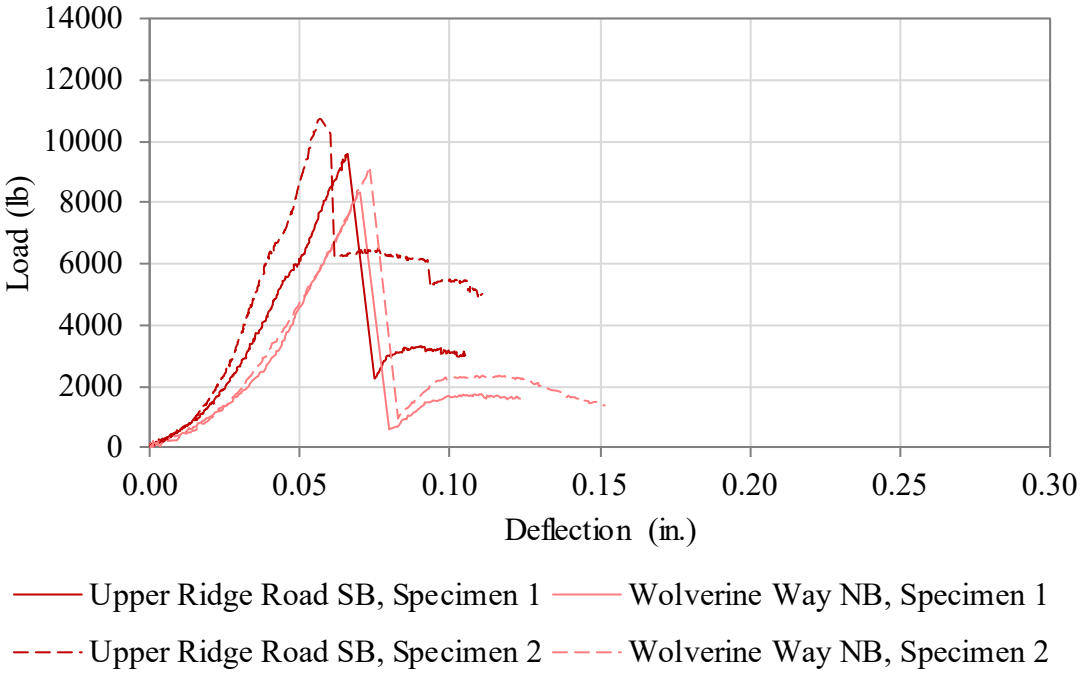

Figure 4-7: Typical load-deflection plot for specimens containing TSMR.

after initial cracking, TSMR specimens exhibited different behavior than that of conventional specimens; however, before initial cracking, no notable difference in behavior between conventional and TSMR specimens was apparent.

The average flexural strength for specimens containing TSMR for testing at 28 days, 3 months, and 1 year was greater than that of the conventional specimens by only 21, 35, and 2 psi, respectively. Differences in corresponding displacement ranged from negligible to 0.003 in. The *t*-tests performed to compare the flexural strength and deflection values of TSMR and conventional concrete resulted in *p*-values as high as 0.979 and 0.919, respectively. All *p*-values are greater than 0.05, which indicates that insufficient evidence is available to statistically differentiate between the two types of concrete.

Table 4-7: Results of Flexural Strength Testing

Concrete Type	Flexural Strength (psi)								
	28 days			3 months			1 year		
	Avg.	St. Dev.	*p* -value	Avg.	St. Dev.	*p* -value	Avg.	St. Dev.	*p* -value
Conventional	613	60	0.709	734	82	0.561	925	93	0.979
TSMR	634	88		770	77		927	98	

Table 4-8: Deflection Results Corresponding to Peak Flexural Stress

Concrete Type	Deflection (in.)								
	28 days			3 months			1 year		
	Avg.	St. Dev.	*p* -value	Avg.	St. Dev.	*p* -value	Avg.	St. Dev.	*p* -value
Conventional	0.0630	0.0058	0.912	0.0653	0.0198	0.919	0.0670	0.0058	0.391
TSMR	0.0623	0.0094		0.0664	0.0072		0.0700	0.0025	

4.2.5 *Splitting Tensile Strength Testing*

Test results from splitting tensile strength testing are provided in Figure 4-8 and Table 4-9. After reaching their peak loads, specimens containing conventional concrete broke suddenly, with the load immediately decreasing to zero. In contrast, specimens containing TSMR were able to maintain measurable loads beyond their peak loads, with the TSMR fibers holding the specimens together and enabling a more ductile failure.

Peak loads recorded during splitting tensile strength testing varied little between TSMR and conventional specimens, with all tensile strength values for a given testing period being within 143 psi of each other. In fact, at 2 years, the TSMR specimens and conventional specimens had the same average tensile strength of 653 psi. The *t*-tests performed on data from splitting tensile strength tests performed at 28 days, 3 months, 1 year, and 2 years resulted in *p*-

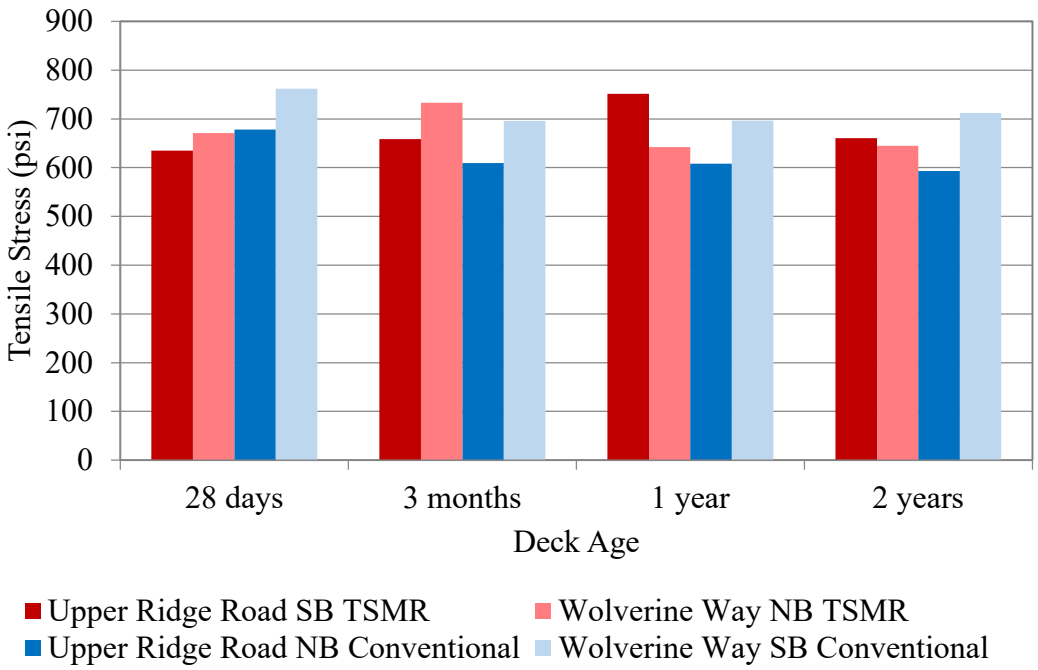

Figure 4-8: Average peak tensile stress values.

Table 4-9: Results of Splitting Tensile Strength Testing

Concrete Type	Tensile Strength (psi)											
	28 days			3 months			1 year			2 years		
	Avg.	St. Dev.	*p*-value	Avg.	St. Dev.	*p*-value	Avg.	St. Dev.	*p*-value	Avg.	St. Dev.	*p*-value
Conventional	720	94	0.261	653	74	0.362	653	62	0.689	653	73	0.997
TSMR	653	43		696	46		679	87		653	43	

values of 0.261, 0.362, 0.689, and 0.997, respectively, as summarized in Table 4-9. These values indicate that insufficient evidence is available to statistically differentiate between the two types of concrete.

4.2.6 Toughness Calculations

Toughness values were computed for both compressive and flexural strength testing as presented in Figures 4-9 and 4-10 and Tables 4-10 and 4-11. Average toughness values obtained from compressive strength testing are shown in Figure 4-9 and Table 4-10. The values represent areas under the corresponding stress-strain curves. The toughness of the TSMR specimens was substantially greater than that of the conventional concrete specimens. At testing periods of 28 days, 3 months, 1 year, and 2 years, the average toughness of the TSMR specimens was 152, 87, 153, and 164 percent greater, respectively, than that of the conventional concrete specimens. The difference would have been even more pronounced had the tests on TSMR specimens been allowed to run until the specimens were unable to maintain any load; instead, they were necessarily terminated prior to complete failure because of limitations in the maximum allowable displacement of the test machine. *T*-tests resulted in *p*-values of 0.000, 0.201, 0.005, and 0.034 for toughness calculated at 28 days, 3 months, 1 year, and 2 years, respectively, as shown in Table 4-10. These values indicate that sufficient evidence is available to reject the null hypothesis and accept the alternative hypothesis that the toughness of specimens containing TSMR is different than that of specimens containing conventional concrete at testing periods of 28 days, 1 year, and 2 years.

Average toughness values obtained from flexural strength testing are shown in Figure 4-10 and Table 4-11. In this case, the values represent areas under the corresponding load-deflection curves. Like the toughness values computed from compressive strength testing, the

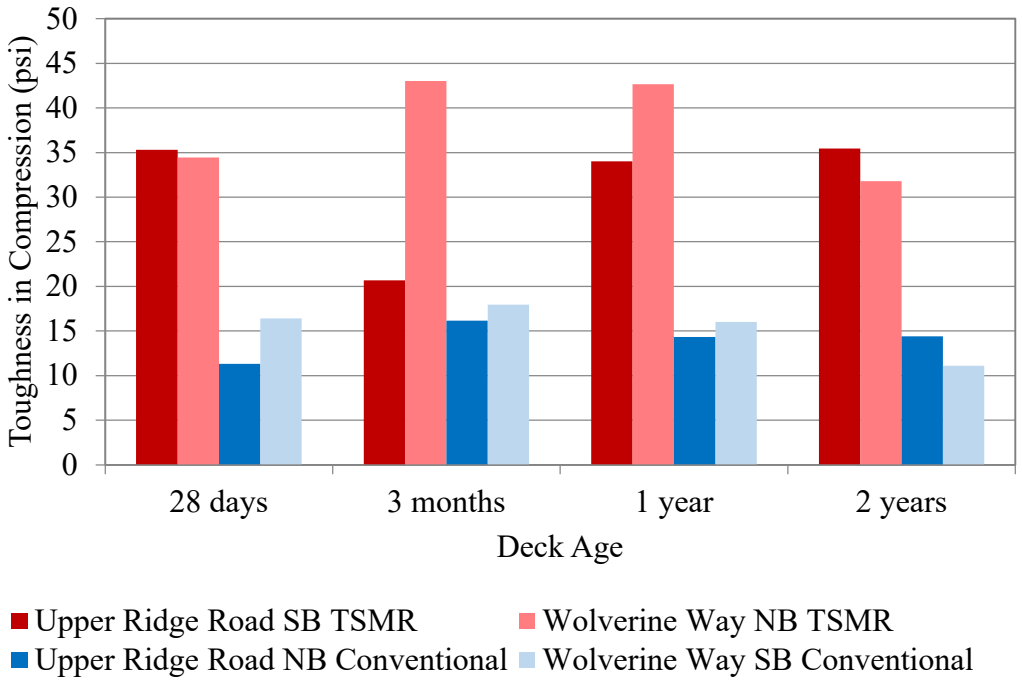

Figure 4-9: Average toughness values for cylindrical specimens.

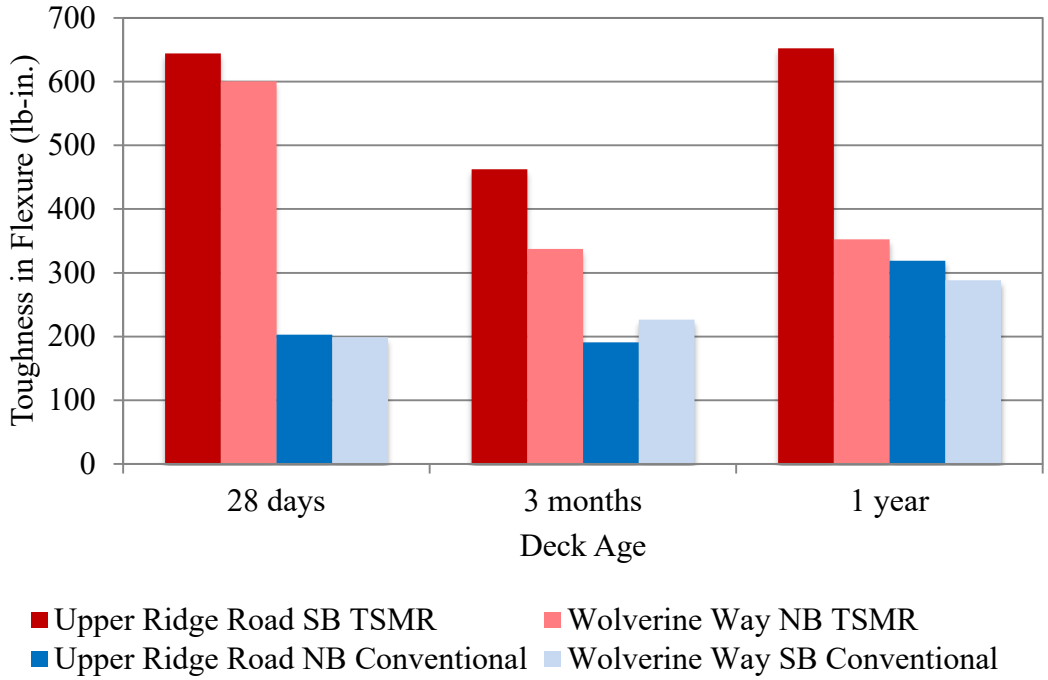

Figure 4-10: Average toughness values for beam specimens.

Table 4-10: Results of Toughness Calculations for Cylindrical Specimens

Concrete Type	Toughness in Compression (psi)											
	28 days			3 months			1 year			2 years		
	Avg.	St. Dev.	*p*-value	Avg.	St. Dev.	*p*-value	Avg.	St. Dev.	*p*-value	Avg.	St. Dev.	*p*-value
Conventional	13.9	3.2	0.000	17.1	1.7	0.201	15.2	1.4	0.005	12.8	3.5	0.034
TSMR	34.9	2.6		31.9	18.0		38.4	6.0		33.6	10.7	

Table 4-11: Results of Toughness Calculations for Beam Specimens

Concrete Type	Toughness in Flexure (lb-in.)								
	28 days			3 months			1 year		
	Avg.	St. Dev.	*p*-value	Avg.	St. Dev.	*p*-value	Avg.	St. Dev.	*p*-value
Conventional	200.7	31.8	0.000	208.6	28.0	0.051	303.5	43.9	0.119
TSMR	622.5	51.9		400.0	118.0		502.0	178.0	

toughness values computed from flexural strength testing are greater for TSMR specimens than for conventional concrete specimens; however, with respect to toughness values computed from flexural strength testing, the difference between the TSMR specimens and conventional concrete specimens decreased over time. At testing periods of 28 days, 3 months, and 1 year, the average toughness of the TSMR specimens was 210, 92, and 65 percent greater, respectively, than that of the conventional concrete specimens. The *p*-values corresponding to these test results were 0.000, 0.051, and 0.119, indicating that sufficient evidence is available to reject the null hypothesis and accept the alternative hypothesis that the toughness of specimens containing TSMR is different than that of specimens containing conventional concrete at a testing period of 28 days.

4.3 Field Testing Results

The results of sensor monitoring, Schmidt rebound hammer testing, distress surveys, and chloride concentration testing are presented in the following sections. Specific dates for the field testing are given in Table 4-12 with the corresponding ages of the bridge decks. For convenience in subsequent discussion of the results, however, deck ages are rounded to 3 months for testing performed before the decks experienced winter conditions and normal trafficking, 1 year for testing performed after the decks experienced one winter season with normal trafficking, and 2 years for testing performed after the decks experienced two winter seasons with normal trafficking. For results for which a statistical analysis was performed to evaluate differences between conventional and TSMR concrete, *p*-values less than or equal to 0.05 allowed rejection of the null hypothesis. Supporting field data are provided in Appendix E.

Table 4-12: Field Testing Schedule

Location	Test Date	Approx. Bridge Deck Age	Test Performed			
			Sensor Monitoring	Schmidt Rebound Hammer	Distress Survey	Chloride Concentration
Upper Ridge Road SB	October 2017	3 months		X	X	X
	July 2018	1 year			X	X
	May 2019	2 years	X	X	X	X
Upper Ridge Road NB	October 2017	3 months		X	X	X
	July 2018	1 year			X	X
	May 2019	2 years	X	X	X	X
Wolverine Way SB	August 2017	3 months			X	
	October 2017	6 months		X		X
	July 2018	1 year			X	X
	May 2019	2 years	X	X	X	X
Wolverine Way NB	August 2017	3 months			X	
	October 2017	6 months		X		X
	July 2018	1 year			X	X
	May 2019	2 years	X	X	X	X

4.3.1 Sensor Monitoring

The data collected from the sensors installed in the bridge decks are presented in Figures 4-11 to 4-13 and Tables 4-13 to 4-14. Because the sensor located at Wolverine Way SB did not function correctly, no data are provided for that deck; therefore, *t*-tests could not be performed on data from the sensors. However, based on data collected from other sensors that were installed in the Wolverine Way SB deck for separate research purposes, the behavior of the deck at Wolverine Way SB is assumed to have been similar to that of the other conventional deck, Upper Ridge Road NB, during the monitoring period.

The internal concrete deck temperatures are shown in Figure 4-11. Wolverine Way NB, Upper Ridge Road NB, and Upper Ridge Road SB were constructed at 0, 104 and 106 days, respectively, which correspond to the beginning points of these data sets in Figure 4-11. In

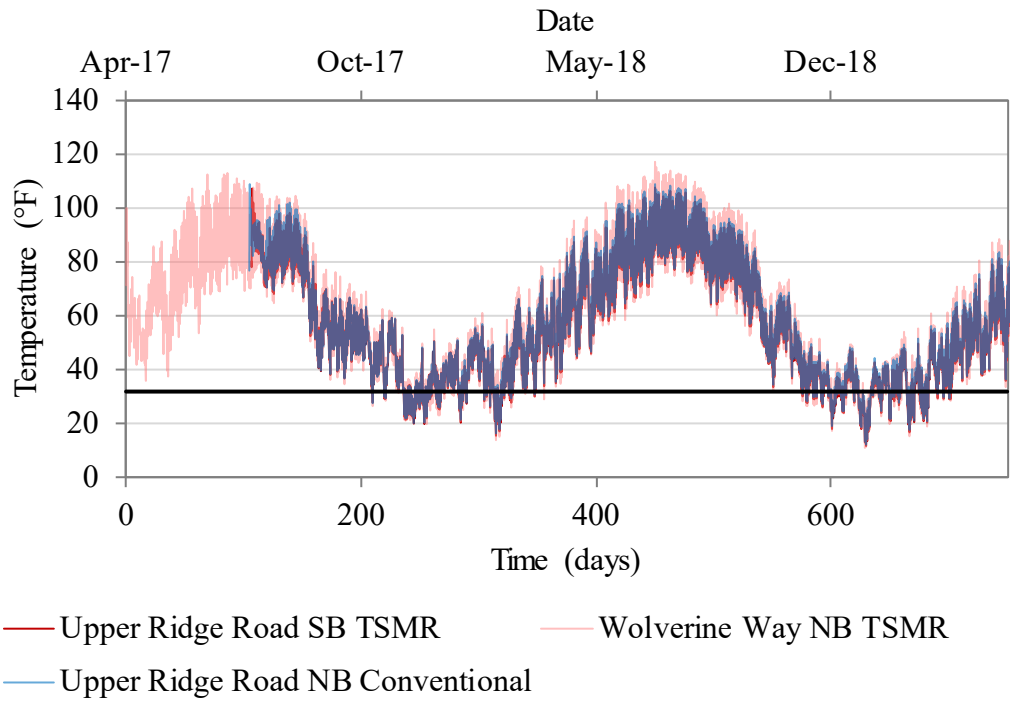

Figure 4-11: Internal concrete temperatures from sensor readings.

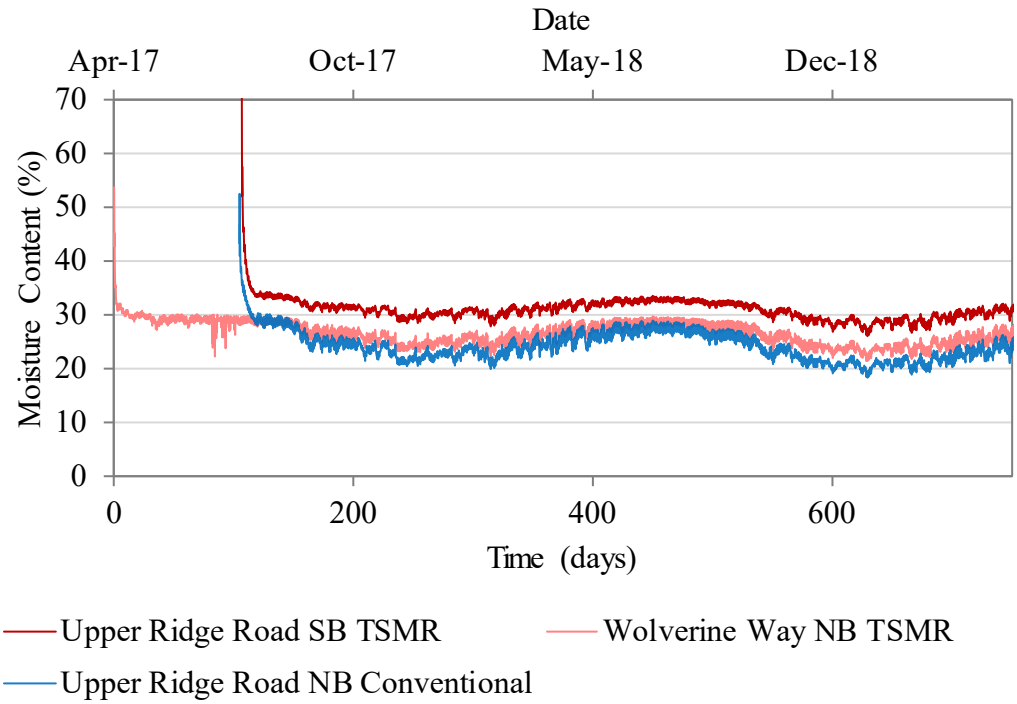

Figure 4-12: Internal concrete moisture contents from sensor readings.

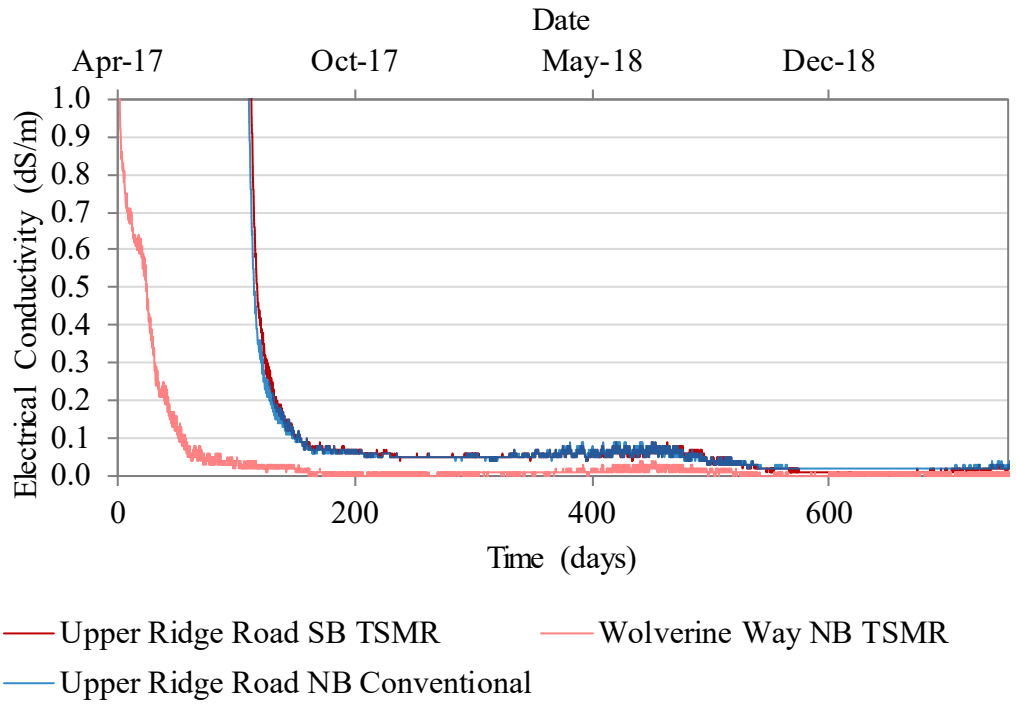

Figure 4-13: Internal concrete electrical conductivity values from sensor readings.

general, both TSMR decks behaved similarly to the conventional deck, and therefore the data indicate that the addition of TSMR does not affect the ability of a concrete matrix to absorb or release heat.

Moisture contents are shown in Figure 4-12 and summarized in Table 4-13. The moisture content of all the decks decreased as the temperature decreased below 32°F, indicated by the horizontal line in Figure 4-11. Because the sensors measured only liquid water, a reduction in apparent water content would occur as a portion of the water changed to ice within the concrete matrix, causing artificially low moisture content readings during winter months. The fluctuating temperatures above and below 32°F and corresponding oscillations in moisture content suggest freezing and thawing within the deck. The apparent moisture content of the Wolverine Way NB deck, which was constructed with concrete containing TSMR, and the Upper Ridge Road NB

Table 4-13: Results of Internal Concrete Moisture Content Monitoring

Location	Moisture Content (%)					
	200 days		400 days		600 days	
	Avg.	St. Dev.	Avg.	St. Dev.	Avg.	St. Dev.
Upper Ridge Road SB TSMR	31.5	0.240	32.2	0.364	27.6	0.557
Wolverine Way NB TSMR	26.8	0.567	27.9	0.682	22.9	0.683
Upper Ridge Road NB Conventional	24.9	0.469	26.4	0.782	19.8	0.509

Table 4-14: Results of Internal Concrete Electrical Conductivity Monitoring

Location	Electrical Conductivity (dS/m)					
	200 days		400 days		600 days	
	Avg.	St. Dev.	Avg.	St. Dev.	Avg.	St. Dev.
Upper Ridge Road SB TSMR	0.0662	0.0049	0.0612	0.0080	0.0100	0.0000
Wolverine Way NB TSMR	0.0071	0.0046	0.0137	0.0049	0.0058	0.0050
Upper Ridge Road NB Conventional	0.0629	0.0046	0.0654	0.0083	0.0200	0.0000

deck, which was constructed with conventional concrete, converged to similar average values between 24 and 26 percent by the end of the monitoring period. However, the Upper Ridge Road SB deck, which was constructed with concrete containing TSMR, had higher values that averaged around 31 percent. Given the similar results between the Wolverine Way NB and Upper Ridge Road NB decks, this higher moisture content cannot be attributed to the use of TSMR; further research would be needed to explain this difference.

The electrical conductivity for bridge decks at Upper Ridge Road NB, Upper Ridge Road SB, and Wolverine Way NB are shown in Figure 4-13 and summarized in Table 4-14. In general,

being a surrogate measure of diffusivity, the electrical conductivity decreased consistently during the first couple of months as concrete curing progressed and then stabilized with only marginal changes occurring for the remainder of the monitoring period. The electrical conductivity for the Wolverine Way NB deck required about twice as much time to stabilize as the decks at Upper Ridge Road, probably related to differences in ambient environmental conditions during the weeks following construction of those decks. The Upper Ridge Road NB and Upper Ridge Road SB decks stabilized at a value of 0.04 dS/m until about 500 days, when the electrical conductivity decreased again to a value closer to that of the Wolverine Way NB deck. Given that the sensor results for the Upper Ridge Road SB and Upper Ridge Road NB decks were practically identical, the data suggest that the addition of TSMR does not affect the electrical conductivity of the concrete.

4.3.2 Schmidt Rebound Hammer Testing

The average rebound numbers for the 3-month and 2-year testing periods are provided in Figure 4-14 and Table 4-15, in which a higher rebound number indicates stiffer concrete. The average rebound number varied little between the TSMR decks and conventional decks. For testing at 3 months, the average rebound numbers of the TSMR and conventional decks were 42 and 45, respectively. For testing at 2 years, the average rebound numbers of the TSMR and conventional decks differed by only one point, with values of 51 and 50, respectively. Therefore, the stiffness of the TSMR concrete was very similar to that of conventional concrete. The *t*-tests

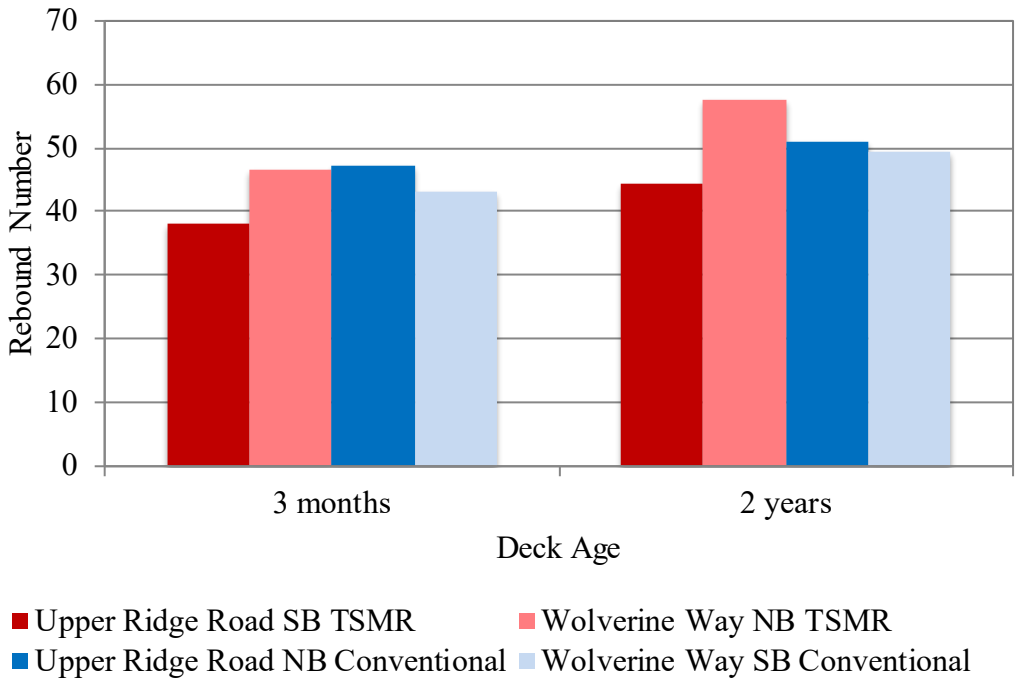

Figure 4-14: Average Schmidt rebound numbers.

Table 4-15: Results of Schmidt Rebound Hammer Testing

Concrete Type	Rebound Number					
	3 months			2 years		
	Avg.	St. Dev.	*p* -value	Avg.	St. Dev.	*p* -value
Conventional	45.3	2.8	0.638	50.1	1.2	0.916
TSMR	42.3	6.0		51.0	9.2	

performed to compare the rebound numbers of TSMR and conventional concrete for the 3-month and 2-year testing periods resulted in *p*-values of 0.638 and 0.916, respectively, as shown in Table 4-15. The *p*-values are greater than the specified threshold of 0.05, which indicates that insufficient evidence is available to statistically differentiate between the two types of concrete.

4.3.3 Distress Surveys

Based on the results of the distress surveys, Figures 4-15 to 4-18 present crack maps prepared for all four bridge decks. Yellow lines indicate cracking observed at 3 months, orange lines indicate additional cracking observed at 1 year, and red lines indicate additional cracking observed at 2 years from the time of construction. Figures 4-19 and 4-20 show average crack densities and maximum crack widths of the bridge decks containing TSMR and conventional concrete, and Tables 4-16 and 4-17 summarize the test results. Separate crack maps for all four bridge decks for the 3-month, 1-year, and 2-year testing periods are provided in Appendix F.

Regarding crack density, the conventional decks exhibited notably more cracking than the TSMR decks, as shown in Figures 4-15 to 4-18. Even at 3 months, the conventional decks exhibited 142 percent greater crack density than the TSMR decks, with values of 0.029 and 0.012 ft/ft^2, respectively. With time, the crack-reducing effect of the TSMR fibers became even more pronounced. At 1 year and 2 years, the average crack densities of the conventional decks reached 0.171 and 0.387 ft/ft^2, respectively, while the average crack densities of the TSMR decks remained at much lower values of 0.042 and 0.103 ft/ft^2, respectively. Therefore, at 1 year and 2 years, the crack density of the conventional decks was 307 and 276 percent greater, respectively, than that of the TSMR decks. Nonetheless, because of the small sample sizes and the comparatively high variability in crack density between the two conventional decks and between the two TSMR decks, the *t*-tests performed to compare the crack densities of TSMR and conventional concrete for the 3-month, 1-year, and 2-year testing periods resulted in *p*-values of 0.688, 0.162, and 0.123, respectively, as shown in Table 4-16. The *p*-values are greater than the specified threshold of 0.05, which indicates that insufficient evidence is available to statistically differentiate between the two types of concrete.

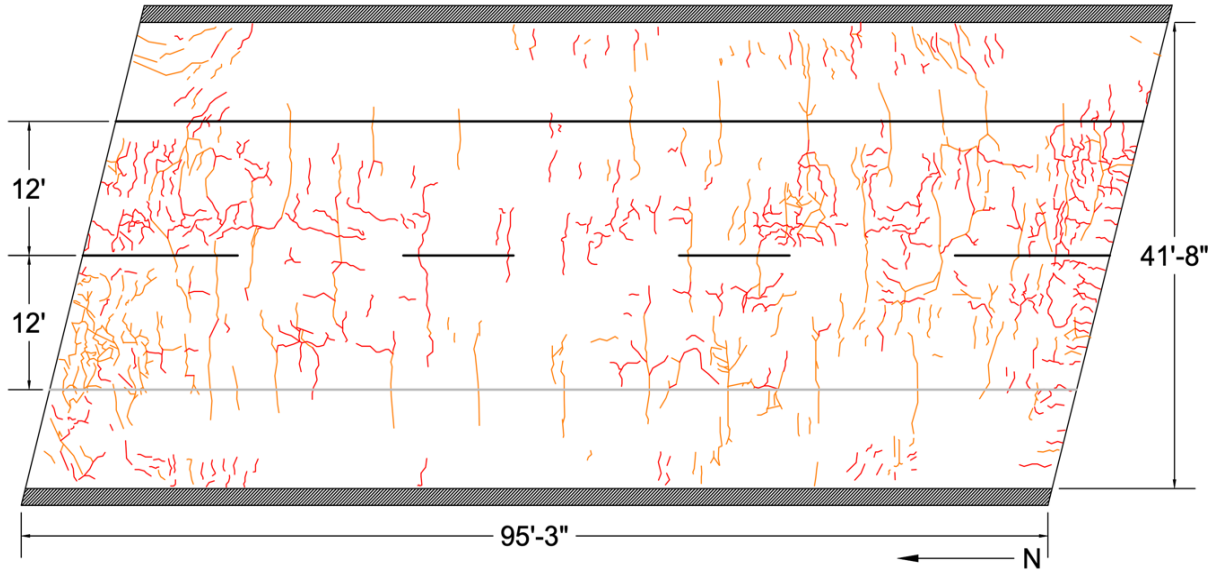

Figure 4-15: Crack map for the Upper Ridge Road NB conventional deck.

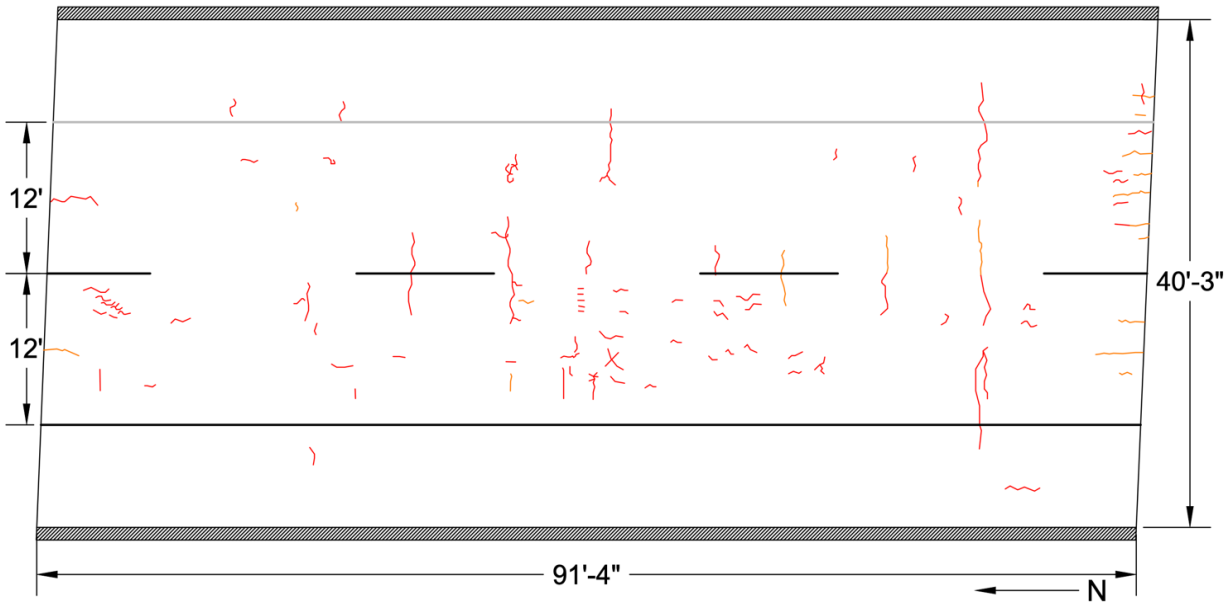

Figure 4-16: Crack map for the Upper Ridge Road SB TSMR deck.

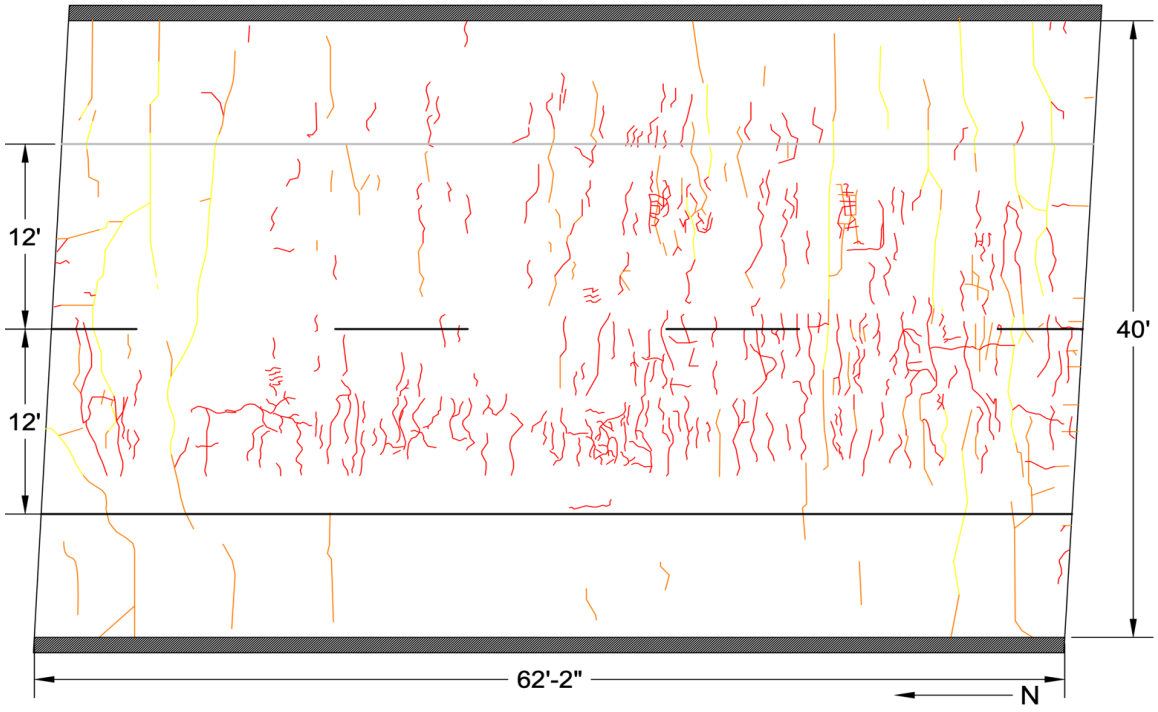

Figure 4-17: Crack map for the Wolverine Way SB conventional deck.

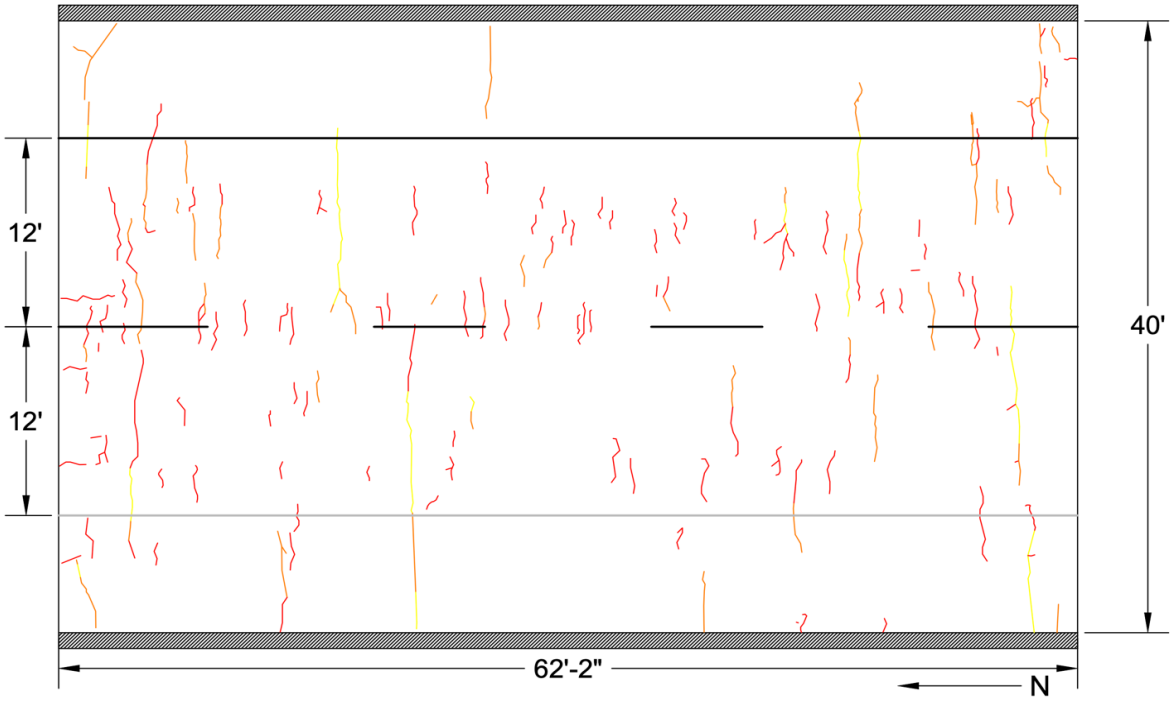

Figure 4-18: Crack map for the Wolverine Way NB TSMR deck.

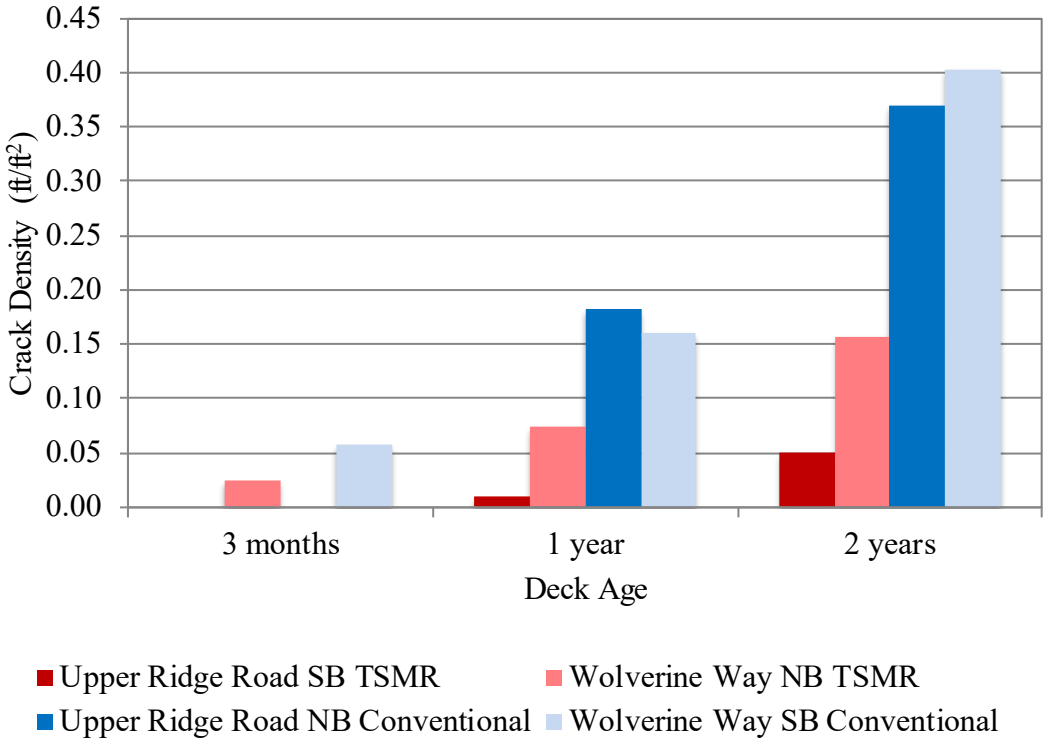

Figure 4-19: Average crack densities.

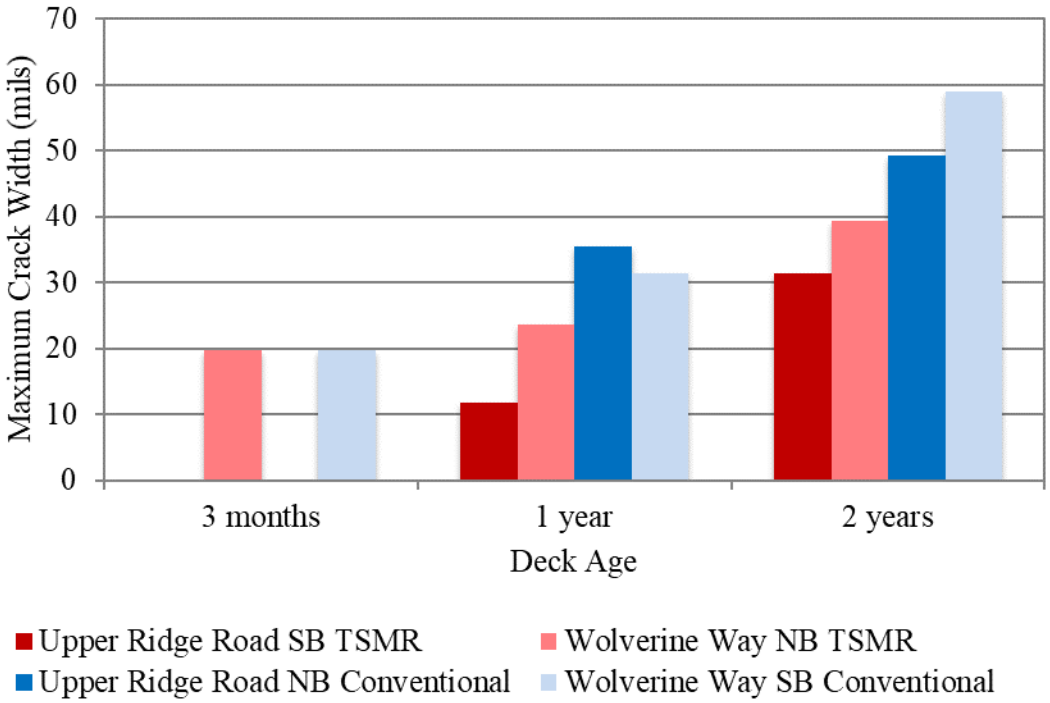

Figure 4-20: Maximum crack widths.

Table 4-16: Results of Distress Surveys for Crack Density

Concrete Type	Crack Density (ft/ft^2)								
	3 months			1 year			2 years		
	Avg.	St. Dev.	*p*-value	Avg.	St. Dev.	*p*-value	Avg.	St. Dev.	*p*-value
Conventional	0.029	0.041	0.688	0.171	0.016	0.162	0.387	0.024	0.123
TSMR	0.012	0.017		0.042	0.045		0.103	0.075	

Table 4-17: Results of Distress Surveys for Maximum Crack Width

Concrete Type	Maximum Crack Width (mils)								
	3 months			1 year			2 years		
	Avg.	St. Dev.	*p*-value	Avg.	St. Dev.	*p*-value	Avg.	St. Dev.	*p*-value
Conventional	10	14	1.000	33	3	0.202	54	7	0.103
TSMR	10	14		18	8		35	6	

Regarding crack width, the TSMR fibers in the Wolverine Way NB and Upper Ridge Road SB bridge decks exhibited the ability to limit the expansion of existing cracks. At 3 months, both the conventional decks and the TSMR decks had a maximum crack width of 9.8 mils. In just 1 year, the average maximum crack width on the conventional decks expanded to 33.5 mils, while the average maximum crack width on the TSMR decks expanded to only 17.7 mils. After 2 years, the average maximum crack widths on the conventional decks and the TSMR decks were 54.1 and 35.4 mils, respectively. Therefore, the average maximum crack width on conventional decks was 89 percent and 53 percent greater than that of the TSMR decks after 1 year and 2 years, respectively, from the time of construction. Nonetheless, again because of the small sample sizes and the comparatively high variability in maximum crack width between the two conventional decks and between the two TSMR decks, the *t*-tests performed to compare the

crack densities of TSMR and conventional concrete resulted in *p*-values greater than the specified threshold of 0.05, as shown in Table 4-17, which indicates that insufficient evidence is available to statistically differentiate between the two types of concrete.

The bridge designs also affected the cracking behavior of the bridge decks. The bridge decks located at Wolverine Way, which were constructed using full-depth monolithic concrete and steel girders, exhibited more cracking than the decks located at Upper Ridge Road, which were constructed with precast half-deck panels and prestressed concrete girders. At the 3-month testing period, the decks at Wolverine Way had an average crack density of 0.041 ft/ft^2, while the decks at Upper Ridge Road had no visible cracks. At the 1-year and 2-year testing periods, the average crack density of the bridge decks at Wolverine Way was 21 and 33 percent greater, respectively, than that of the decks at Upper Ridge Road. The higher flexibility of steel girders compared to prestressed concrete girders (Zhou et al. 2004), as well as the higher amount of construction trafficking experienced by the decks located at Wolverine Way, which were constructed prior to those located at Upper Ridge Road, may have caused these differences in cracking. In the absence of these confounding variables, the decks constructed with precast half-deck panels would have been expected to exhibit more cracking than those constructed with full-depth monolithic concrete (Guthrie and Yaede 2014). Further research would be needed to investigate the effects of bridge design on the cracking behavior of the bridge decks.

4.3.4 Chloride Concentration Testing

Average chloride concentration results from testing at 1 year and 2 years are provided in Figures 4-21 to 4-24. For samples collected over cracked concrete, the crack depths and widths are provided in Appendix E. Chloride concentrations measured before the decks experienced

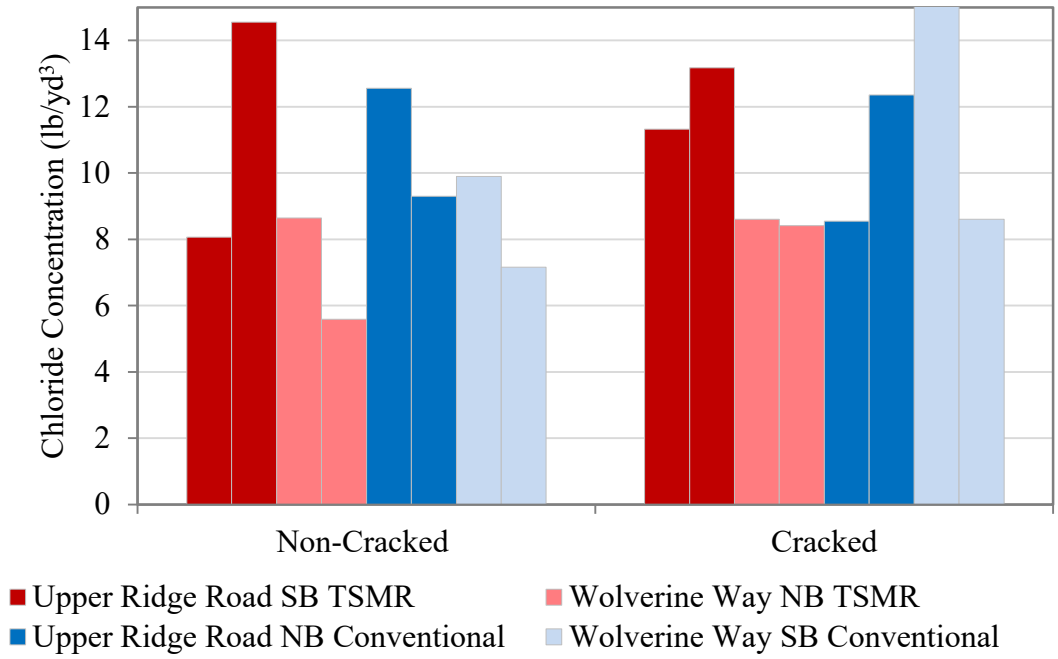

Figure 4-21: Chloride concentrations for 1-year testing at a depth of 0.0 to 0.5 in.

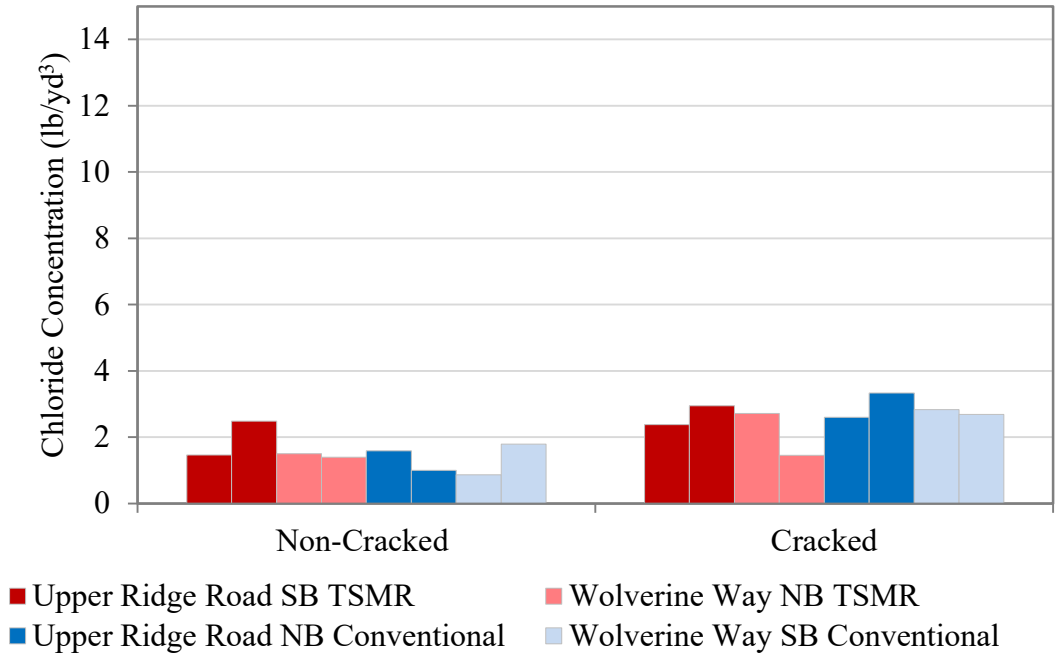

Figure 4-22: Chloride concentrations for 1-year testing at a depth of 0.5 to 1.0 in.

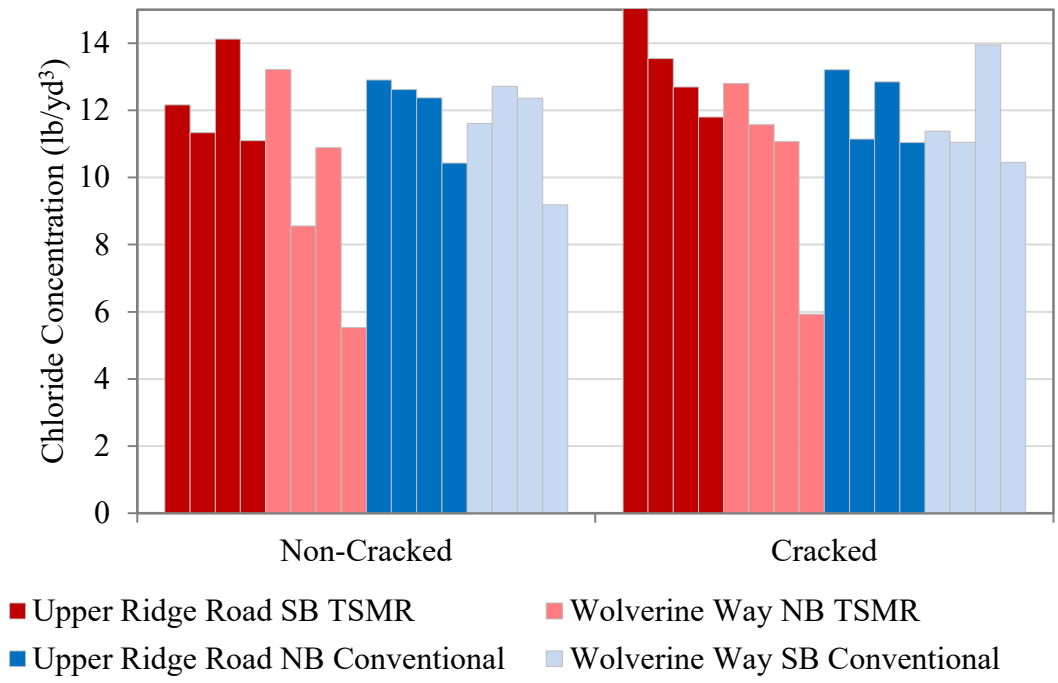

Figure 4-23: Chloride concentrations for 2-year testing at a depth of 0.0 to 0.5 in.

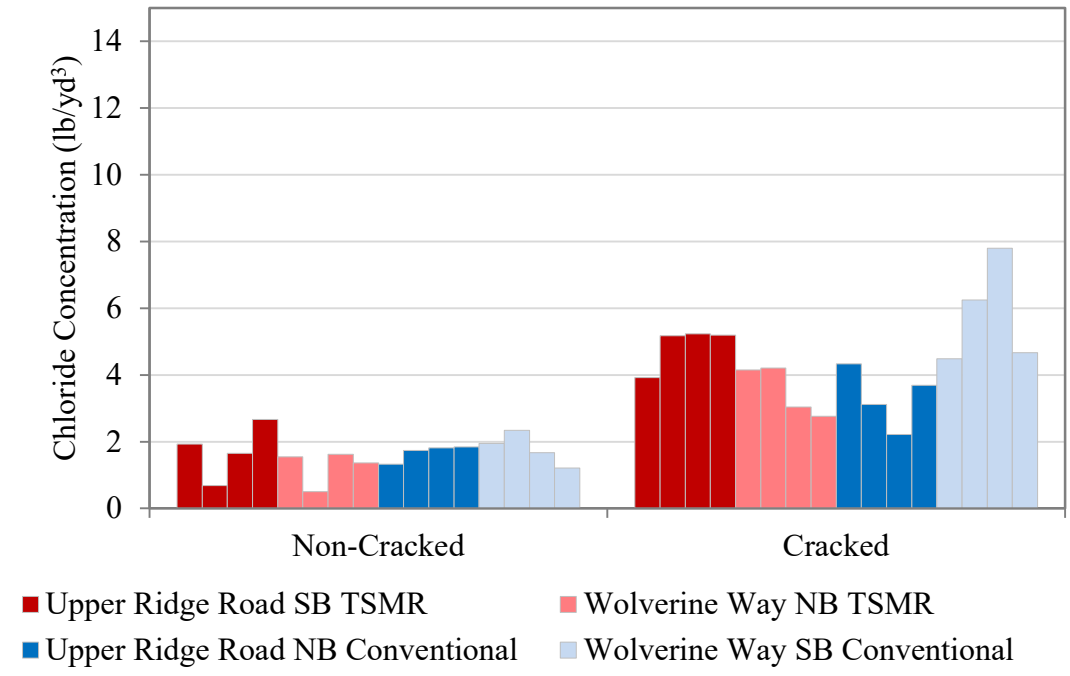

Figure 4-24: Chloride concentrations for 2-year testing at a depth of 0.5 to 1.0 in.

winter conditions and normal trafficking were extremely low, ranging from 0.1 to 0.8 lb/yd^3 at a depth of 0.0 to 0.5 in. across the four bridge decks. The presence of these low but measurable chloride concentrations in the new decks may be attributable to salt inherent in the aggregate used for concrete production; many aggregates are mined from areas previously covered by the historic Lake Bonneville. At 1 year, after the decks experienced one winter season with normal trafficking, chloride concentrations increased as a result of the use of deicing salts on the bridge decks. Specifically, the average chloride concentrations for all samples collected over intact concrete at depths of 0.0 to 0.5 in. and 0.5 to 1.0 in. were 9.5 and 1.5 lb/yd^3, respectively. At 2 years, after the decks experienced two winter seasons with normal trafficking, the average chloride concentrations for all samples collected over intact concrete at depths of 0.0 to 0.5 in. and 0.5 to 1.0 in. increased to 11.3 and 1.6 lb/yd^3, respectively.

The data also show that the chloride concentrations for samples collected over cracked concrete increased more rapidly than those for samples collected over non-cracked concrete. At 1 year, the chloride concentrations for the cracked concrete at depths of 0.0 to 0.5 in. and 0.5 to 1.0 in. were, on average, 32 and 73 percent greater than those for the non-cracked concrete. At 2 years, the chloride concentrations for samples collected over cracked concrete at depths of 0.0 to 0.5 in. and 0.5 to 1.0 in. were, on average, 5 and 172 percent greater than those for samples collected over non-cracked concrete. Therefore, the data indicate that the presence of cracks markedly increases the rate at which chloride ions penetrate the bridge decks.

The inclusion of TSMR in the bridge decks did not change the rate at which chloride ions penetrated cracked or non-cracked concrete. The *t*-test for chloride concentrations measured over cracked concrete resulted in *p*-values ranging from 0.230 to 0.991, and the *t*-test for chloride concentrations measured over non-cracked concrete resulted in *p*-values ranging from 0.302 to

0.826, as shown in Tables 4-18 and 4-19. Therefore, insufficient evidence is available to statistically differentiate between the two types of concrete.

As described previously, the bridge decks constructed with concrete containing TSMR experienced less cracking than the bridge decks constructed with conventional concrete. The chloride concentration data indicate that, although TSMR fibers themselves do not directly affect the rate at which chloride ions penetrate the concrete, the fibers prevent cracking, which, in turn, limits the penetration of chloride ions into the decks. Therefore, the use of TSMR would be expected to decrease the area of a bridge deck affected by cracking and subsequent chloride-induced corrosion damage and thereby increase the service life of the bridge deck.

Table 4-18: Results of Chloride Concentration Testing at a Depth of 0.0 to 0.5 in.

Concrete Type		Chloride Concentration (lb/yd^3)					
		1 year			2 years		
		Avg.	St. Dev.	*p* -value	Avg.	St. Dev.	*p* -value
Conventional	Non-Cracked	9.7	2.2	0.826	11.8	0.7	0.556
TSMR		9.2	3.8		10.9	2.7	
Conventional	Cracked	14.6	9.6	0.430	11.9	1.1	0.991
TSMR		10.4	2.3		11.9	2.3	

Table 4-19: Results of Chloride Concentration Testing at a Depth of 0.5 to 1.0 in.

Concrete Type		Chloride Concentration (lb/yd^3)					
		1 year			2 years		
		Avg.	St. Dev.	*p* -value	Avg.	St. Dev.	*p* -value
Conventional	Non-Cracked	1.3	0.4	0.302	1.7	0.1	0.317
TSMR		1.7	0.5		1.5	0.4	
Conventional	Cracked	2.9	0.3	0.230	4.6	1.4	0.682
TSMR		2.4	0.7		4.2	0.8	

4.4 Summary

Laboratory testing, field testing, and data analyses were performed for this research. For shrinkage testing, the conventional and TSMR beam specimens exhibited similar average changes in height after 4 months. The electrical impedance measurements did not indicate a notable difference between specimens comprising concrete with TSMR and those comprising conventional concrete. Even with the addition of 40 lb of TSMR per cubic yard of concrete, which was expected to aid in the transfer of electrical current through the concrete matrix due to the conductive nature of the steel fibers, the electrical impedance values of the TSMR specimens were approximately the same as those of the conventional specimens.

During compressive strength, flexural strength, and splitting tensile strength testing, all specimens containing conventional concrete exhibited a brittle failure, in which the load immediately decreased to zero after reaching the peak stress. In contrast, specimens containing TSMR exhibited an extremely ductile failure. The ability of the TSMR specimens to maintain a substantial amount of load at high strain levels indicates that, after initial cracking, TSMR fibers were able to act as bridges across the cracks, preventing formation of larger cracks that would have led to quicker failure. Therefore, after initial cracking, TSMR specimens exhibited different behavior than that of conventional specimens; however, before initial cracking, no notable difference in behavior between conventional and TSMR specimens was apparent.

The toughness of the TSMR cylindrical and beam specimens was substantially greater than that of the conventional concrete specimens. For cylindrical specimens at testing periods of 28 days, 3 months, 1 year, and 2 years, the average toughness of the TSMR specimens was 152, 87, 153, and 164 percent greater, respectively, than that of the conventional concrete specimens. For beam specimens at testing periods of 28 days, 3 months, and 1 year, the average toughness of

the TSMR specimens was 210, 92, and 65 percent greater, respectively, than that of the conventional concrete specimens.

Sensors installed in the bridge decks provided internal concrete temperature, moisture content, and electrical conductivity data. Regarding temperature, in general, both TSMR decks behaved similarly to the conventional deck, and therefore the data indicate that the addition of TSMR does not affect the ability of a concrete matrix to absorb or release heat. The apparent moisture content of the Wolverine Way NB deck, which was constructed with concrete containing TSMR, and the Upper Ridge Road NB deck, which was constructed with conventional concrete, converged to similar average values between 24 and 26 percent by the end of the monitoring period. Given that the electrical conductivity results for the Upper Ridge Road SB and Upper Ridge Road NB decks were practically identical, the data suggest that the addition of TSMR does not affect the electrical conductivity of the concrete.

The average Schmidt rebound number varied little between the TSMR decks and conventional decks. For testing at 2 years, the average rebound numbers of the TSMR and conventional decks differed by only one point, with values of 51 and 50, respectively. Therefore, the stiffness of the TSMR concrete was very similar to that of conventional concrete.

Distress surveys showed that the conventional decks exhibited notably more cracking than the TSMR decks. At 1 year and 2 years, the crack density of the conventional decks was 307 and 276 percent greater, respectively, than that of the TSMR decks. Furthermore, the TSMR fibers in the Wolverine Way NB and Upper Ridge Road SB bridge decks exhibited the ability to limit the expansion of existing cracks. The average maximum crack width on conventional decks was 89 percent and 53 percent greater than that of the TSMR decks after 1 year and 2 years, respectively, from the time of construction.

For all of the decks, chloride concentrations increased every year as a result of the use of deicing salts on the bridge decks during winter. At 1 year, the average chloride concentrations for all samples collected over intact concrete at depths of 0.0 to 0.5 in. and 0.5 to 1.0 in. were 9.5 and 1.5 lb/yd^3, respectively. At 2 years, the average chloride concentrations for all samples collected over intact concrete at depths of 0.0 to 0.5 in. and 0.5 to 1.0 in. increased to 11.3 and 1.6 lb/yd^3, respectively. The data also show that the chloride concentrations for samples collected over cracked concrete increased more rapidly than those for samples collected over non-cracked concrete. Although TSMR fibers themselves do not directly affect the rate at which chloride ions penetrated cracked or non-cracked concrete, the fibers do prevent cracking, which, in turn, limits the penetration of chloride ions into the decks. Therefore, the use of TSMR would be expected to decrease the area of a bridge deck affected by cracking and subsequent chloride-induced corrosion damage and thereby increase the service life of the bridge deck.

5 CONCLUSION

5.1 Summary

The objective of this research was to investigate the effects of TSMR fibers on 1) the mechanical properties of concrete used in bridge deck construction and 2) the early cracking behavior of concrete bridge decks. This research involved the evaluation of four newly constructed bridge decks through a series of laboratory and field tests.

In the spring and summer of 2017, UDOT constructed four new bridge decks along the Mountain View Corridor in West Valley City, Utah, two at Upper Ridge Road and two at Wolverine Way. The two-lane Wolverine Way SB bridge deck and the Upper Ridge Road NB bridge deck were constructed using a conventional concrete mixture containing portland cement and fly ash as binders with a water-cementitious materials ratio of 0.40. The two-lane Wolverine Way NB bridge deck and the Upper Ridge Road SB bridge deck were constructed using the same conventional concrete mixture but with an addition of 40 lb of TSMR per cubic yard of concrete. Prior to concrete placement, each of the four bridge decks was instrumented with a sensor connected to a data logger. The sensors measured the internal temperature, moisture content, and electrical conductivity of the concrete at hourly intervals. A battery-powered data logger was mounted inside a secure junction box to facilitate automated data collection.

Twelve cylinder and six beam specimens cast during construction of each bridge deck were subjected to several laboratory tests over a period of 2 years. Nondestructive tests, including shrinkage and electrical impedance tests, were performed on specimens prior to

destructive tests such as compressive strength, flexural strength, and splitting tensile strength tests.

Schmidt rebound hammer testing, distress surveys, and chloride concentration tests were performed to evaluate the performance of the bridge decks at different ages of the concrete. Tests were performed at approximately 3 months, 1 year, and 2 years from the time of construction of the bridge decks, thereby providing a comparison of data collected before the decks experienced winter conditions and normal trafficking, after the decks experienced one winter season with normal trafficking, and after the decks experienced two winter seasons with normal trafficking.

Statistical analyses were performed to determine the significance of the addition of TSMR in the concrete bridge decks. The null hypothesis in each *t*-test was that the given value of the specimens with TSMR was equal to that of the specimens without TSMR, and the alternative hypothesis was that the given value of the specimens with TSMR was different than that of the specimens without TSMR.

5.2 Findings

Laboratory testing, field testing, and data analyses were performed for this research. For shrinkage testing, the conventional and TSMR beam specimens exhibited similar average changes in height after 4 months. The electrical impedance measurements did not indicate a notable difference between specimens comprising concrete with TSMR and those comprising conventional concrete.

During compressive strength, flexural strength, and splitting tensile strength testing, all specimens containing conventional concrete exhibited a brittle failure, in which the load immediately decreased to zero after reaching the peak stress. In contrast, specimens containing TSMR exhibited an extremely ductile failure. The ability of the TSMR specimens to maintain a

substantial amount of load at high strain levels indicates that, after initial cracking, TSMR fibers were able to act as bridges across the cracks, preventing formation of larger cracks that would have led to quicker failure. Although no notable difference in behavior between conventional and TSMR specimens was apparent before initial cracking, the toughness of the TSMR specimens was substantially greater than that of the conventional concrete specimens.

Sensors installed in the bridge decks provided internal concrete temperature, moisture content, and electrical conductivity data. Regarding temperature, in general, both TSMR decks behaved similarly to the conventional deck, and therefore the data indicate that the addition of TSMR does not affect the ability of a concrete matrix to absorb or release heat. The apparent moisture content of the Wolverine Way NB deck, which was constructed with concrete containing TSMR, and the Upper Ridge Road NB deck, which was constructed with conventional concrete, converged to similar average values by the end of the monitoring period. Given that the electrical conductivity results for the Upper Ridge Road SB and Upper Ridge Road NB decks were practically identical, the data suggest that the addition of TSMR does not affect the electrical conductivity of the concrete.

The average Schmidt rebound number varied little between the TSMR decks and conventional decks. Therefore, the stiffness of the TSMR concrete was very similar to that of conventional concrete.

Distress surveys showed that the conventional decks exhibited notably more cracking than the TSMR decks. The TSMR fibers in the Wolverine Way NB and Upper Ridge Road SB bridge decks exhibited the ability to limit both crack density and crack width.

For all of the decks, chloride concentrations increased every year as a result of the use of deicing salts on the bridge decks during winter. However, the chloride concentrations for

samples collected over cracked concrete increased more rapidly than those for samples collected over non-cracked concrete. Although TSMR fibers themselves do not directly affect the rate at which chloride ions penetrated cracked or non-cracked concrete, the fibers do prevent cracking, which, in turn, limits the penetration of chloride ions into the decks. Therefore, the use of TSMR would be expected to decrease the area of a bridge deck affected by cracking and subsequent chloride-induced corrosion damage and thereby increase the service life of the bridge deck.

5.3 Recommendations

Based on the results of the distress surveys performed on the bridge decks studied in this research, the use of TSMR in concrete bridge decks is recommended to provide additional protection against cracking and reduce the occurrence of larger cracks. In addition, the use of TSMR is recommended for use when extreme loading conditions, such as earthquakes, are expected, as concrete containing TSMR exhibits high levels of toughness; the use of TSMR would also be expected to provide increased post-cracking structural capacity during the service life of a bridge deck.

Given that the future cost of concrete containing TSMR may decrease compared to the costs associated with early implementation efforts, such as the project documented in this research, further research to study the economic viability of the use of TSMR is highly recommended. Researching the use of TSMR in decks with overlays would also be valuable to determine if TSMR improves overlay performance and thereby offsets the extra cost of TSMR. Finally, analyzing the use of TSMR in additional decks involving different structural configurations, service conditions, and contractors may also be of interest for future research studies.

REFERENCES

Balakumaran, S. S. G., Weyers, R. E., and Brown, M. C. (2017). "Influence of Cracks on Corrosion Initiation in Bridge Decks." *ACI Materials Journal*, 114(1), 161-170.

Banthia, N., and Trottier, J.-F. (1991). "Deformed steel fiber—cementitious matrix bond under impact." *Cement and Concrete Research*, 21(1), 158-168.

Barton, J., Baxter, J., Guthrie, W. S., and Mazzeo, B. A. (2019). "Vertical Electrical Impedance Scanner for Nondestructive Concrete Bridge Deck Assessment without a Direct Rebar Connection." *Materials Evaluation*, 77(10).

Basheer, P. A. M., Chidiact, S. E., and Long, A. E. (1996). "Predictive Models for Deterioration of Concrete Structures." *Construction and Building Materials*, 10(1), 27-37.

Bateman, K. D. (2018). *Estimating Phase Durations for Chloride-Induced Corrosion Damage of Concrete Bridge Decks in Utah*. M.S. thesis, Department of Civil and Environmental Engineering, Brigham Young University, Provo, UT.

Baxter, J. S. (2019). *Vertical Electrical Impedance Measurements of Concrete Bridge Decks*. Ph.D. dissertation, Department of Electrical and Computer Engineering, Brigham Young University, Provo, UT.

Bentz, D. P., Guthrie, W. S., Jones, S. Z., and Martys, N. S. (2014). "Predicting Service Life of Steel Reinforced Concrete Exposed to Chlorides." *Concrete International*, 36(9), 55-64.

Bioubakhsh, S. (2011). *The Penetration of Chloride in Concrete Subject to Wetting and Drying: Measurement and Modeling*. Ph.D. dissertation, Department of Civil, Environmental, and Geomatic Engineering, University College London, London, England.

Birdsall, A. W., Guthrie, W. S., and Bentz, D. P. (2007). "Effects of Initial Surface Treatment Timing on Chloride Concentrations in Concrete Bridge Decks." *Transportation Research Record: Journal of the Transportation Research Board*, 2028, 103-110.

Concrete News. (2015). "Steel Reinforcing Fibers: Micro Rebar." *Concrete Products*, SEMCO Publishing, <http://www.concreteproducts.com/equipment/innovations/9179-steel-reinforcing-fibers-micro-rebar.html#.WpOZRmaZPMI> (Accessed Aug. 15, 2017).

Core Construction Products (undated). Helix Micro Rebar, <http://www.core-construction-products.com/products-leed-energy-star-net-zero-energy-efficient-insulation-concrete-building-materials-homes-east-usa/helix-steel-micro-rebar-reinforcement.html> (Accessed May 20, 2019).

Dunker, K. F., and Rabbat, B. G. (1993). "Why Americas Bridges are Crumbling." *Scientific American*, 266(3), 66-72.

Ghetasi, A., and Harris, D. K. (2014). "Effect of Deck Deterioration on Overall System Behavior, Resilience and Remaining Life of Composite Steel Girder Bridges." *Proceedings of the Structures Congress 2014*, Structural Engineering Institute, American Society of Civil Engineers, Boston, MA.

Grace, N., Hanson, J., and AbdelMessih, H. (2004). *Inspection and Deterioration of Bridge Decks Constructed Using Stay-in-Place Metal Forms and Epoxy-Coated Reinforcement*. Research Report R, Michigan Department of Transportation, Lansing, MI.

Granju, J.-L., and Balouch, S. U. (2005). "Corrosion of Steel Fibre Reinforced Concrete from the Cracks." *Cement and Concrete Research*, 35(3), 572-577.

Grzybowski, M., and Shah, S. P. (1990). "Shrinkage Cracking of Fiber Reinforced Concrete." *ACI Materials Journal*, 87(2), 138-148.

Gucunski, N., Imani, A., Romero, F., Nazarian, S., Yuan, D., Wiggenhauser, H., Shokouhi, P., Taffe, A., and Kutrubes, D. (2013). *Nondestructive Testing to Identify Concrete Bridge Deck Deterioration*. Report S2-R06A-RR-1, Transportation Research Board, Washington, D.C.

Guthrie, W. S., Nolan, C. D., and Bentz, D. P. (2011). "Effect of Initial Timing of Scarification and Overlay Treatment on Chloride Concentrations in Concrete Bridge Decks." *Transportation Research Record: Journal of the Transportation Research Board*, 2220, 66-74.

Guthrie, W. S., Waters, T., and Reese, G.B. (2015). "Comparison of Moisture Content and Electrical Conductivity of Lightweight and Normal-Weight Concrete Bridge Decks: Instrumentation and Monitoring." *Proceedings of the Sixteenth International Conference on Cold Regions Engineering*, American Society of Civil Engineers, Salt Lake City, UT.

Guthrie, W. S., and Yaede, J. M. (2013). "Internal Curing of Concrete Bridge Decks in Utah." *Transportation Research Record: Journal of the Transportation Research Board*, 2342(1), 121–128.

Guthrie, W. S., and Yaede, J. (2014). "Evolution of Early-Age Cracking in Concrete Bridge Decks Incorporating Pre-Stressed Concrete Panels and Internally Cured Concrete." *Transportation Research Board 93rd Annual Meeting Compendium of Papers*, Transportation Research Board of the National Academies, Washington DC.

Hansson, C. M., Poursaee, A., and Jaffer, S. J. (2012). "Corrosion of Reinforcing Bars in Concrete." *The Masterbuilder*, 106-124, <https://ceramrtr.ceramika.agh.edu.pl/~szyszkin/mm/Corrosion%20Of%20Reinforcing%20Bars%20In%20Concrete.pdf> (Accessed Aug. 27, 2020).

Helix Steel (undated). "Twisted Steel Micro Rebar." Helix Steel, Ann Arbor, MI, <http://www.helixsteel.com> (Accessed Apr. 26, 2017).

Hema, J., Guthrie, W. S., and Fonseca, F. S. (2004). *Concrete Bridge Deck Condition Assessment and Improvement Strategies*. Report UT-04.16, Utah Department of Transportation, Salt Lake City, UT.

Homma, D., Mihashi, H., and Nishiwaki, T. (2009). "Self-Healing Capability of Fiber Reinforced Cementitious Composites." *Journal of Advanced Concrete Technology*, 7(2), 217-228.

Katzer, J. (2006). "Steel Fibers and Steel Fiber Reinforced Concrete in Civil Engineering." *The Pacific Journal of Science and Technology*, 7(1), 53-58.

Lee, S.-J., Yoo, D.-Y., and Moon, D.-Y. (2019). "Effects of Hooked-End Steel Fiber Geometry and Volume Fraction on the Flexural Behavior of Concrete Pedestrian Decks." *Applied Sciences*, 9(6), 1241.

Lindquist, W. D., Darwin, D., and Browning, J. P. (2005). *Cracking and Chloride Contents in Reinforced Concrete Bridge Decks*. Report KU-01-09, Kansas Department of Transportation, Lawrence, KS.

Marsh, D. (2015). "A New Twist on Optimization." *Concrete Products*, SEMCO Publishing, <http://www.concreteproducts.com/features/9371-a-new-twist-on-optimization.html#.WpOYQWaZPMJ> (Accessed Apr. 26, 2017).

Master Builders Solutions. (2016). "Shrinkage of Concrete." BASF Corporation, Cleveland, OH, <https://assets.master-builders-solutions.basf.com/en-us/shrinkage_of_concrete_ctif.pdf> (Accessed Mar. 26, 2020).

Mazzeo, B. A., Baxter, J., Barton, J., and Guthrie, W. S. (2017). "Vertical Impedance Measurements of Concrete Bridge Deck Cover Condition without a Direct Electrical Connection to the Reinforcing Steel." *AIP Conference Proceedings*, 1806(1).

Mehta, P. K., and Burrows, R. W. (2001). "Building Durable Structures in the 21st Century." *Concrete International*, 57-63, <https://citeseerx.ist.psu.edu/viewdoc/download?doi=10.1.1.475.5570&rep=rep1&type=pdf> (Accessed Aug. 27, 2020).

Mindess, S. F., Young, J. F., and Darwin, D. F. (2003). "Fiber Reinforced Concrete." *Concrete,* Second Edition, Prentice Hall, Upper Saddle River, NJ, 599-617.

Mishra, G. (2017). “Fiber Reinforced Concrete–Types, Properties and Advantages.” *The Constructor*, <https://theconstructor.org/concrete/fiber-reinforced-concrete/150/> (Accessed Jan. 17, 2020).

Naaman, A. E. (1976). “Pull-Out Mechanism in Steel Fiber-Reinforced Concrete.” *Journal of the Structural Division*, 102(8), 1537-1548.

NACE International. (2012). *Corrosion Control Plan for Bridges*. NACE International, Houston, TX, <https://www.roadsbridges.com/sites/rb/files/CorrosionControlPlanForBridges.pdf> (Accessed Aug. 27, 2020).

NACE International (undated). “Highways and Bridges – Corrosion Resources for Highways and Bridges.” NACE International, Houston, TX, <https://www.nace.org/resources/industries-nace-serves/highways-bridges> (Accessed Feb. 23, 2018).

Nataraja, M. C., Dhang, N., and Gupta, A. P. (1999). “Stress-Strain Curves for Steel-Fiber Reinforced Concrete under Compression.” *Cement and Concrete Composites*, 21(5-6), 383-390.

Pinkerton, L. R., Stecher, J. L., and Novak, J. (2013). “Twisted Steel Micro Reinforcement.” *Concrete International*, 35(10), 57-61.

Safiuddin, M., Kaish, A., Woon, C.-O., and Raman, S. (2018). “Early-Age Cracking in Concrete: Causes, Consequences, Remedial Measures, and Recommendations.” *Applied Sciences*, 8(10), 1730.

Schmitt, T. R., and Darwin, D. (1995). “Cracking in Concrete Bridge Decks.” University of Kansas, Center for Research, Lawrence, KS.

Shannag, M. J., Brincker, R., and Hansen, W. (1997). “Pullout Behavior of Steel Fibers from Cement-Based Composites.” *Cement and Concrete Research*, 27(6), 925-936.

Singh, H. (2017). *Steel Fiber Reinforced Concrete: Behavior, Modeling and Design.* Springer Science and Business Media, Singapore, 20-37.

Suryavanshi, A. K., Swamy, R. N., and McHugh, S. (1998). “Chloride Penetration into Reinforced Concrete Slabs.” *Canadian Journal of Civil Engineering*, 25(1), 87-95.

Vairagade, V. S., and Kene, K. S. (2012). “Introduction to Steel Fiber Reinforced Concrete on Engineering Performance of Concrete.” *International Journal of Scientific and Technology Research*, 1(4), 139-140.

Van Chanh, N. (2005). “Steel Fiber Reinforced Concrete.” <https://www.semanticscholar.org/paper/STEEL-FIBER-REINFORCED-CONCRETE-FIBER-Concrete/60001cca99b66f94d048e381ecb13b915dc09d08> (Accessed Jan. 15, 2020).

Voigt, G. F. (2002). “Early Cracking of Concrete Pavement: Causes and Repairs.” *Proceedings of the Federal Aviation Administration Airport Technology Transfer Conference*, <http://citeseerx.ist.psu.edu/viewdoc/download;jsessionid=AB984C9A9697A3C9356C70A2C574D742?doi=10.1.1.587.1150&rep=rep1&type=pdf> (Accessed Aug. 27, 2020).

Vondran, G. L. (1991). “Applications of Steel Fiber Reinforced Concrete.” *Concrete International*, 13(11), 44-49.

Wardhana, K., and Hadipriono, F. C. (2003). “Analysis of Recent Bridge Failures in the United States.” *Journal of Performance of Constructed Facilities*, 17(3), 144-150.

Wilson, C. (2013). “Using Micro-Reinforced Concrete.” *Insulated Concrete Form Builder Magazine*, <https://www.icfmag.com/articles/features/2013-11_Reinforced-Concrete.html> (Accessed Apr. 25, 2016).

Wu, H.-C. (1999). *Performance of Epoxy-Coated Reinforcement in Iowa Bridge Decks*.” M.S. thesis, Department of Civil, Construction, and Environmental Engineering, Iowa State University, Ames, IA.

Zatar, W. (2014). *Assessing the Service Life of Corrosion-Deteriorated Reinforced Concrete Member Highway Bridges in West Virginia*. College of Information Technology and Engineering, Marshall University, Huntington, WV, <https://rosap.ntl.bts.gov/view/dot/28036> (Accessed Aug. 27, 2020).

Zhou, S., Rizos, D. C., and Petrou, M. F. (2004). “Effects of Superstructure Flexibility on Strength of Reinforced Concrete Bridge Decks.” *Computers & Structures*, 82(1), 13-23.

APPENDIX A SENSOR, SAMPLING, AND TESTING LOCATIONS

Figures A-1 to A-8 show the location of the sensors installed in the bridge decks prior to construction. Figures A-9 to A-12 show the locations where concrete used for beam and cylindrical specimens was sampled during construction. Figures A-13 to A-16 show the approximate locations where concrete cover depth measurements, Schmidt rebound hammer testing, and chloride concentration sampling were performed. For chloride concentration testing, successive tests at a given location were performed 1 ft from the previous test, measured longitudinally in the direction of traffic.

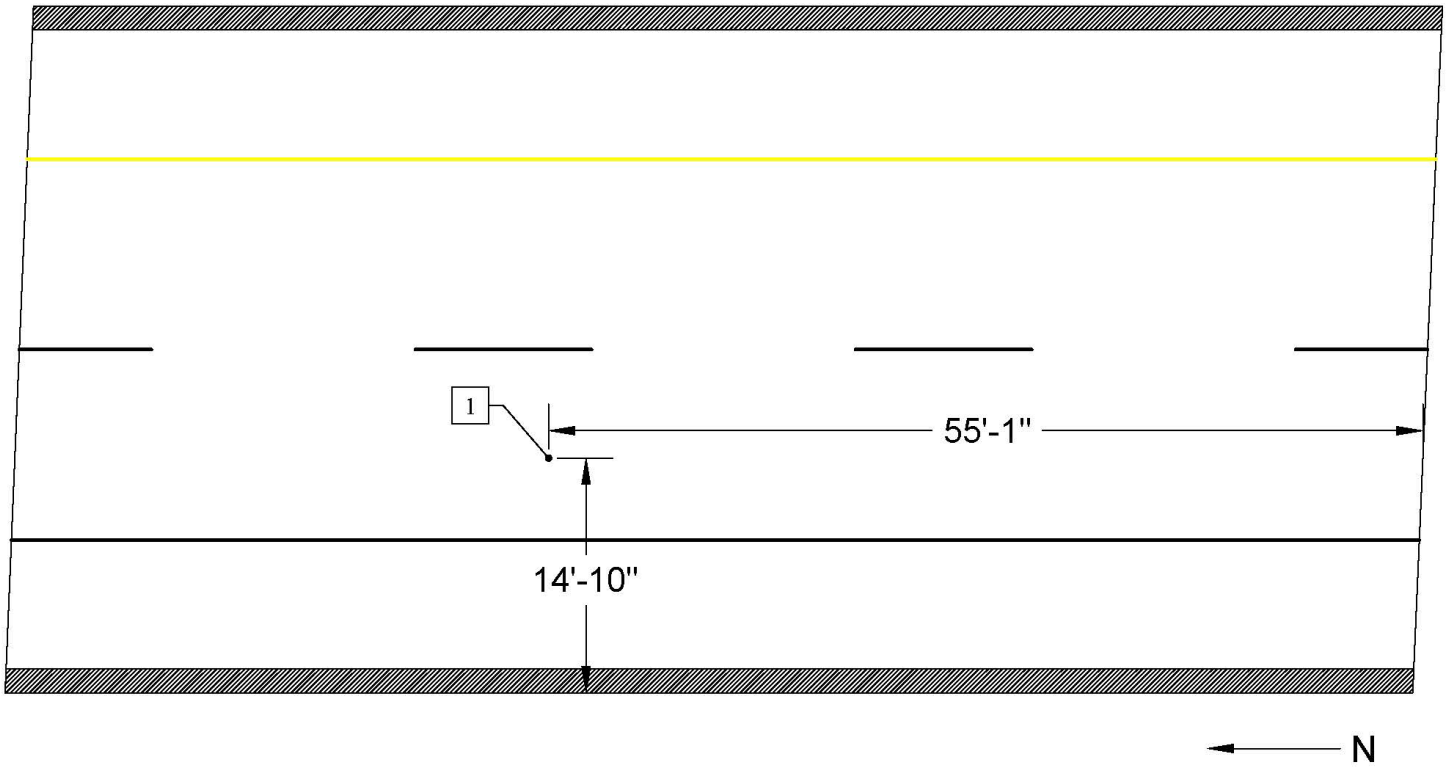

Figure A-1: Location of sensor installed in Upper Ridge Road SB deck.

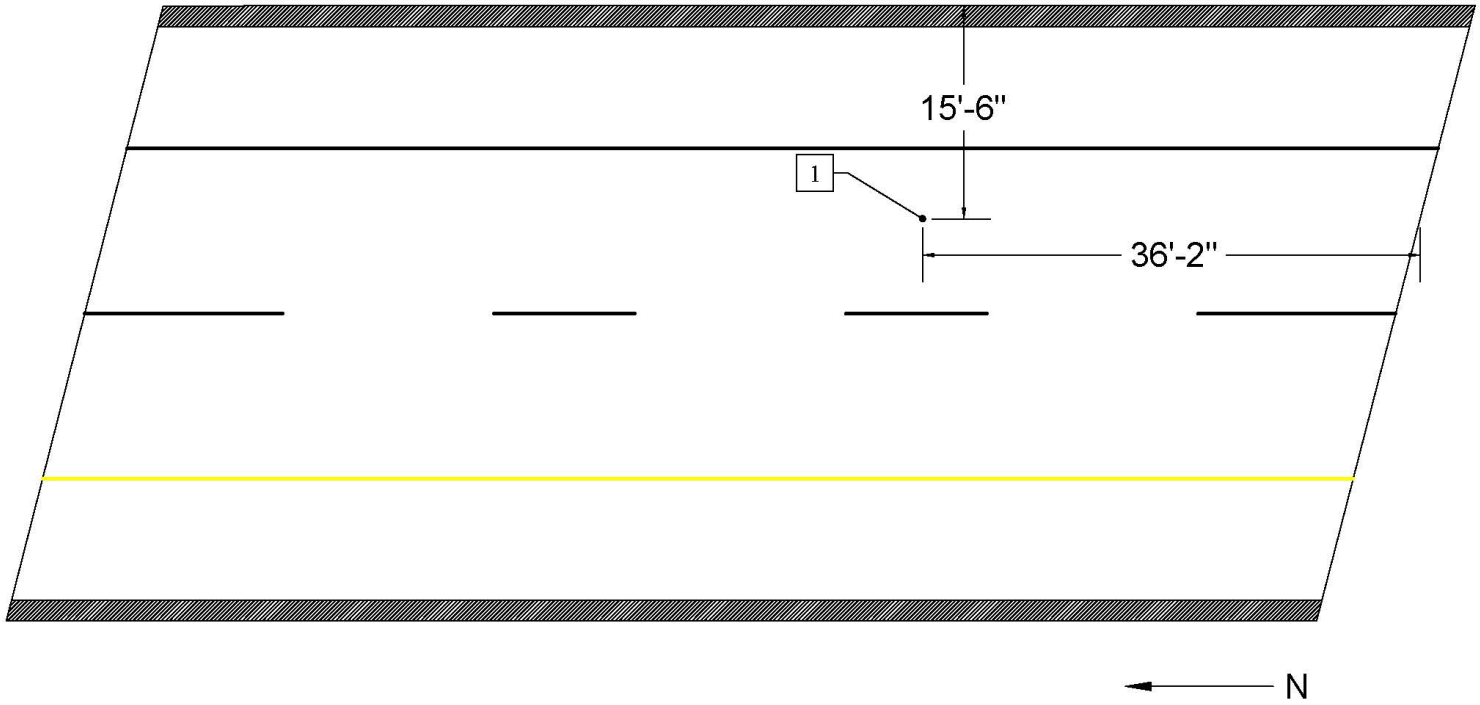

Figure A-2: Location of sensor installed in Upper Ridge Road NB deck.

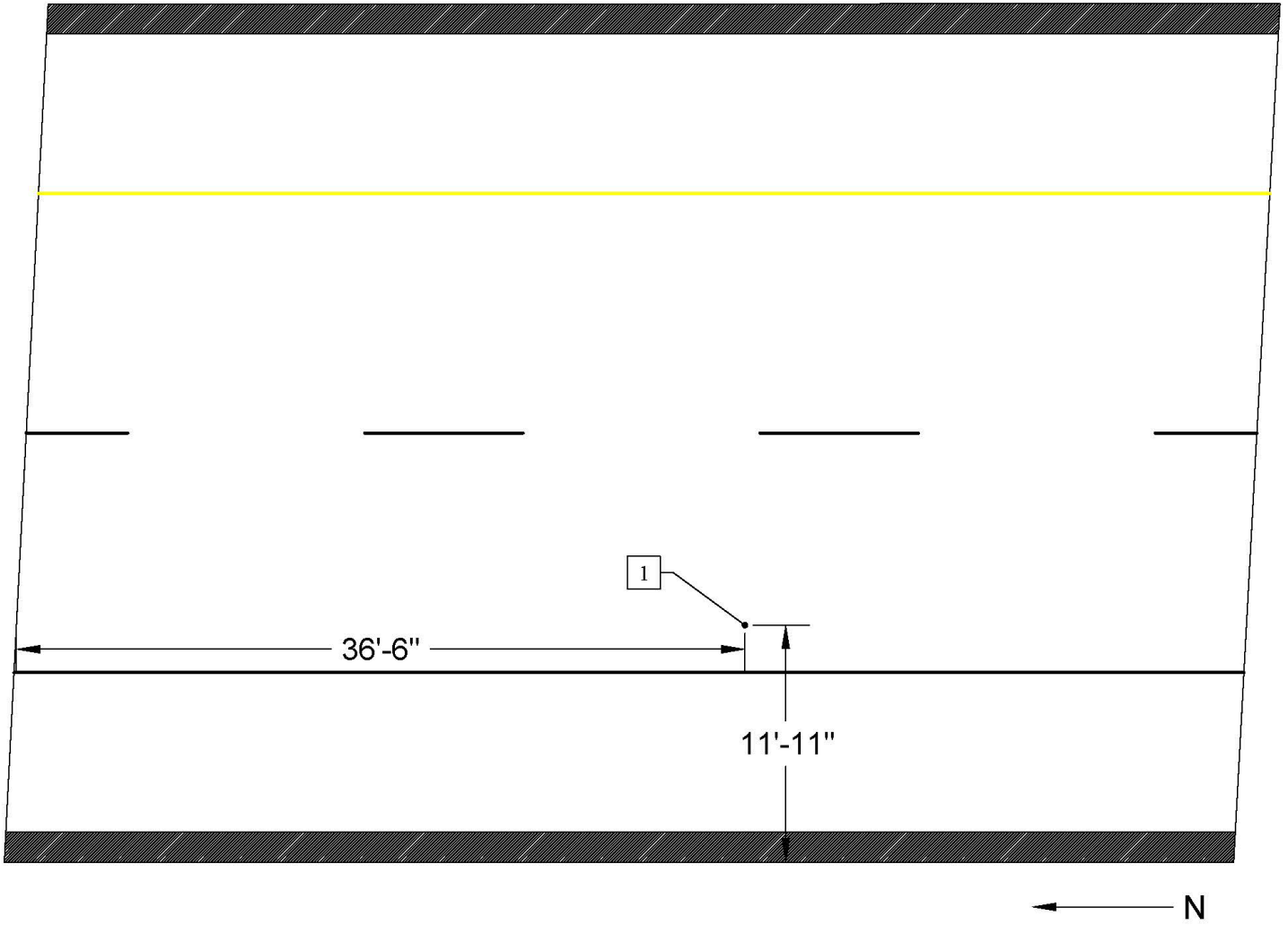

Figure A-3: Location of sensor installed in Wolverine Way SB deck.

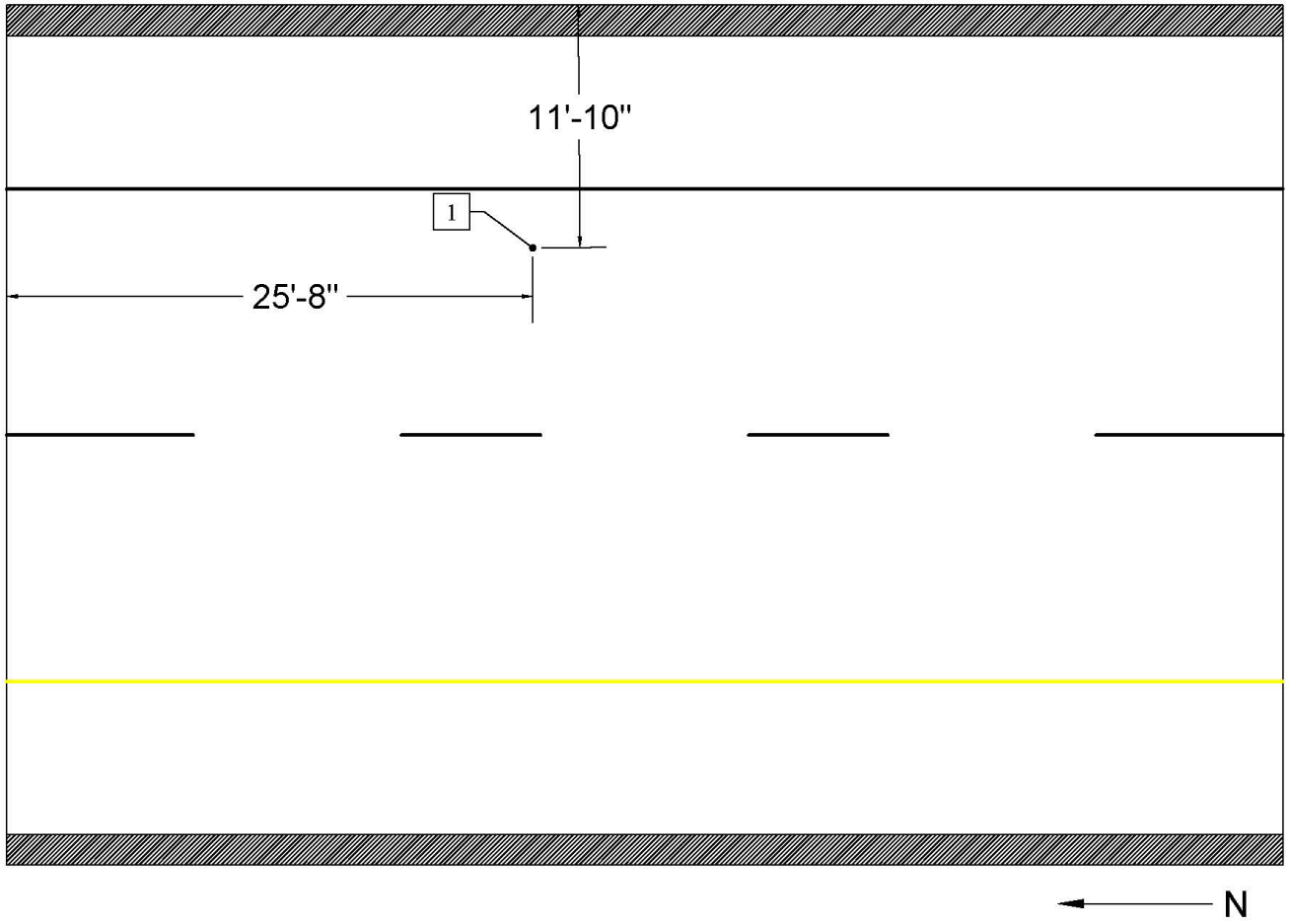

Figure A-4: Location of sensor installed in Wolverine Way NB deck.

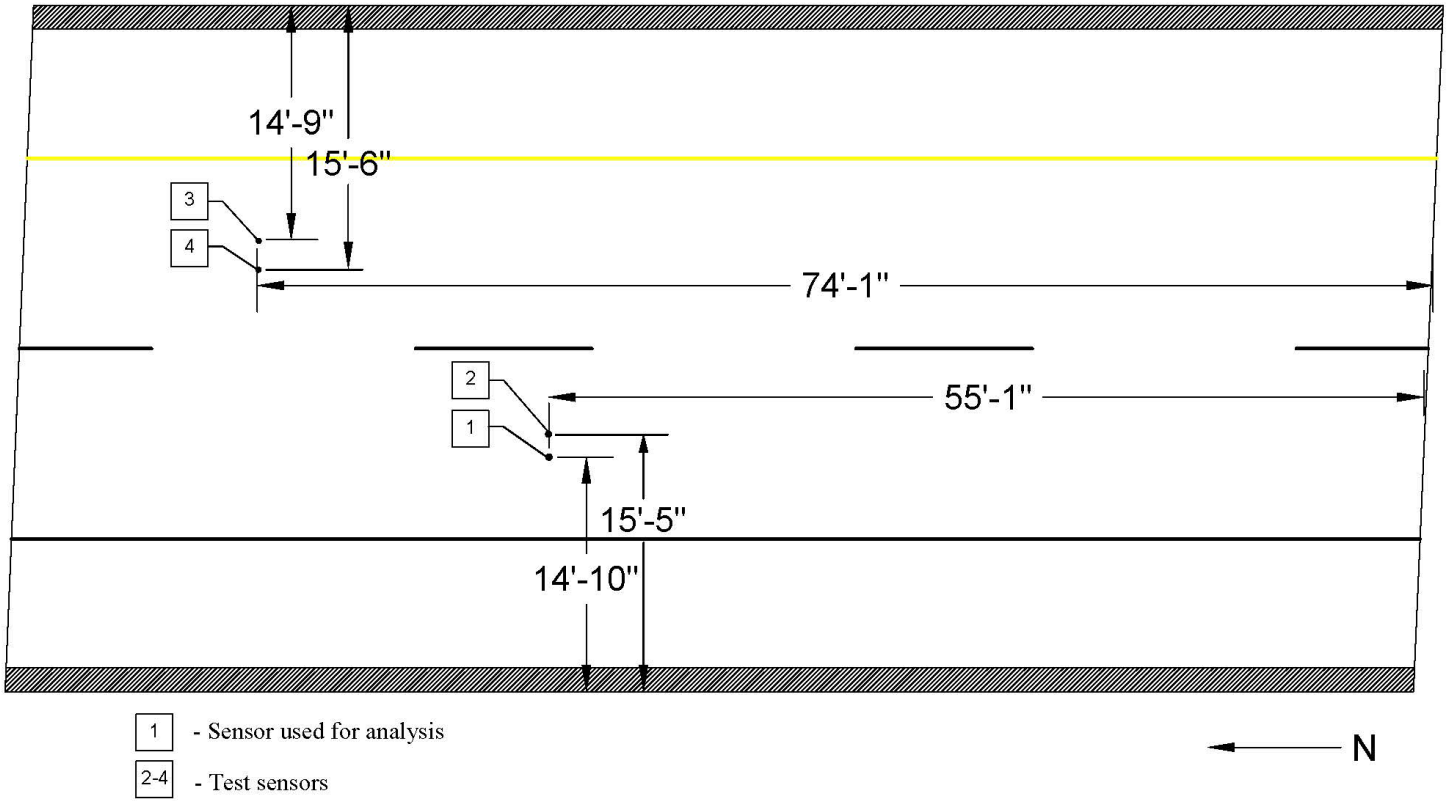

Figure A-5: Location of all sensors installed in Upper Ridge Road SB deck.

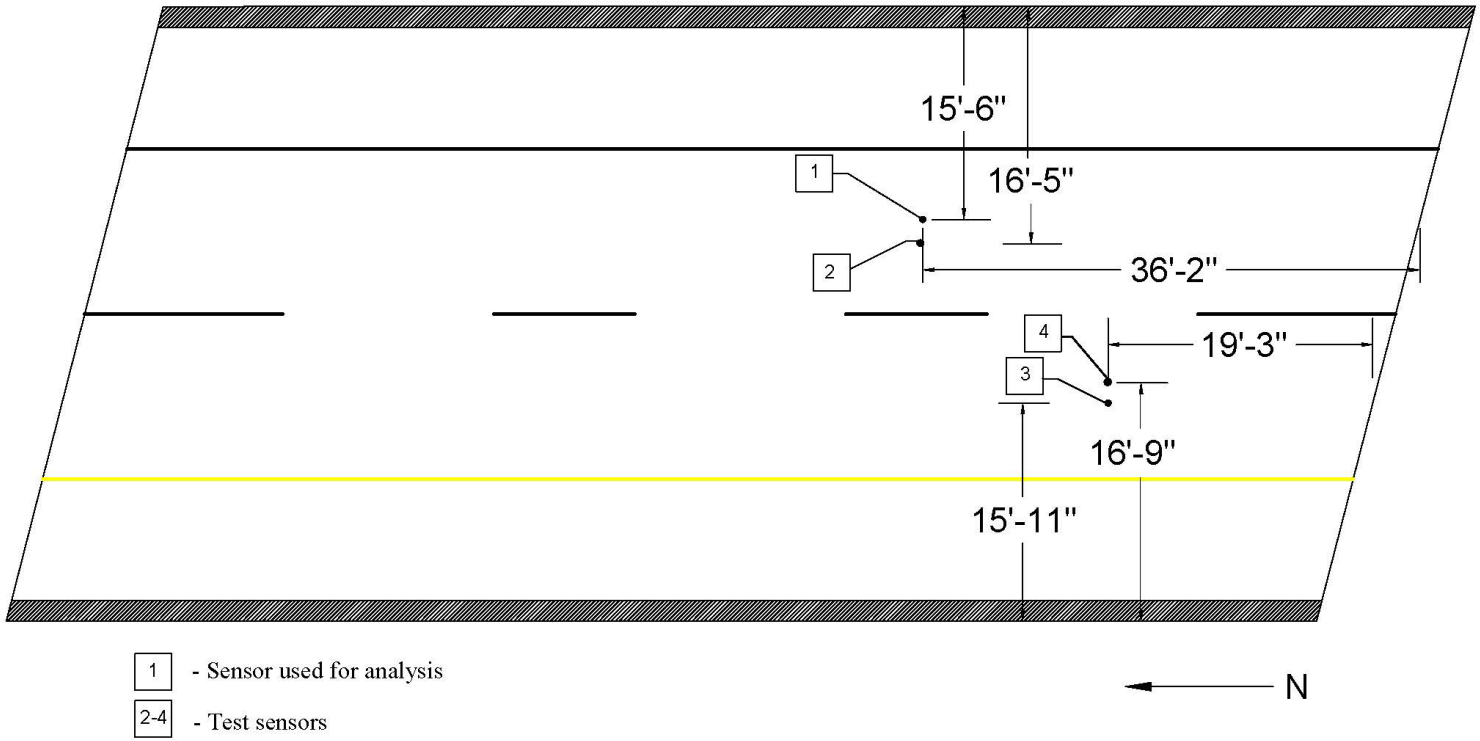

Figure A-6: Location of all sensors installed in Upper Ridge Road NB deck.

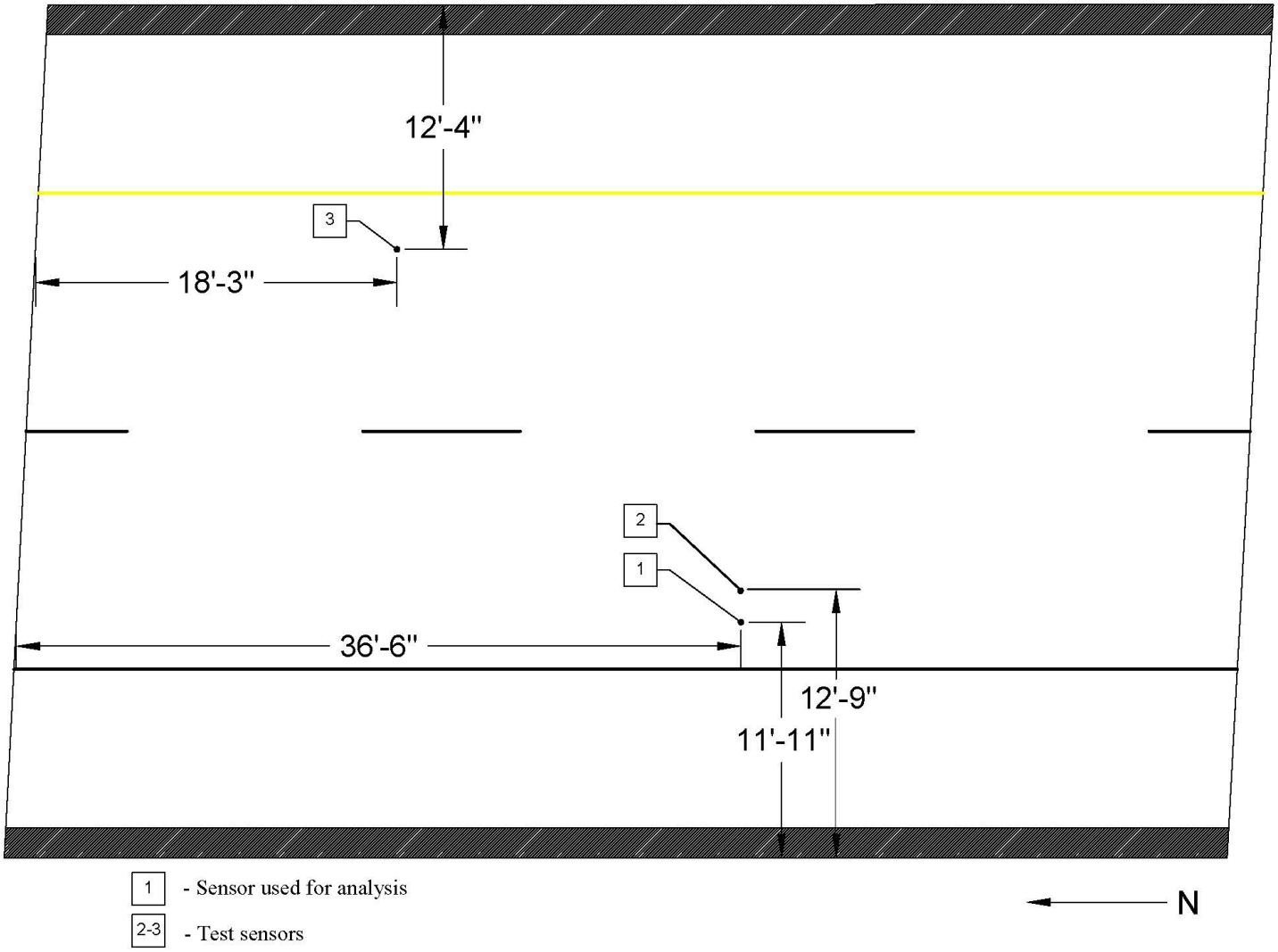

Figure A-7: Location of all sensors installed in Wolverine Way SB deck.

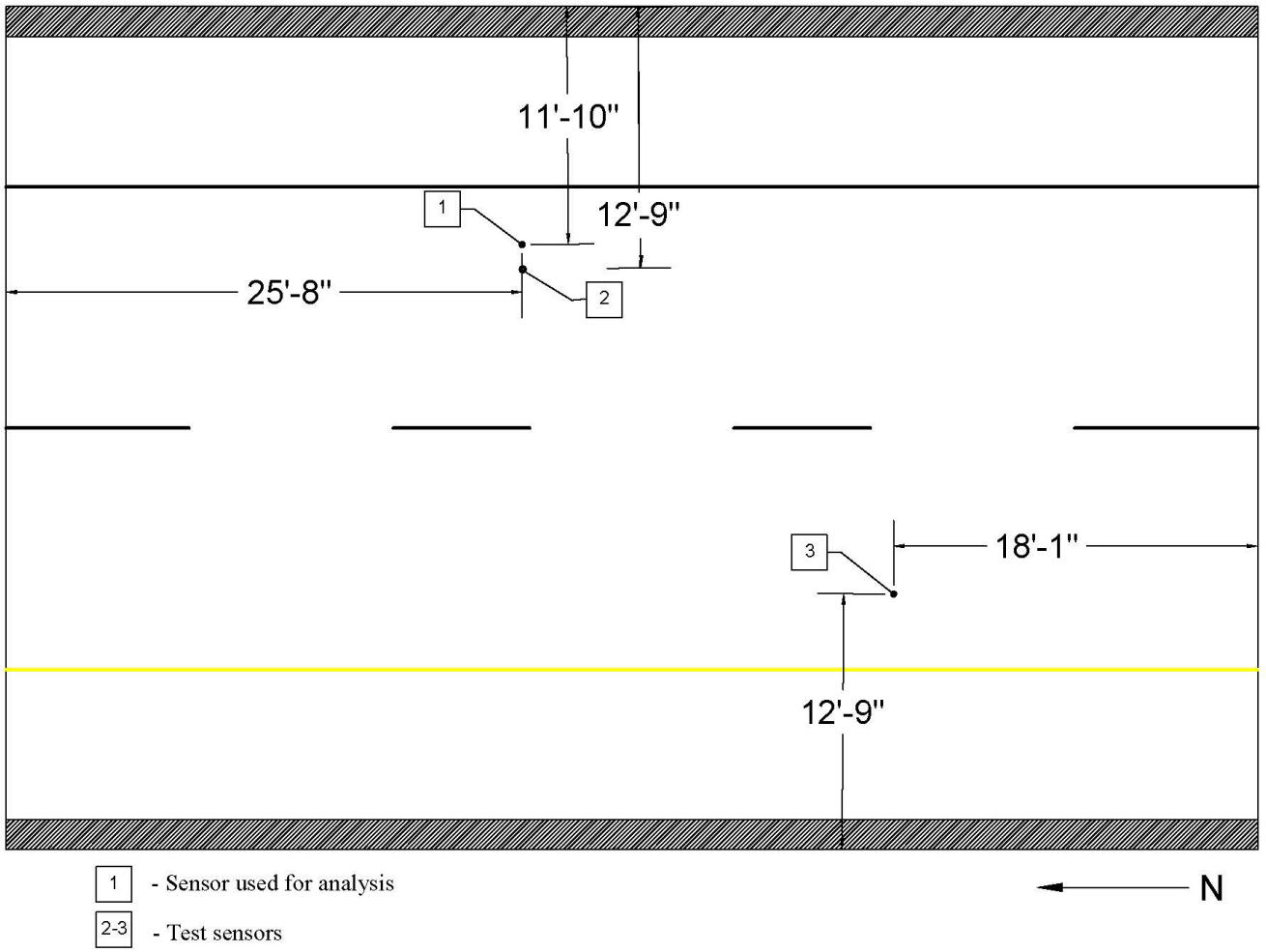

Figure A-8: Location of all sensors installed in Wolverine Way NB deck.

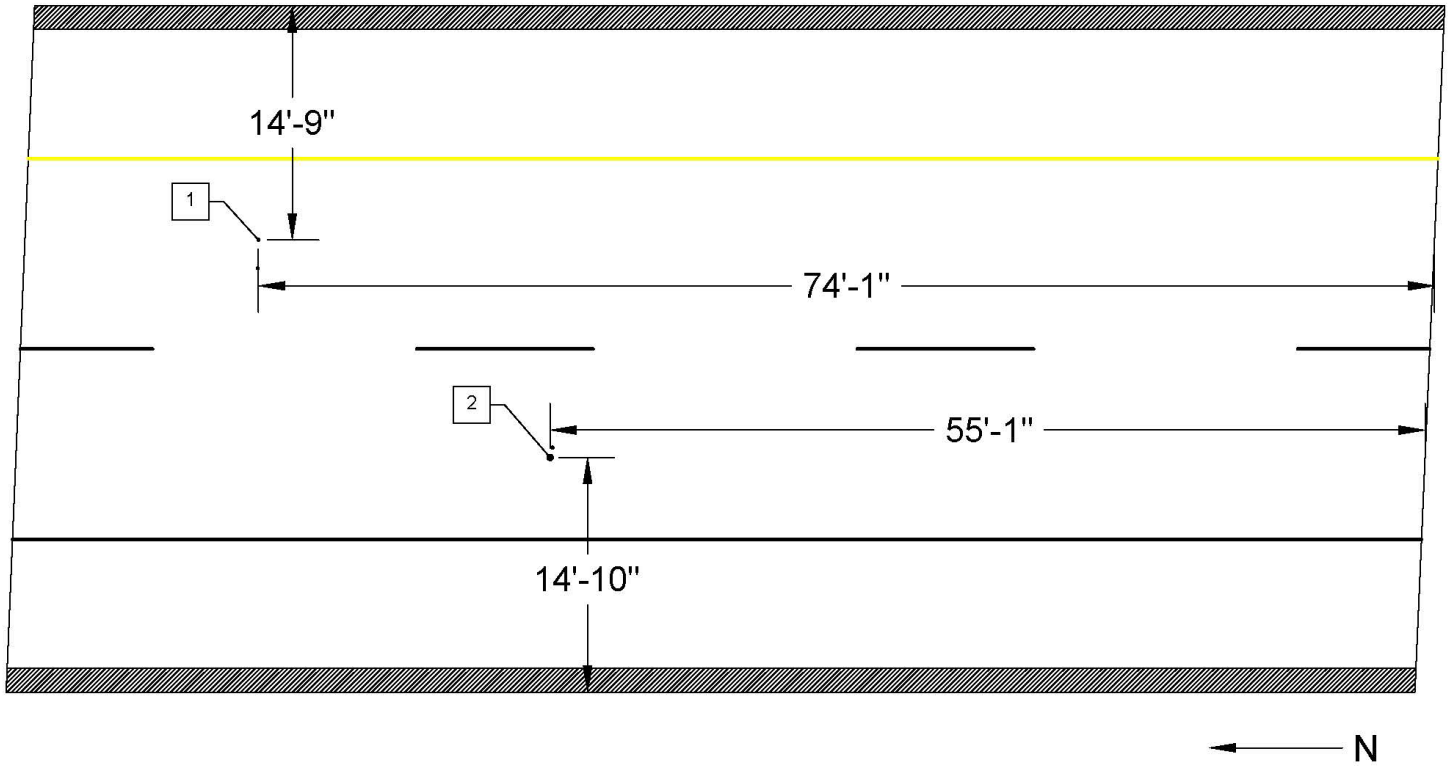

Figure A-9: Sampling locations for concrete collected for cylindrical and beam specimens for Upper Ridge Road SB deck.

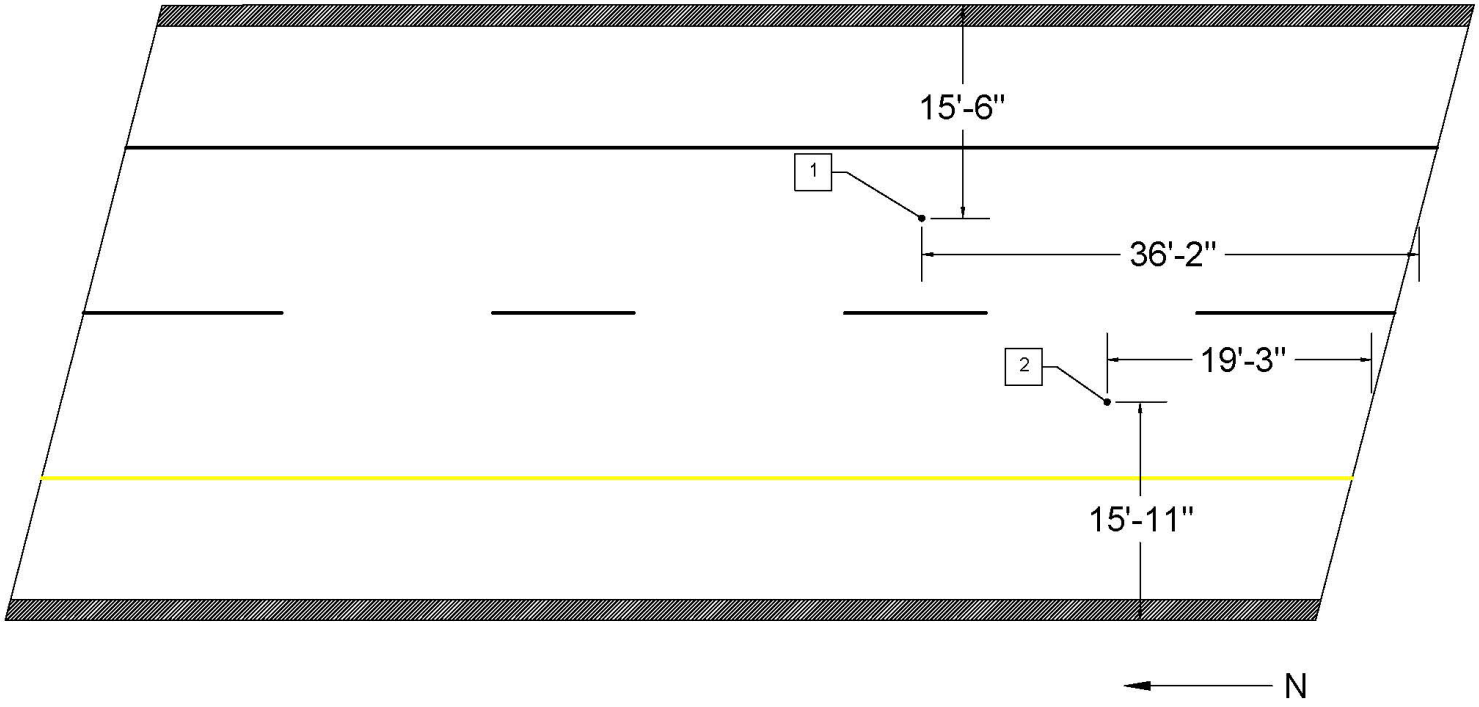

Figure A-10: Sampling locations for concrete collected for cylindrical and beam specimens for Upper Ridge Road NB deck.

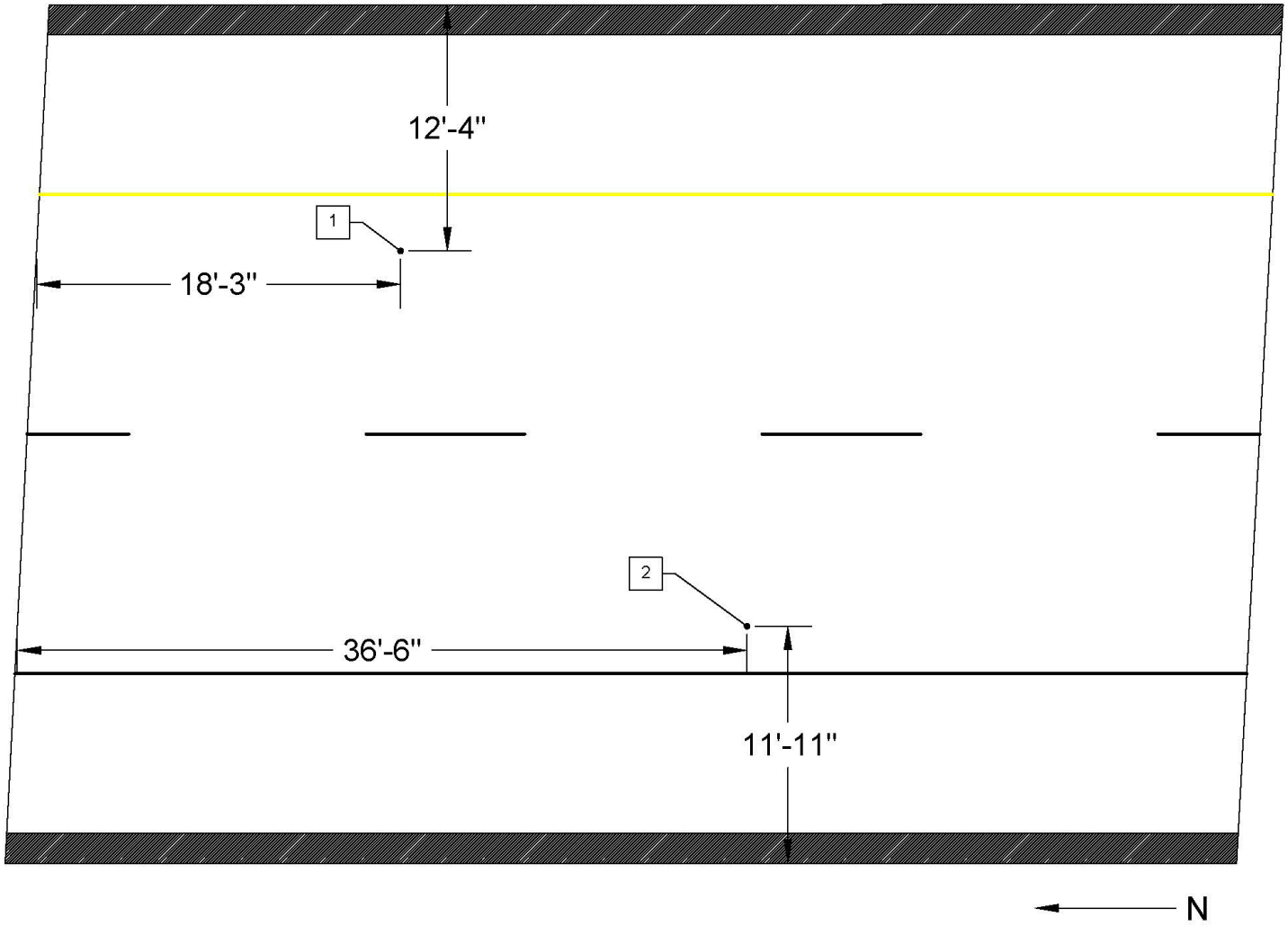

Figure A-11: Sampling locations for concrete collected for cylindrical and beam specimens for Wolverine Way SB deck.

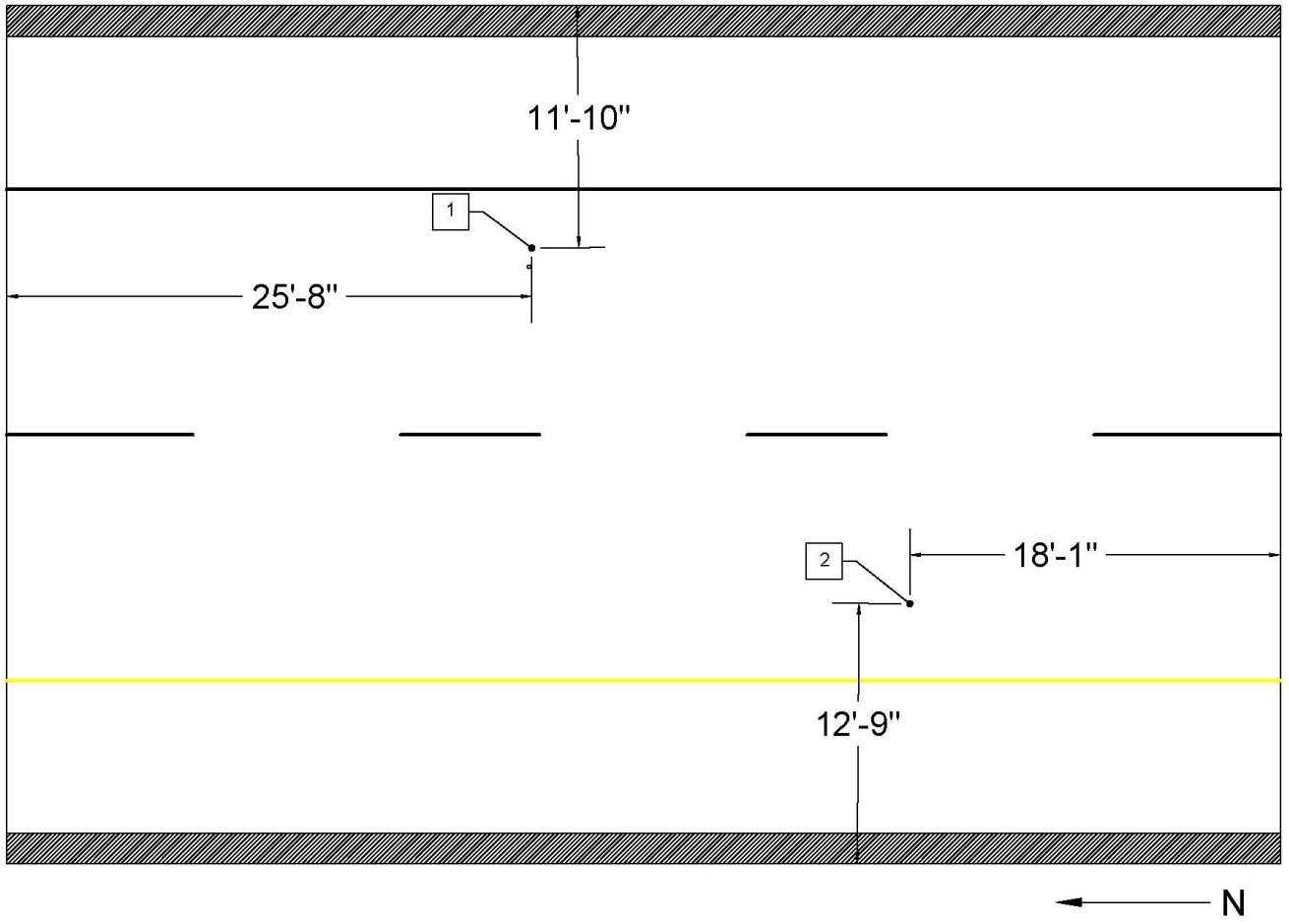

Figure A-12: Sampling locations for concrete collected for cylindrical and beam specimens for Wolverine Way NB deck.

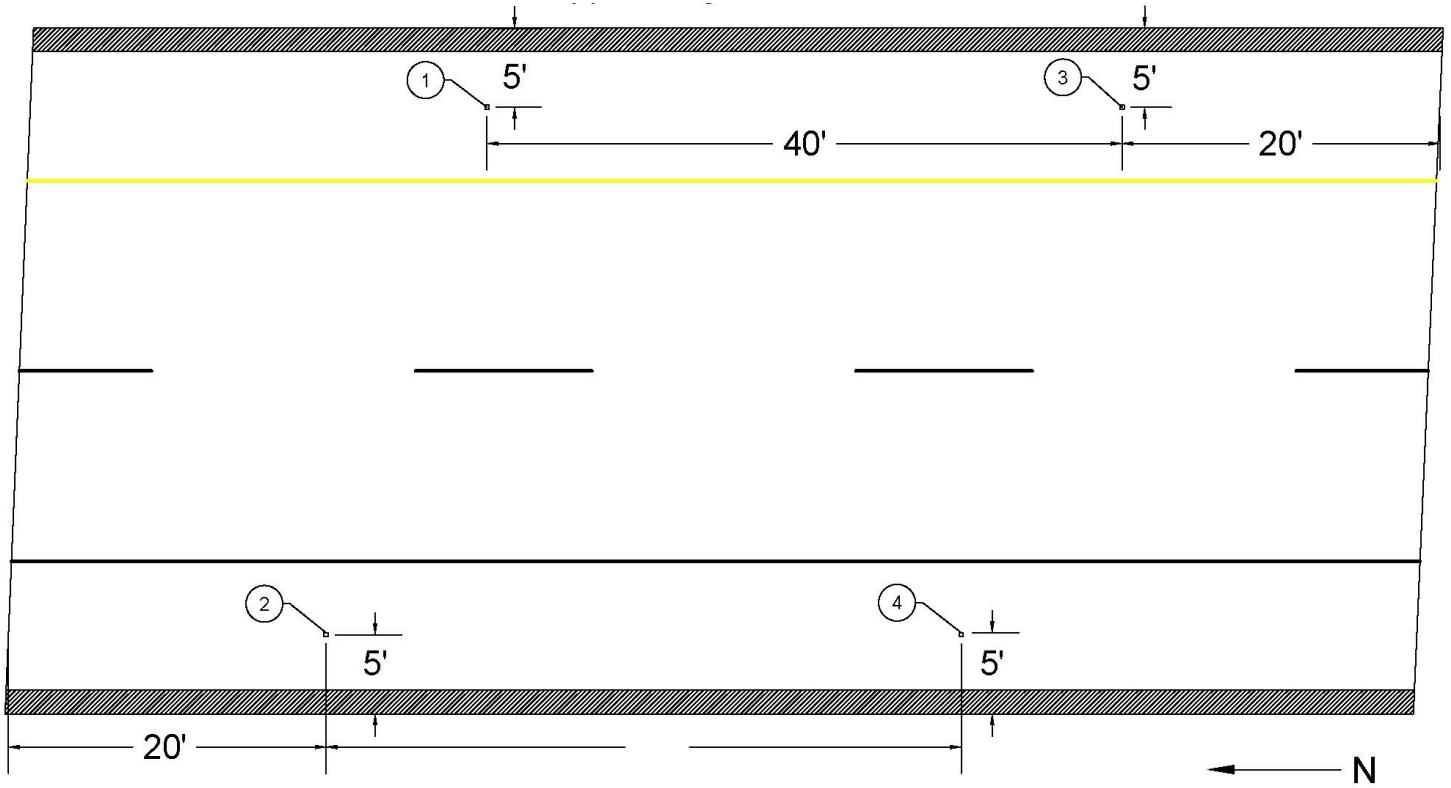

Figure A-13: Approximate locations for cover depth, Schmidt rebound hammer, and chloride concentration testing for Upper Ridge Road SB deck.

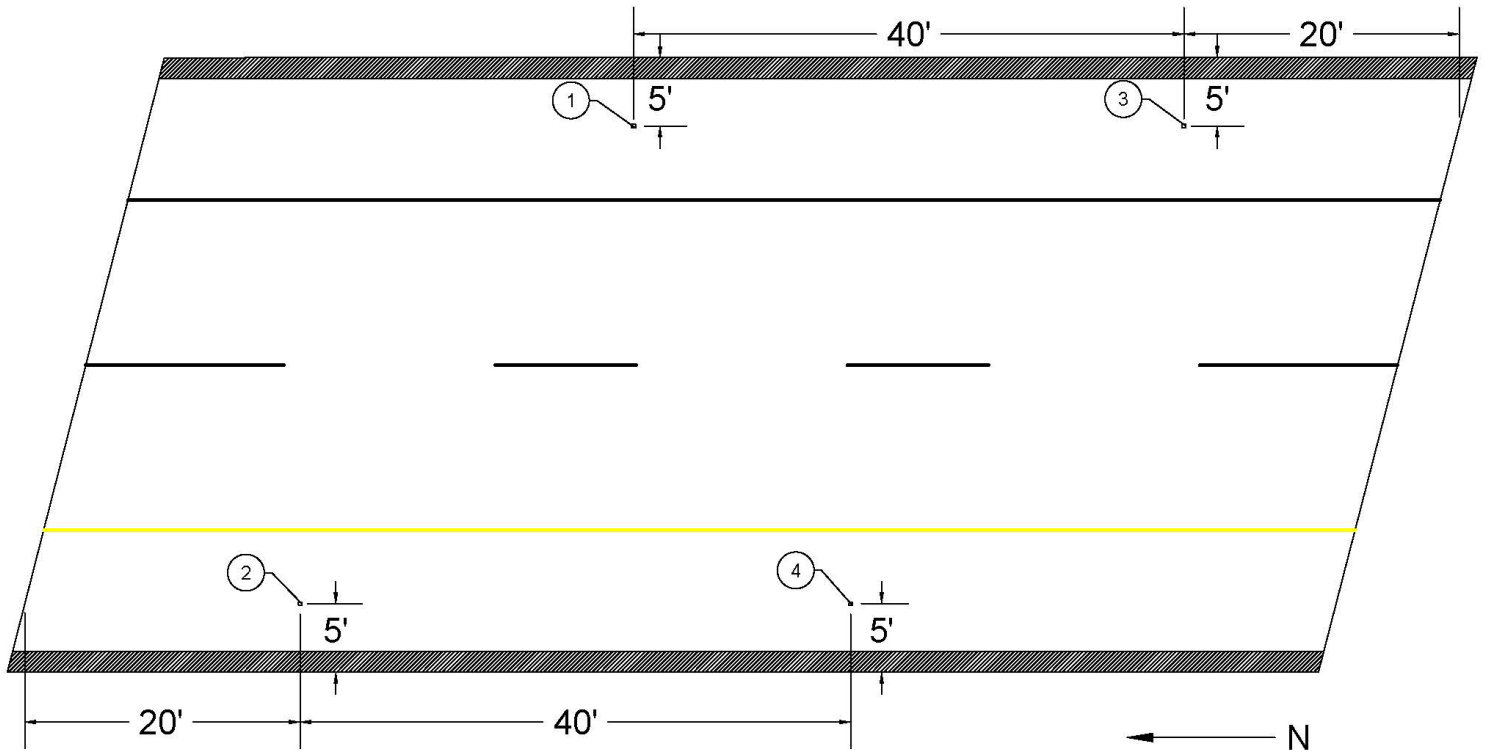

Figure A-14: Approximate locations for cover depth, Schmidt rebound hammer, and chloride concentration testing for Upper Ridge Road NB deck.

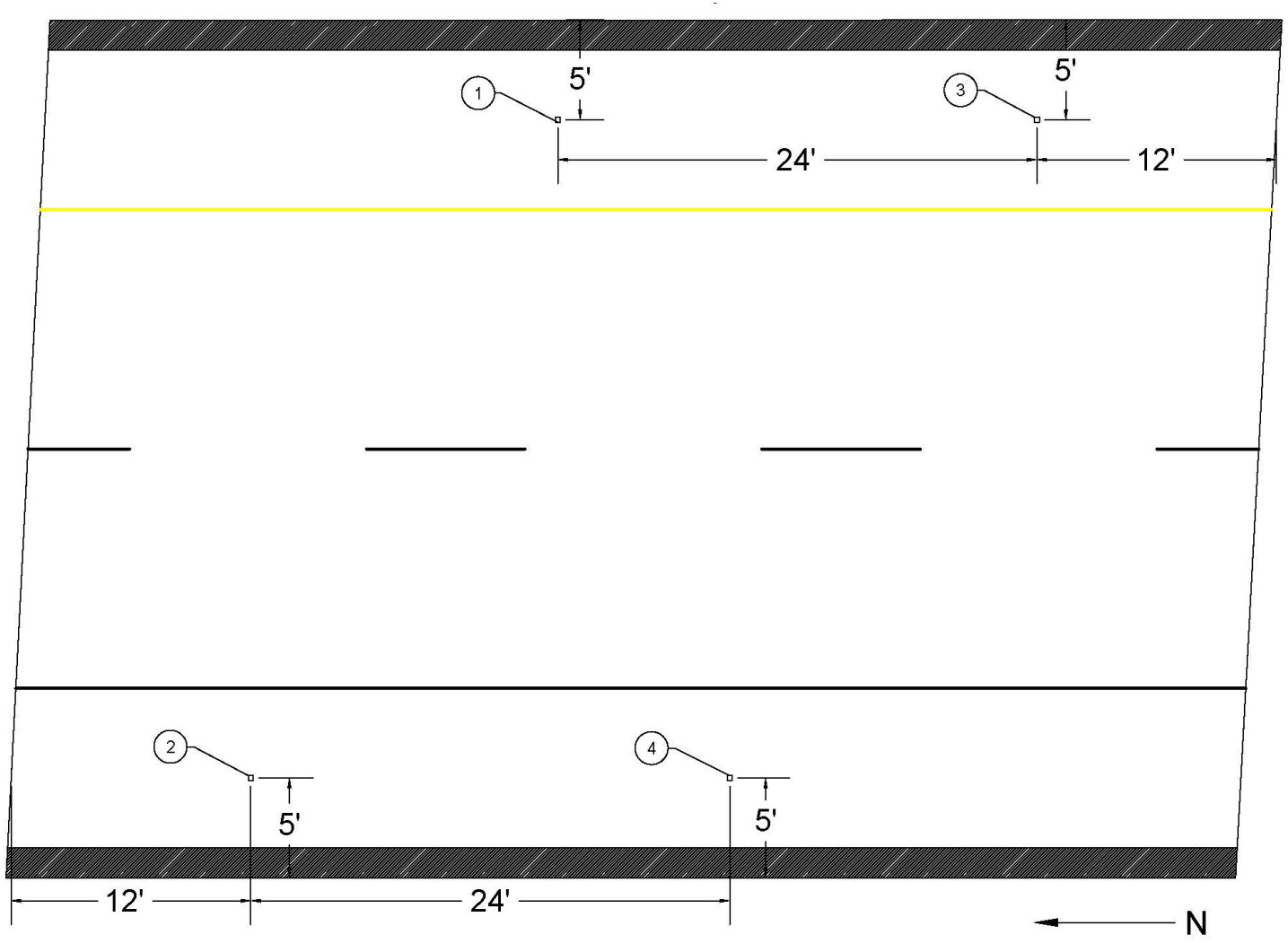

Figure A-15: Approximate locations for cover depth, Schmidt rebound hammer, and chloride concentration testing for Wolverine Way SB deck.

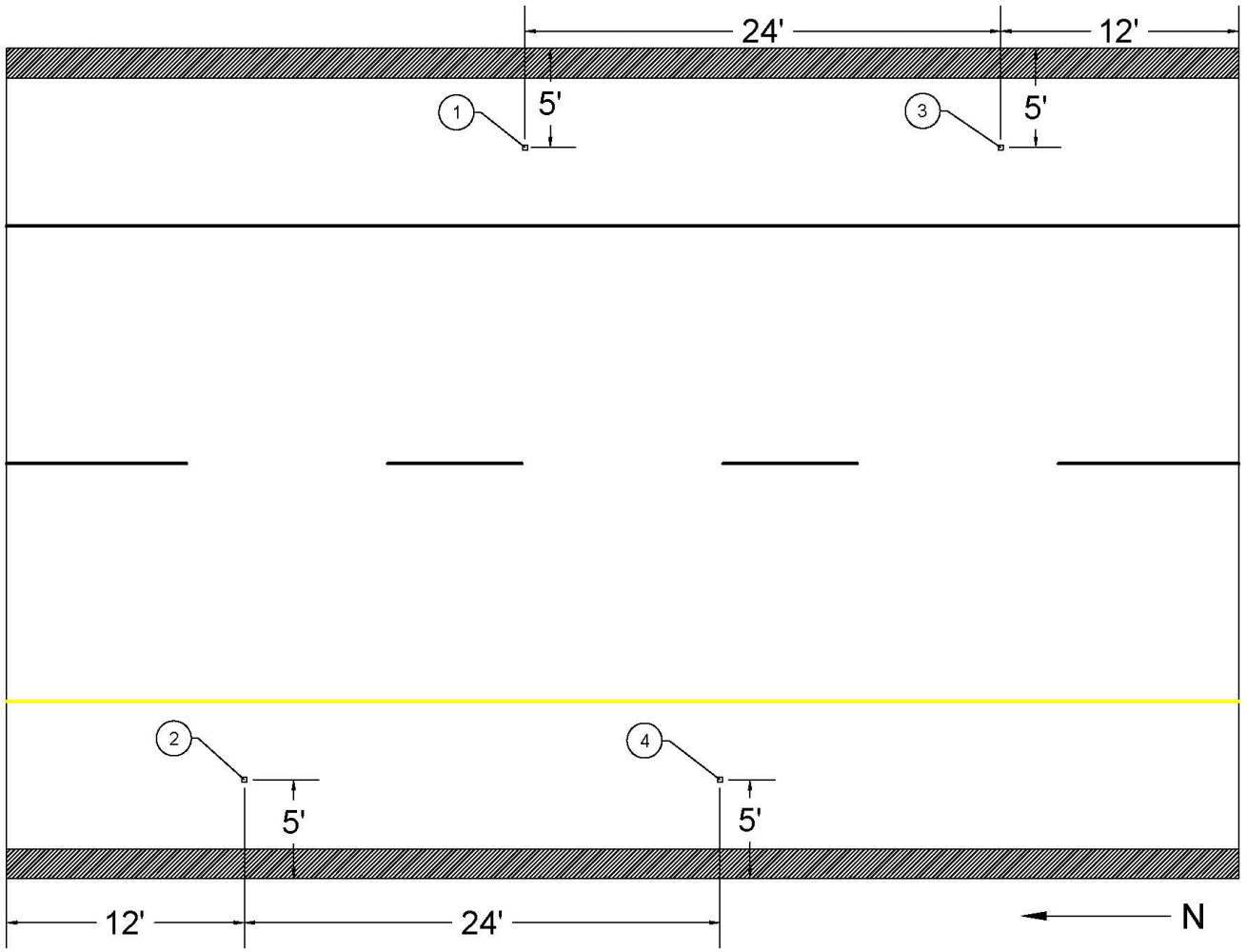

Figure A-16: Approximate locations for cover depth, Schmidt rebound hammer, and chloride concentration testing for Wolverine Way NB deck.

APPENDIX B SUPPORTING LABORATORY DATA

Tables B-1 gives an example of micrometer readings and corresponding shrinkage calculations. Table B-2 shows the results of electrical impedance testing. Table B-3 provides the results of compressive strength testing. Tables B-4 to B-7 give the properties of cylindrical specimens used for impedance and compressive strength testing. Table B-8 provides the results of flexural strength testing. Tables B-9 to B-11 provide the properties of beam specimens used for impedance and flexural strength testing. Table B-12 gives the results of splitting tensile strength testing, and Tables B-13 to B-16 provide the properties of specimens used for splitting tensile strength testing. Tables B-17 and B-18 show the calculated toughness of cylindrical and beam specimens, respectively.

Table B-1: Example of Shrinkage Readings and Calculations

Time	Micrometer Reading (mils)				Shrinkage (mils)			
	Upper Ridge Road NB Conventional		Upper Ridge Road SB TSMR		Upper Ridge Road NB Conventional		Upper Ridge Road SB TSMR	
	Specimen 1	Specimen 2	Specimen 1	Specimen 2	Specimen 1	Specimen 2	Specimen 1	Specimen 2
8/1/17 8:14	210.650	200.728	190.512	-78.130	0.591	0.709	0.177	0.079
8/1/17 13:57	210.650	200.728	190.512	-78.150	0.591	0.709	0.177	0.059
8/1/17 15:25	210.650	200.748	190.512	-78.150	0.591	0.728	0.177	0.059
8/1/17 18:10	210.630	200.728	190.492	-78.169	0.571	0.709	0.157	0.039
8/1/17 20:23	210.610	200.709	190.492	-78.169	0.551	0.689	0.157	0.039
8/1/17 21:20	210.669	200.748	190.512	-78.150	0.610	0.728	0.177	0.059
8/2/17 8:09	210.630	200.709	190.492	-78.169	0.571	0.689	0.157	0.039
8/2/17 10:16	210.630	200.709	190.492	-78.150	0.571	0.689	0.157	0.059
8/2/17 17:24	210.610	200.689	190.492	-78.169	0.551	0.669	0.157	0.039
8/2/17 17:45	210.650	200.728	190.512	-78.150	0.591	0.709	0.177	0.059
8/2/17 20:12	210.610	200.689	190.472	-78.169	0.551	0.669	0.138	0.039
8/3/17 8:13	210.610	200.669	190.472	-78.169	0.551	0.650	0.138	0.039
8/3/17 13:30	210.591	200.669	190.472	-78.169	0.531	0.650	0.138	0.039
8/3/17 14:00	210.591	200.650	190.472	-78.189	0.531	0.630	0.138	0.020
8/3/17 15:25	210.610	200.669	190.472	-78.169	0.551	0.650	0.138	0.039
8/3/17 17:23	210.610	200.689	190.492	-78.169	0.551	0.669	0.157	0.039
8/3/17 19:35	210.650	200.709	190.512	-78.150	0.591	0.689	0.177	0.059
8/4/17 8:44	210.571	200.630	190.472	-78.189	0.512	0.610	0.138	0.020
8/4/17 9:15	210.591	200.650	190.472	-78.189	0.531	0.630	0.138	0.020
8/4/17 9:22	210.610	200.650	190.492	-78.189	0.551	0.630	0.157	0.020
8/4/17 11:11	210.630	200.669	190.492	-78.169	0.571	0.650	0.157	0.039
8/4/17 14:06	210.591	200.650	190.472	-78.189	0.531	0.630	0.138	0.020
8/4/17 17:55	210.591	200.650	190.492	-78.189	0.531	0.630	0.157	0.020
8/4/17 20:18	210.571	200.630	190.472	-78.209	0.512	0.610	0.138	0.000
8/4/17 22:07	210.571	200.610	190.453	-78.209	0.512	0.591	0.118	0.000
8/5/17 8:03	210.571	200.610	190.472	-78.209	0.512	0.591	0.138	0.000
8/5/17 13:08	210.571	200.630	190.472	-78.189	0.512	0.610	0.138	0.020
8/5/17 17:29	210.551	200.591	190.453	-78.209	0.492	0.571	0.118	0.000
8/6/17 13:09	210.551	200.571	190.453	-78.228	0.492	0.551	0.118	-0.020
8/6/17 19:57	210.531	200.551	190.433	-78.248	0.472	0.531	0.098	-0.039
8/7/17 11:54	210.512	200.531	190.413	-78.268	0.453	0.512	0.079	-0.059
8/7/17 12:45	210.512	200.531	190.413	-78.268	0.453	0.512	0.079	-0.059
8/7/17 20:24	210.492	200.512	190.413	-78.287	0.433	0.492	0.079	-0.079
8/8/17 8:05	210.531	200.512	190.413	-78.268	0.472	0.492	0.079	-0.059
8/8/17 12:58	210.453	200.472	190.374	-78.307	0.394	0.453	0.039	-0.098
8/8/17 13:53	210.472	200.472	190.374	-78.307	0.413	0.453	0.039	-0.098
8/8/17 20:39	210.472	200.472	190.374	-78.307	0.413	0.453	0.039	-0.098
8/9/17 8:30	210.413	200.413	190.335	-78.346	0.354	0.394	0.000	-0.138
8/9/17 13:01	210.433	200.433	190.354	-78.346	0.374	0.413	0.020	-0.138
8/9/17 14:07	210.492	200.492	190.394	-78.307	0.433	0.472	0.059	-0.098
8/9/17 15:23	210.472	200.453	190.374	-78.327	0.413	0.433	0.039	-0.118

Table B-2: Electrical Impedance

Bridge Location	Sample Location	Electrical Impedance (10^x Ohms)						
		Beam Specimens			Cylindrical Specimens			
		28 Days	3 Months	1 Year	28 Days	3 Months	1 Year	2 Years
Upper Ridge Road SB	1	3.675	4.497	5.263	3.806	4.967	6.174	4.334
TSMR	2	3.563	4.338	5.226	3.783	4.671	6.055	6.565
Wolverine Way NB	1	3.737	4.344	6.544	3.946	4.531	6.475	6.129
TSMR	2	3.767	4.295	6.467	3.868	4.573	6.472	6.430
Upper Ridge Road NB	1	3.800	4.737	5.485	3.800	5.004	6.176	6.515
Conventional	2	3.625	4.955	5.648	3.738	5.280	6.223	5.100
Wolverine Way SB	1	4.281	4.511	6.492	4.186	4.616	6.390	6.119
Conventional	2	3.889	4.574	6.467	4.093	4.612	6.482	5.486

Table B-3: Compressive Strength and Corresponding Strain of Cylindrical Specimens

Bridge Location	Sample Location	Compressive Strength (psi)				Corresponding Strain (in./in.)			
		28 Days	3 Months	1 Year	2 Years	28 Days	3 Months	1 Year	2 Years
Upper Ridge Road SB	1	4039	5061	5071	4325	0.0068	0.0077	0.0072	0.0100
TSMR	2	4479	5547	5357	5484	0.0079	0.0067	0.0073	0.0096
Wolverine Way NB	1	5377	5852	6396	5654	0.0081	0.0098	0.0075	0.0057
TSMR	2	4875	5448	3974	4593	0.0082	0.0091	0.0082	0.0077
Upper Ridge Road NB	1	3963	5897	5896	5427	0.0079	0.0075	0.0072	0.0105
Conventional	2	4312	5215	5011	4698	0.0073	0.0073	0.0078	0.0079
Wolverine Way SB	1	5887	6585	6569	5326	0.0091	0.0093	0.0084	0.0054
Conventional	2	5022	5685	5553	5328	0.0087	0.0095	0.0080	0.0065

Table B-4: Properties of Specimens for Electrical Impedance and Compressive Strength Testing at 28 Days

Bridge Location	Sample Location	Length (in.)					Diameter (in.)					Weight (lb)	Density (lb/ft^3)
		1	2	3	4	Avg.	1	2	3	4	Avg.		
Upper Ridge Road SB	1	8.034	8.054	8.047	8.035	8.042	4.033	4.043	4.006	4.002	4.021	8.080	136.7
TSMR	2	8.106	8.032	8.031	8.038	8.051	4.036	4.024	4.002	3.990	4.013	8.103	137.5
Wolverine Way NB	1	8.040	8.044	8.052	8.052	8.047	4.006	3.994	4.035	4.020	4.013	8.184	138.9
TSMR	2	8.063	8.052	8.085	8.062	8.066	4.045	4.034	4.040	4.014	4.033	8.082	135.5
Upper Ridge Road NB	1	8.042	8.044	8.047	8.044	8.044	4.041	4.040	4.006	3.998	4.021	8.337	141.0
Conventional	2	8.116	8.129	8.119	8.100	8.116	4.049	4.040	3.985	4.000	4.018	8.235	138.3
Wolverine Way SB	1	8.031	8.063	8.000	8.031	8.031	3.994	3.991	4.025	4.036	4.011	8.296	141.3
Conventional	2	8.000	8.031	8.031	8.000	8.016	3.991	4.002	4.033	4.030	4.014	8.149	138.8

Table B-5: Properties of Specimens for Electrical Impedance and Compressive Strength Testing at 3 Months

Bridge Location	Sample Location	Length (in.)					Diameter (in.)					Weight (lb)	Density (lb/ft^3)
		1	2	3	4	Avg.	1	2	3	4	Avg.		
Upper Ridge Road SB	1	8.031	8.000	8.000	8.031	8.016	4.055	4.041	4.010	4.010	4.029	7.975	134.9
TSMR	2	8.031	8.031	8.000	8.000	8.016	4.074	4.033	3.997	3.994	4.024	8.163	138.4
Wolverine Way NB	1	8.125	8.031	8.000	8.000	8.039	3.993	3.996	4.013	4.065	4.017	8.233	139.7
TSMR	2	8.031	8.000	7.969	8.000	8.000	4.016	4.003	4.037	4.025	4.020	8.088	137.6
Upper Ridge Road NB	1	7.969	8.000	7.969	7.969	7.977	4.039	4.039	4.050	3.987	4.029	8.163	138.7
Conventional	2	8.000	8.063	8.000	7.969	8.008	4.047	4.038	4.017	4.004	4.026	8.092	137.2
Wolverine Way SB	1	8.000	8.000	8.031	8.031	8.016	3.993	3.989	4.023	4.030	4.009	8.221	140.4
Conventional	2	8.031	8.031	8.000	8.031	8.023	3.992	3.988	4.034	4.024	4.009	8.030	137.0

Table B-6: Properties of Specimens for Electrical Impedance and Compressive Strength Testing at 1 Year

Bridge Location	Sample Location	Length (in.)					Diameter (in.)					Weight (lb)	Density (lb/ft^3)
		1	2	3	4	Avg.	1	2	3	4	Avg.		
Upper Ridge Road SB	1	8.031	8.031	8.031	8.000	8.023	4.033	4.047	4.002	4.017	4.025	7.966	134.9
TSMR	2	7.969	8.031	8.000	8.000	8.000	4.054	4.040	4.009	4.003	4.027	8.058	136.7
Wolverine Way NB	1	8.000	7.938	8.031	8.031	8.000	4.056	4.000	4.023	4.042	4.030	8.107	137.3
TSMR	2	8.000	8.000	8.000	8.000	8.000	4.024	4.003	4.022	4.034	4.021	7.945	135.2
Upper Ridge Road NB	1	8.000	8.000	8.094	8.063	8.039	4.067	4.043	4.038	4.011	4.040	8.207	137.7
Conventional	2	8.063	8.000	8.063	8.031	8.039	4.024	4.027	4.021	4.008	4.020	7.998	135.5
Wolverine Way SB	1	8.000	8.000	8.000	8.000	8.000	4.010	4.003	4.052	4.010	4.019	8.194	139.5
Conventional	2	8.000	8.000	8.000	8.000	8.000	4.017	4.003	4.037	4.028	4.021	7.966	135.5

Table B-7: Properties of Specimens for Electrical Impedance and Compressive Strength Testing at 2 Years

Bridge Location	Sample Location	Length (in.)					Diameter (in.)					Weight (lb)	Density (lb/ft^3)
		1	2	3	4	Avg.	1	2	3	4	Avg.		
Upper Ridge Road SB	1	8.060	8.070	8.081	8.097	8.077	4.126	4.084	4.184	4.021	4.103	7.964	128.8
TSMR	2	8.004	8.009	8.019	8.006	8.009	4.008	4.042	3.991	4.001	4.010	7.989	136.5
Wolverine Way NB	1	8.055	8.070	8.046	8.042	8.053	3.994	4.018	4.029	4.037	4.019	8.153	137.9
TSMR	2	8.014	8.035	8.018	8.023	8.022	4.025	4.019	4.033	4.032	4.027	7.937	134.2
Upper Ridge Road NB	1	8.044	8.035	8.043	8.070	8.048	4.032	4.036	4.002	4.000	4.017	8.111	137.4
Conventional	2	8.042	8.064	8.084	8.033	8.056	4.031	4.016	4.000	4.003	4.012	8.044	136.5
Wolverine Way SB	1	8.064	8.066	8.074	8.066	8.067	3.997	4.004	4.033	4.017	4.013	8.104	137.3
Conventional	2	8.127	8.111	8.120	8.129	8.122	4.024	4.003	4.042	4.030	4.024	7.985	133.6

Table B-8: Flexural Strength and Corresponding Deflection of Beam Specimens

Bridge Location	Sample Location	Flexural Strength (psi)			Corresponding Deflection (in.)		
		28 Days	3 Months	1 Year	28 Days	3 Months	1 Year
Upper Ridge Road SB	1	541	792	852	0.0530	0.0659	0.0668
TSMR	2	613	864	1015	0.0609	0.0566	0.0721
Wolverine Way NB	1	753	684	1007	0.0753	0.0701	0.0719
TSMR	2	628	738	831	0.0601	0.0732	0.0694
Upper Ridge Road NB	1	533	768	993	0.0602	0.0474	0.0717
Conventional	2	611	834	953	0.0700	0.0524	0.0643
Wolverine Way SB	1	676	657	965	0.0567	0.0704	0.0719
Conventional	2	631	678	788	0.0650	0.0910	0.0602

Table B-9: Properties of Specimens for Electrical Impedance and Flexural Strength Testing at 28 Days

Bridge Location	Sample Location	Length (in.)					Height (in.)			Width (in.)			Weight (lb)	Density (lb/ft^3)
		1	2	3	4	Avg.	1	2	Avg.	1	2	Avg.		
Upper Ridge Road SB	1	20.031	20.000	20.031	20.063	20.031	6.035	6.034	6.034	6.063	6.158	6.110	59.6	139.4
TSMR	2	20.031	20.000	20.000	20.031	20.016	6.017	6.004	6.010	6.073	6.140	6.107	60.8	143.0
Wolverine Way NB	1	20.031	20.125	20.250	20.188	20.148	6.149	6.055	6.102	6.001	5.966	5.983	60.8	142.8
TSMR	2	20.063	20.063	20.063	20.094	20.070	6.093	6.029	6.061	6.029	6.024	6.027	59.2	139.5
Upper Ridge Road NB	1	19.969	19.938	20.000	19.969	19.969	6.036	6.048	6.042	6.102	6.235	6.168	60.8	141.2
Conventional	2	20.031	20.000	20.031	20.000	20.016	6.034	6.024	6.029	6.063	6.020	6.041	59.2	140.3
Wolverine Way SB	1	20.031	20.094	20.125	20.063	20.078	6.024	6.036	6.030	6.134	6.098	6.116	61.0	142.4
Conventional	2	20.000	20.094	20.188	20.125	20.102	6.005	5.970	5.987	6.242	6.225	6.233	59.6	137.3

Table B-10: Properties of Specimens for Electrical Impedance and Flexural Strength Testing at 3 Months

Bridge Location	Sample Location	Length (in.)					Height (in.)			Width (in.)			Weight (lb)	Density (lb/ft^3)
		1	2	3	4	Avg.	1	2	Avg.	1	2	Avg.		
Upper Ridge Road SB	1	20.000	19.969	19.969	20.000	19.984	6.022	5.989	6.006	6.025	6.019	6.022	58.2	139.2
TSMR	2	19.938	20.063	20.125	20.063	20.047	6.060	6.148	6.104	6.048	6.052	6.050	59.8	139.6
Wolverine Way NB	1	20.000	20.000	20.063	20.031	20.023	6.001	5.961	5.981	6.090	6.019	6.054	59.4	141.6
TSMR	2	20.031	20.000	20.094	20.125	20.063	6.022	6.046	6.034	6.079	6.101	6.090	59.2	138.8
Upper Ridge Road NB	1	19.969	20.000	20.000	20.031	20.000	6.115	6.144	6.129	6.009	6.008	6.008	60.4	141.7
Conventional	2	19.938	20.000	20.094	20.031	20.016	6.101	6.104	6.103	5.988	5.960	5.974	59.0	139.7
Wolverine Way SB	1	19.969	20.031	19.969	20.031	20.000	6.007	5.964	5.985	6.109	6.180	6.144	60.4	141.9
Conventional	2	20.031	20.031	20.000	20.031	20.023	6.012	5.963	5.987	6.264	6.097	6.181	59.8	139.5

Table B-11: Properties of Specimens for Electrical Impedance and Flexural Strength Testing at 1 Year

Bridge Location	Sample Location	Length (in.)					Height (in.)			Width (in.)			Weight (lb)	Density (lb/ft^3)
		1	2	3	4	Avg.	1	2	Avg.	1	2	Avg.		
Upper Ridge Road SB	1*	19.969	20.000	20.063	20.000	20.008	6.113	6.116	6.114	6.003	5.967	5.985	58.4	137.8
TSMR	2*	19.969	20.063	20.125	20.031	20.047	6.115	6.146	6.130	5.994	5.970	5.982	59.7	140.4
Wolverine Way NB	1	20.063	20.063	20.188	20.250	20.141	6.069	3.032	4.550	6.133	6.179	6.156	61.1	187.3
TSMR	2	20.063	20.063	20.031	20.063	20.055	6.011	5.964	5.987	6.173	6.140	6.157	59.2	138.5
Upper Ridge Road NB	1*	19.938	20.063	20.125	20.063	20.047	6.067	6.122	6.094	6.022	6.050	6.036	59.5	139.4
Conventional	2*	19.938	20.000	20.031	20.031	20.000	6.175	6.250	6.212	6.019	5.989	6.004	59.3	137.3
Wolverine Way SB	1	20.000	20.125	20.125	20.031	20.070	6.017	6.002	6.010	6.119	6.076	6.097	60.3	141.7
Conventional	2	20.031	20.000	19.938	19.938	19.977	6.039	6.044	6.041	6.092	6.167	6.129	57.6	134.5

*Samples that were also subjected to shrinkage testing

Table B-12: Splitting Tensile Strength

Bridge Location	Sample Location	Tensile Strength (psi)			
		28 Days	3 Months	1 Year	2 Years
Upper Ridge Road SB	1	638	642	751	614
TSMR	2	632	675	-	707
Wolverine Way NB	1	716	724	703	667
TSMR	2	625	743	582	623
Upper Ridge Road NB	1	707	628	616	619
Conventional	2	649	591	601	568
Wolverine Way SB	1	856	759	738	727
Conventional	2	668	632	655	697

Table B-13: Properties of Specimens for Splitting Tensile Strength Testing at 28 Days

Bridge Location	Sample Location	Length (in.)					Diameter (in.)					Weight (lb)	Density (lb/ft^3)
		1	2	3	4	Avg.	1	2	3	4	Avg.		
Upper Ridge Road SB	1	2.495	2.502	2.526	2.535	2.514	4.013	3.997	4.059	4.042	4.028	2.475	133.5
TSMR	2	2.644	2.668	2.641	2.652	2.651	4.036	4.018	4.041	4.025	4.030	2.678	136.8
Wolverine Way NB	1	2.538	2.536	2.525	2.528	2.532	4.027	4.034	4.020	4.020	4.025	2.563	137.5
TSMR	2	2.529	2.533	2.551	2.551	2.541	4.036	4.031	4.026	4.014	4.027	2.543	135.8
Upper Ridge Road NB	1	2.391	2.376	2.387	2.399	2.388	4.020	4.015	4.025	4.015	4.019	2.462	140.4
Conventional	2	2.579	2.743	2.672	2.633	2.657	4.018	4.008	4.034	4.011	4.018	2.725	139.8
Wolverine Way SB	1	2.572	2.572	2.568	2.571	2.571	3.992	3.995	4.013	4.010	4.002	2.624	140.2
Conventional	2	2.560	2.566	2.560	2.561	2.562	4.013	4.012	3.995	3.992	4.003	2.565	137.5

Table B-14: Properties of Specimens for Splitting Tensile Strength Testing at 3 Months

Bridge Location	Sample Location	Length (in.)					Diameter (in.)					Weight (lb)	Density (lb/ft^3)
		1	2	3	4	Avg.	1	2	3	4	Avg.		
Upper Ridge Road SB	1	2.382	2.376	2.377	2.386	2.380	4.035	4.029	4.033	4.018	4.029	2.342	133.4
TSMR	2	2.317	2.316	2.312	2.325	2.317	4.265	4.020	4.018	4.013	4.079	2.307	131.6
Wolverine Way NB	1	2.543	2.543	2.562	2.550	2.549	3.997	4.003	4.012	4.015	4.007	2.549	137.0
TSMR	2	2.570	2.568	2.545	2.575	2.564	4.021	4.001	4.002	3.993	4.004	2.614	139.9
Upper Ridge Road NB	1	2.521	2.489	2.493	2.482	2.496	4.014	4.010	4.014	4.010	4.012	2.546	139.5
Conventional	2	2.292	2.229	2.272	2.276	2.267	4.017	4.016	4.011	4.005	4.012	2.239	135.0
Wolverine Way SB	1	2.491	2.516	2.498	2.483	2.497	4.009	4.012	4.016	4.015	4.013	2.532	138.5
Conventional	2	2.531	2.528	2.526	2.524	2.527	4.006	4.012	4.012	4.021	4.013	2.514	135.9

Table B-15: Properties of Specimens for Splitting Tensile Strength Testing at 1 Year

Bridge Location	Sample Location	Length (in.)					Diameter (in.)					Weight (lb)	Density (lb/ft^3)
		1	2	3	4	Avg.	1	2	3	4	Avg.		
Upper Ridge Road SB	1	2.502	2.554	2.648	2.568	2.568	4.006	4.003	4.005	4.006	4.005	2.530	135.1
TSMR	2	2.577	2.578	2.583	2.610	2.587	4.011	4.003	4.012	4.010	4.009	2.543	134.6
Wolverine Way NB	1	2.548	2.542	2.549	2.549	2.547	4.002	4.017	4.015	4.017	4.013	2.506	134.4
TSMR	2	2.561	2.561	2.549	2.562	2.558	4.008	4.012	4.016	4.016	4.013	2.520	134.6
Upper Ridge Road NB	1	2.472	2.604	2.563	2.530	2.542	4.035	4.057	4.025	4.051	4.042	2.562	135.7
Conventional	2	2.666	2.565	2.479	2.565	2.569	4.035	4.081	4.042	4.034	4.048	2.579	134.8
Wolverine Way SB	1	2.536	2.535	2.529	2.523	2.531	4.040	4.037	4.017	4.020	4.028	2.562	137.2
Conventional	2	2.523	2.521	2.526	2.536	2.527	4.040	4.041	4.037	4.035	4.038	2.497	133.3

Table B-16: Properties of Specimens for Splitting Tensile Strength Testing at 2 Years

Bridge Location	Sample Location	Length (in.)					Diameter (in.)					Weight (lb)	Density (lb/ft^3)
		1	2	3	4	Avg.	1	2	3	4	Avg.		
Upper Ridge Road SB	1	1.969	1.943	1.934	1.934	1.945	4.028	4.022	3.900	4.029	3.995	1.889	133.9
TSMR	2	1.848	1.846	1.850	1.853	1.849	4.013	4.029	4.024	4.027	4.023	1.835	134.9
Wolverine Way NB	1	2.067	2.069	2.112	2.060	2.077	4.022	4.021	4.052	4.009	4.026	2.067	135.1
TSMR	2	2.067	2.068	2.067	2.066	2.067	4.028	4.045	4.036	4.026	4.034	2.028	132.7
Upper Ridge Road NB	1	1.927	1.967	1.923	1.941	1.939	4.034	4.054	4.033	4.013	4.033	1.970	137.4
Conventional	2	1.959	1.966	1.950	1.953	1.957	4.032	4.004	4.016	4.024	4.019	1.921	133.7
Wolverine Way SB	1	1.976	1.984	1.997	1.986	1.985	4.024	4.013	4.027	4.030	4.023	2.031	139.0
Conventional	2	1.958	1.954	1.955	1.953	1.955	4.014	4.016	4.022	4.017	4.017	1.965	137.0

Table B-17: Toughness of Cylindrical Specimens

Bridge Location	Sample Location	Toughness (psi)			
		28 Days	3 Months	1 Year	2 year
Upper Ridge Road SB	1	36.8	20.8	35.4	22.7
TSMR	2	33.9	20.6	32.6	48.2
Wolverine Way NB	1	31.7	58.4	38.8	33.8
TSMR	2	37.2	27.7	46.6	29.8
Upper Ridge Road NB	1	10.7	17.9	14.7	18.0
Conventional	2	11.9	14.4	14.0	10.8
Wolverine Way SB	1	17.7	18.1	17.1	10.9
Conventional	2	15.1	17.8	14.9	11.3

Table B-18: Toughness of Beam Specimens

Bridge Location	Sample Location	Flexural Toughness (lb-in.)		
		28 days	3 months	1 year
Upper Ridge Road SB	1	591.1	362.3	608.0
TSMR	2	697.5	563.0	696.0
Wolverine Way NB	1	584.5	283.9	381.5
TSMR	2	616.7	390.7	323.0
Upper Ridge Road NB	1	241.3	210.1	348.9
Conventional	2	164.0	171.1	289.0
Wolverine Way SB	1	194.8	214.0	327.0
Conventional	2	202.9	239.0	249.1

APPENDIX C STRESS-STRAIN AND LOAD-DEFLECTION CURVES FROM LABORATORY TESTING

Figures C-1 to C-8 provide the stress-strain curves generated from data collected during compressive strength testing. Figures C-9 to C-14 provide the load-deflection curves generated from data collected during flexural strength testing.

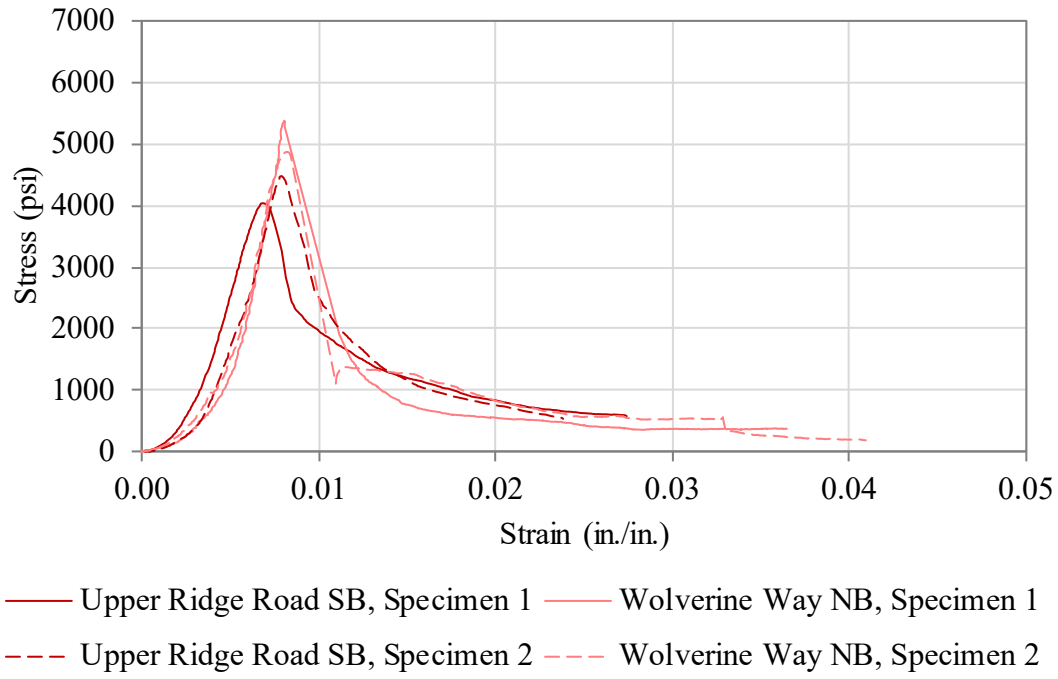

Figure C-1: Stress-strain curves for specimens containing TSMR at 28 days.

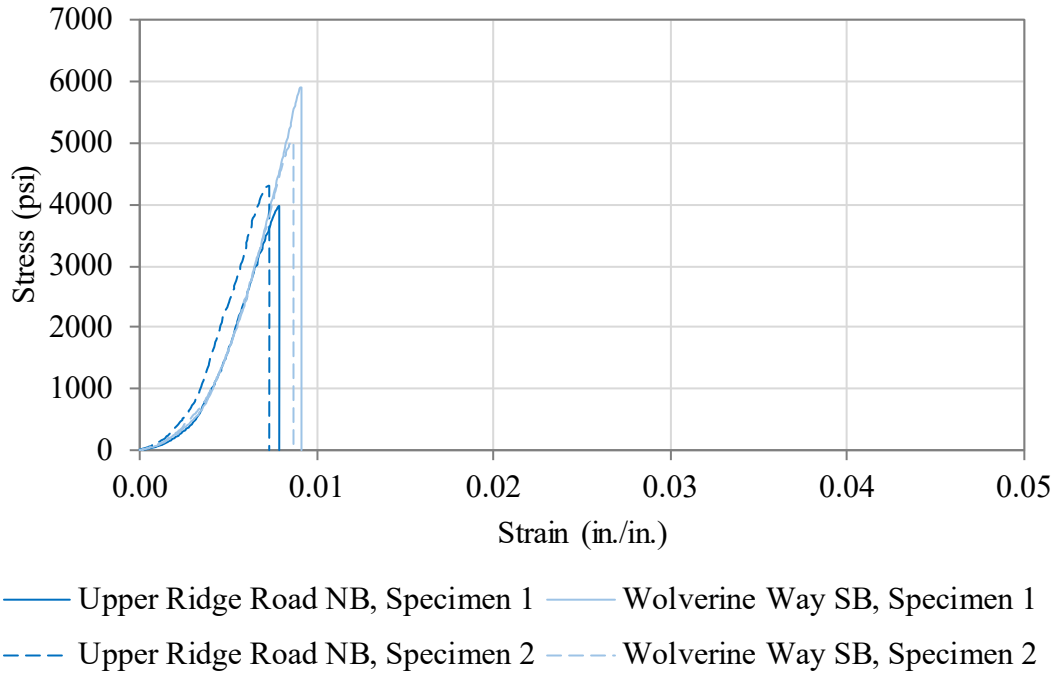

Figure C-2: Stress-strain curves for conventional concrete specimens at 28 days.

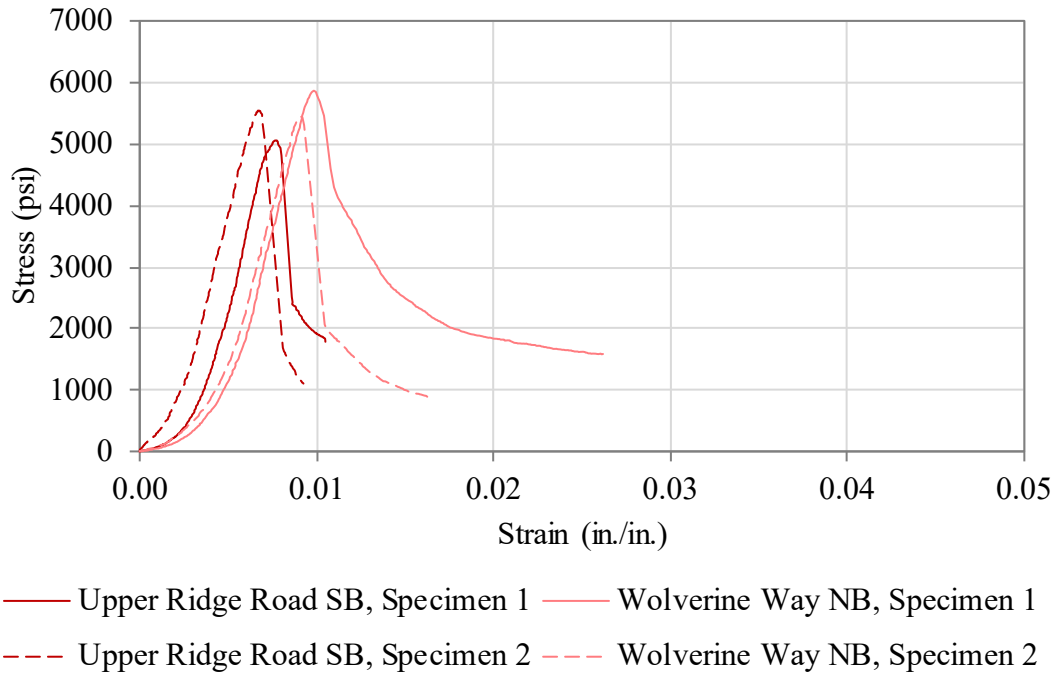

Figure C-3: Stress-strain curves for specimens containing TSMR at 3 months.

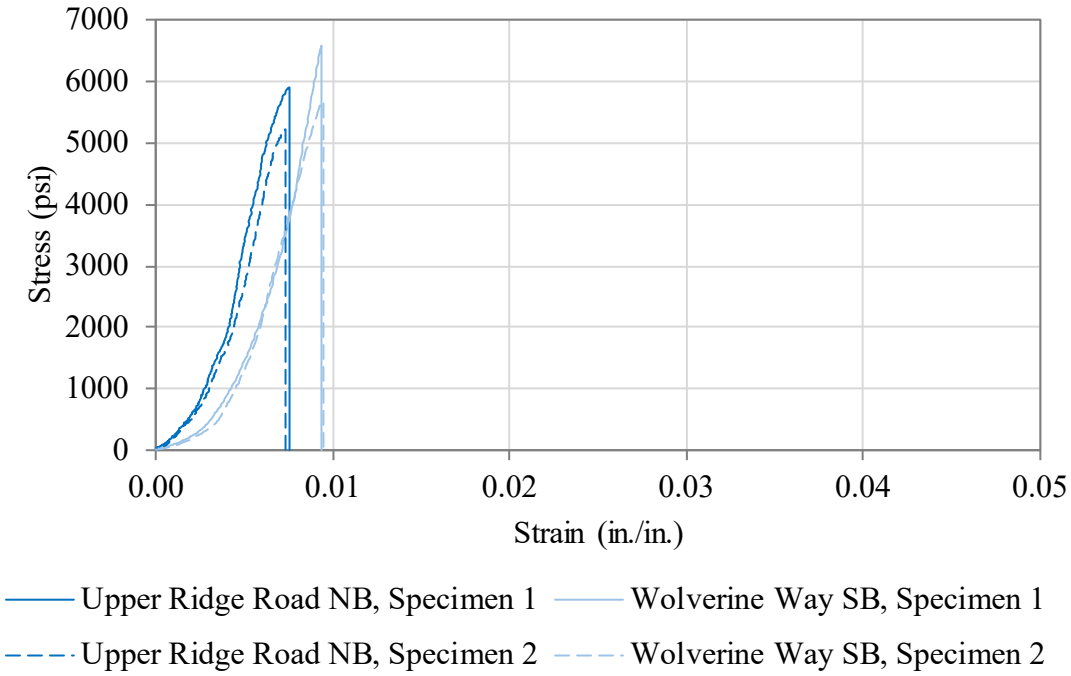

Figure C-4: Stress-strain curves for conventional concrete specimens at 3 months.

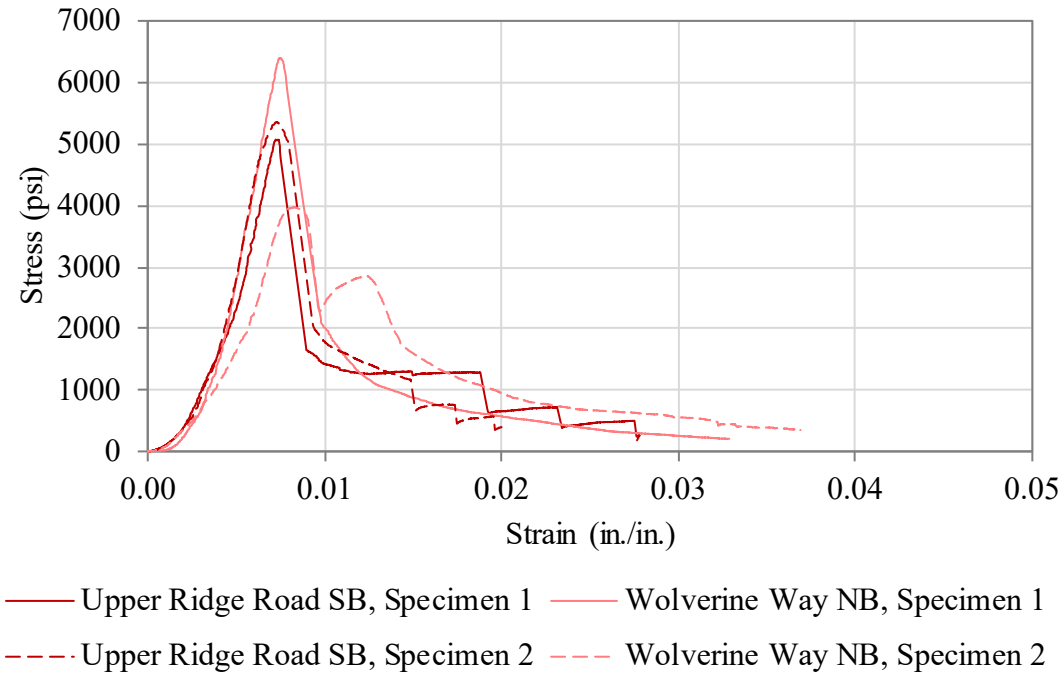

Figure C-5: Stress-strain curves for specimens containing TSMR at 1 year.

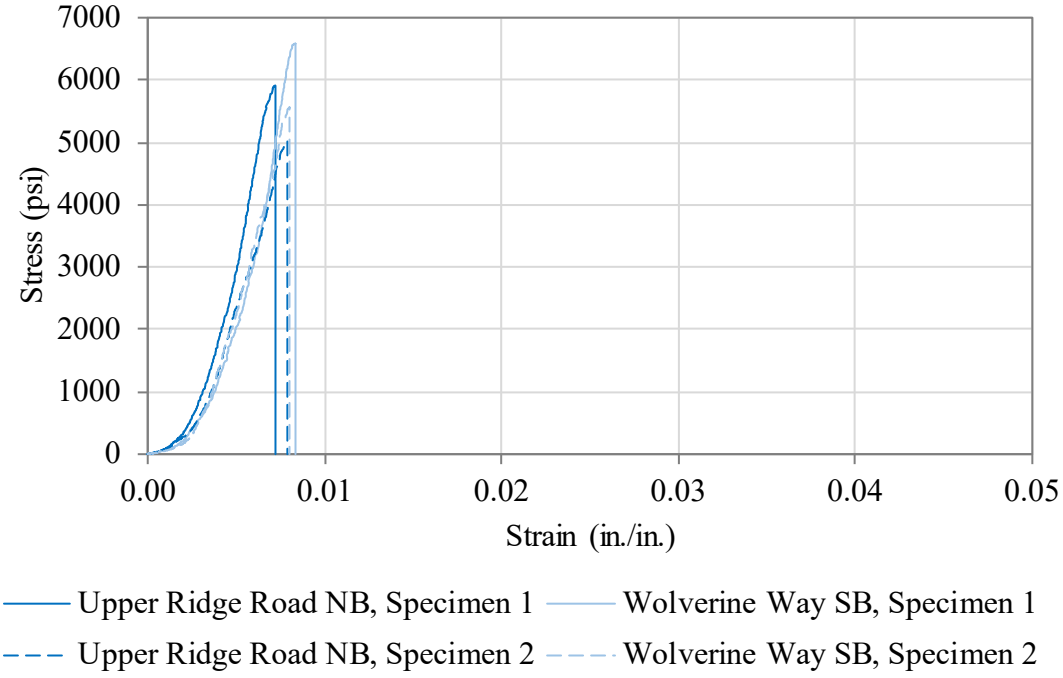

Figure C-6: Stress-strain curves for conventional concrete specimens at 1 year.

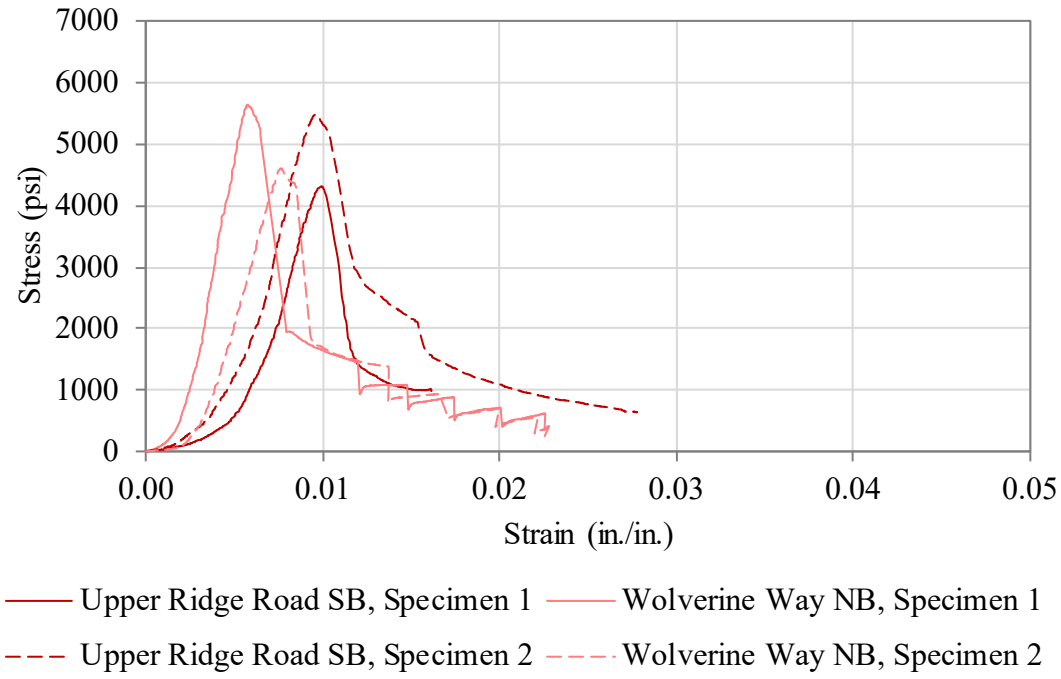

Figure C-7: Stress-strain curves for specimens containing TSMR at 2 years.

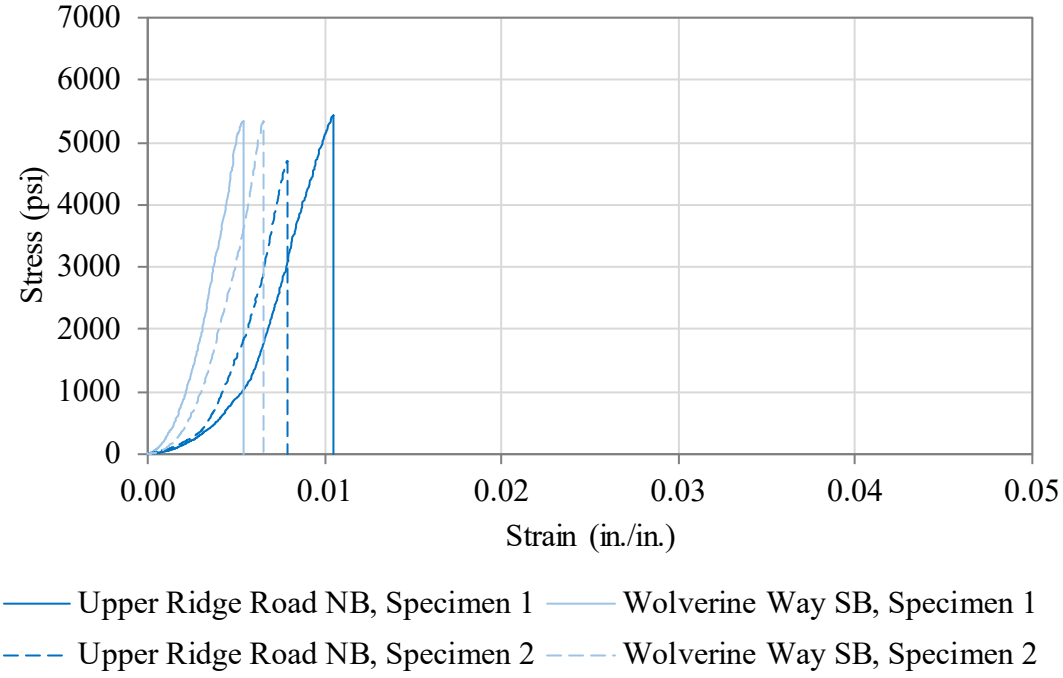

Figure C-8: Stress-strain curves for conventional concrete specimens at 2 years.

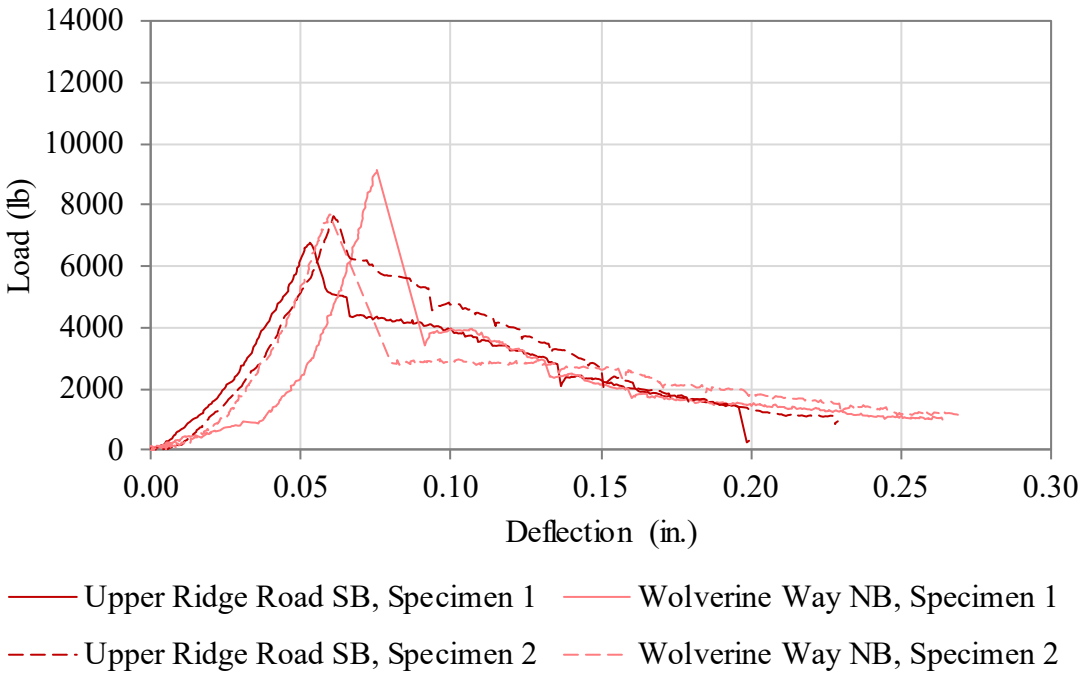

Figure C-9: Load-deflection curves for specimens containing TSMR at 28 days.

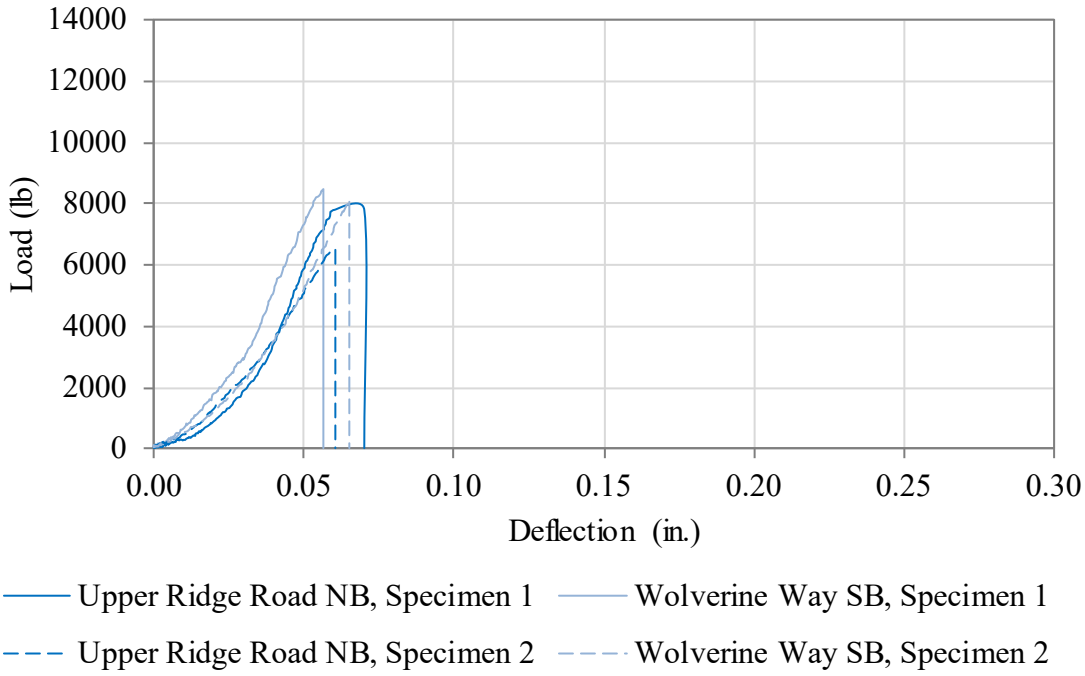

Figure C-10: Load-deflection curves for conventional concrete specimens at 28 days.

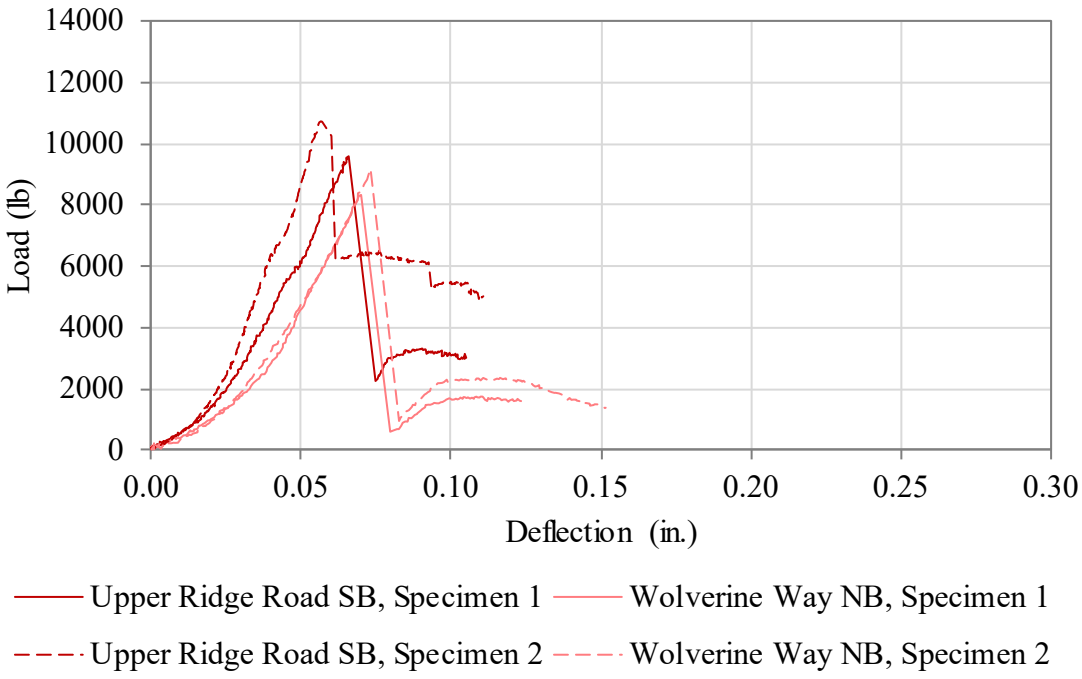

Figure C-11: Load-deflection curves for specimens containing TSMR at 3 months.

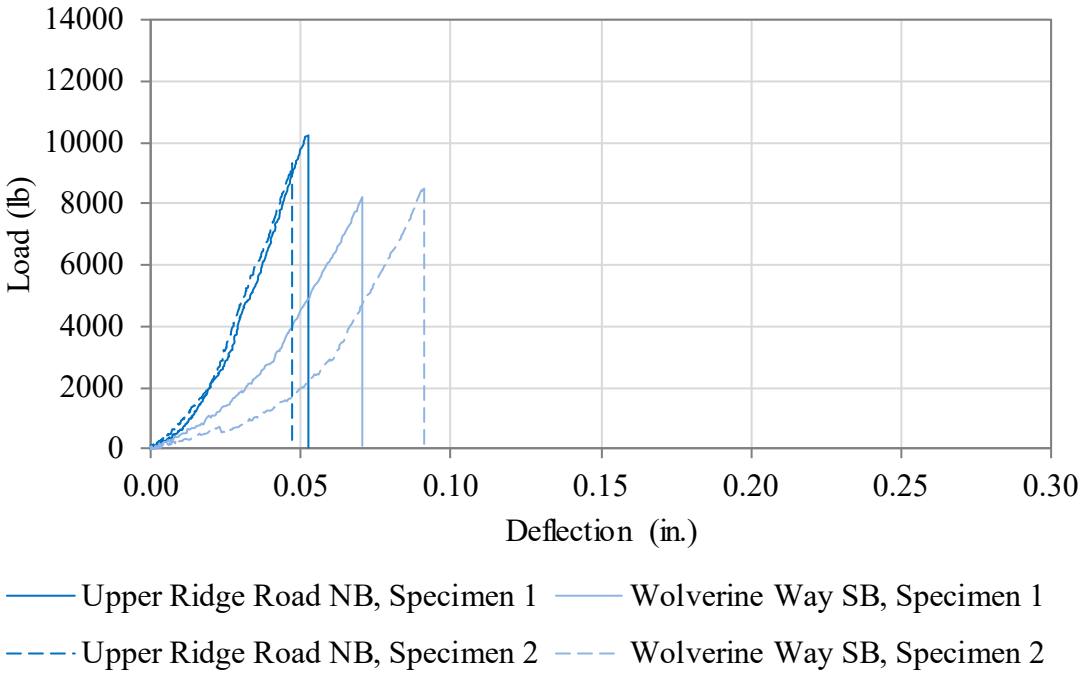

Figure C-12: Load-deflection curves for conventional concrete specimens at 3 months.

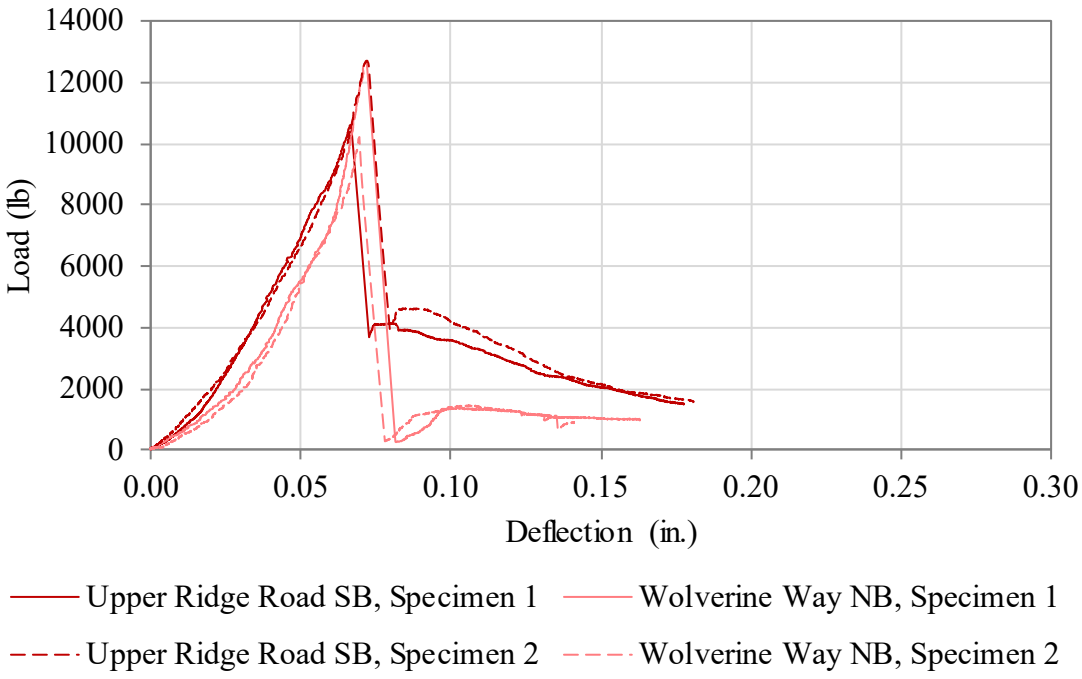

Figure C-13: Load-deflection curves for specimens containing TSMR at 1 year.

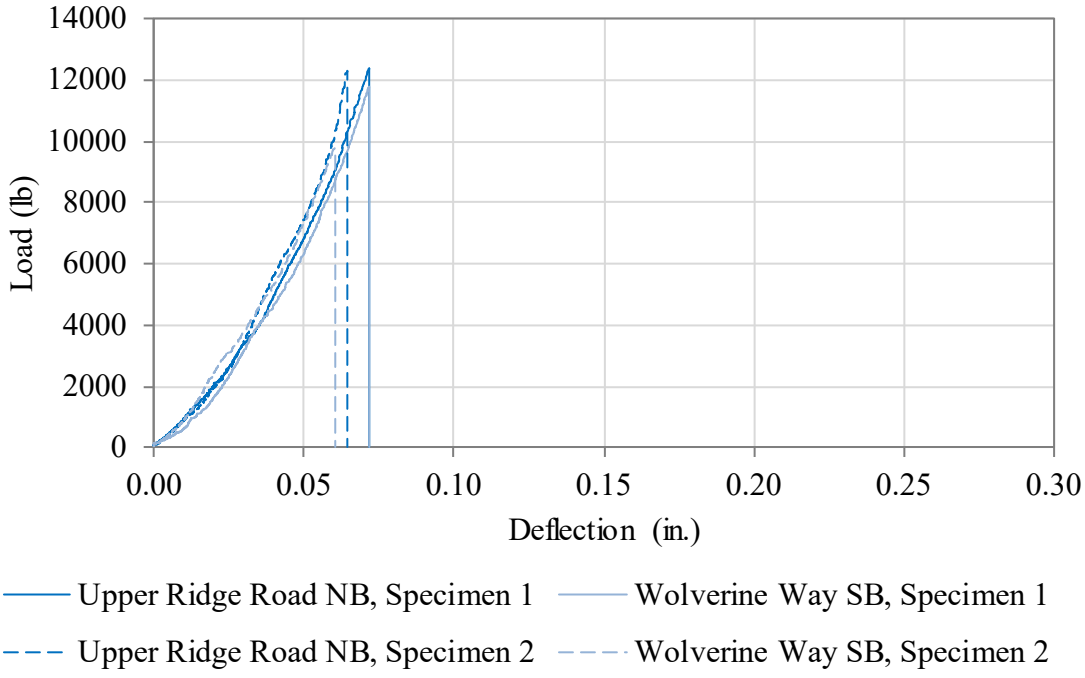

Figure C-14: Load-deflection curves for conventional concrete specimens at 1 year.

APPENDIX D PICTURES OF SPECIMENS AFTER COMPRESSIVE STRENGTH, FLEXURAL STRENGTH, AND SPLITTING TENSILE STRENGTH TESTING

Figures D-1 to D-4 show typical cylindrical specimens after compressive strength testing. Figures D-5 to D-8 show typical beam specimens after flexural strength testing. Figures D-9 to D-12 show typical specimens after splitting tensile strength testing.

Figure D-1: Typical Upper Ridge Road SB TSMR specimen after compressive strength testing.

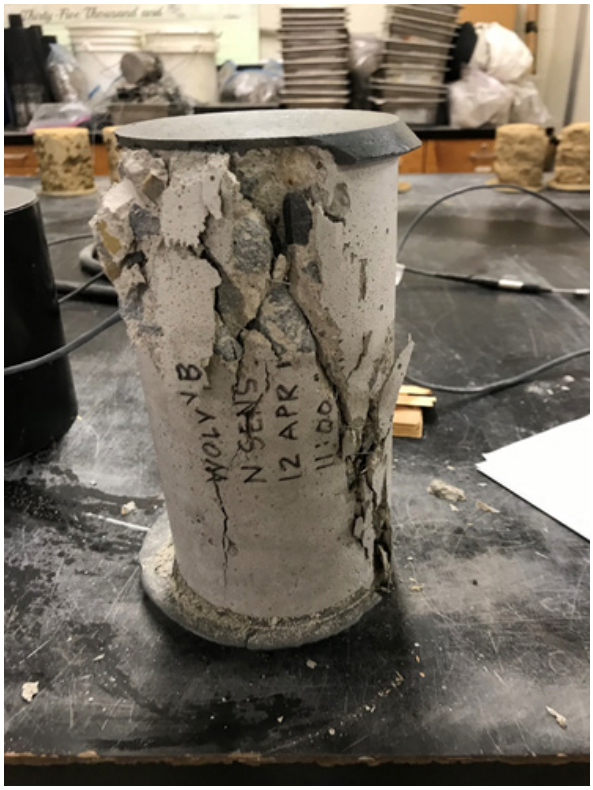

Figure D-2: Typical Wolverine Way NB TSMR specimen after compressive strength testing.

Figure D-3: Typical Upper Ridge Road NB conventional concrete specimen after compressive strength testing.

Figure D-4: Typical Wolverine Way SB conventional concrete specimen after compressive strength testing.

Figure D-5: Typical Upper Ridge Road SB TSMR specimen after flexural strength testing.

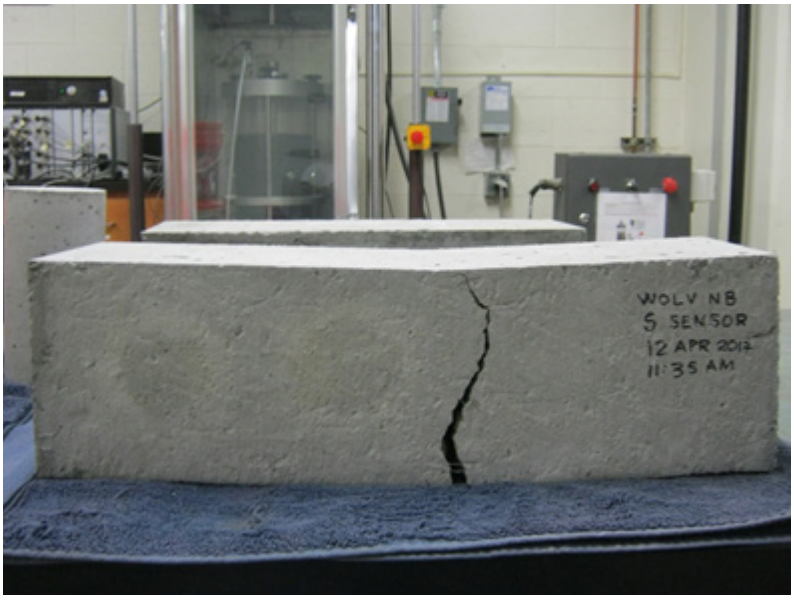

Figure D-6: Typical Wolverine Way NB TSMR specimen after flexural strength testing.

Figure D-7: Typical Upper Ridge Road NB conventional concrete specimen after flexural strength testing.

Figure D-8: Typical Wolverine Way SB conventional concrete specimen after flexural strength testing.

Figure D-9: Typical Upper Ridge Road SB TSMR specimen after splitting tensile strength testing.

Figure D-10: Typical Wolverine Way NB TSMR specimen after splitting tensile strength testing.

Figure D-11: Typical Upper Ridge Road NB conventional concrete specimen after splitting tensile strength testing.

Figure D-12: Typical Wolverine Way SB conventional concrete specimen after splitting tensile strength testing.

APPENDIX E SUPPORTING FIELD DATA

Table E-1 provides an example of data logger output from the sensors installed in the bridge decks. Table E-2 gives Schmidt rebound numbers. Table E-3 shows concrete cover depths at test locations corresponding to those at which chloride concentration testing was performed. Tables E-4, E-5, and E-6 provide chloride concentration data for testing at 3 months, 1 year, and 2 years, respectively. A hyphen indicates that no samples were collected at the specified location at the given testing period. Tables E-7 and E-8 provide the crack properties at chloride concentration testing locations.

Table E-1: Example Data Logger Output

Measurement Time	Port 1* GS3 % VWC	Port 1* GS3 °F Temp	Port 1* GS3 dS/m EC Bulk	Port 2 5TE % VWC	Port 2 5TE °F Temp	Port 2 5TE dS/m EC Bulk	Port 3* GS3 % VWC	Port 3* GS3 °F Temp	Port 3* GS3 dS/m EC Bulk	Port 4* ECH2O-TE % VWC	Port 4* ECH2O-TE °F Temp	Port 4* ECH2O-TE dS/m EC Bulk
9/1/17 0:00	41.19	79.70	0.09	33.01	80.06	0.13	49.56	79.52	0.13	228.89	-8.32	0.26
9/1/17 1:00	41.09	78.62	0.09	32.96	78.80	0.13	49.40	78.26	0.13	228.57	-8.68	0.25
9/1/17 2:00	40.99	77.54	0.08	32.91	77.72	0.13	49.23	77.18	0.12	228.24	-9.04	0.25
9/1/17 3:00	40.91	76.46	0.08	32.83	76.64	0.13	49.08	76.28	0.12	227.91	-9.22	0.24
9/1/17 4:00	40.83	75.56	0.08	32.80	75.74	0.13	48.94	75.20	0.12	227.59	-9.58	0.24
9/1/17 5:00	40.73	74.66	0.08	32.78	74.84	0.13	48.81	74.30	0.12	227.37	-9.76	0.23
9/1/17 6:00	40.63	73.94	0.08	32.72	73.94	0.12	48.68	73.40	0.12	227.04	-9.76	0.23
9/1/17 7:00	40.58	73.04	0.08	32.67	73.04	0.12	48.58	72.50	0.12	226.82	-10.12	0.22
9/1/17 8:00	40.50	72.32	0.08	32.65	72.14	0.12	48.45	71.60	0.12	226.60	-10.84	0.22
9/1/17 9:00	40.50	72.14	0.08	32.65	71.78	0.12	48.43	71.42	0.12	226.49	-10.84	0.22
9/1/17 10:00	40.58	73.04	0.08	32.67	72.68	0.12	48.56	72.14	0.12	226.82	-10.12	0.22
9/1/17 11:00	40.78	75.02	0.08	32.75	74.30	0.13	48.84	74.12	0.12	227.37	-9.94	0.23
9/1/17 12:00	41.06	77.90	0.09	32.86	77.00	0.13	49.24	77.00	0.13	228.24	-9.40	0.25
9/1/17 13:00	41.39	81.32	0.09	33.01	80.24	0.13	49.70	80.42	0.13	229.22	-8.50	0.27
9/1/17 14:00	41.71	84.74	0.09	33.17	83.66	0.14	50.15	84.02	0.13	229.98	-7.06	0.29
9/1/17 15:00	41.98	87.80	0.09	33.33	86.72	0.14	50.55	87.26	0.14	230.85	-6.16	0.30

*Data were not used in this research

Table E-2: Schmidt Rebound Numbers

Bridge Location	Schmidt Rebound Number									
	3 Months					2 Years				
	1	2	3	4	Avg.	1	2	3	4	Avg.
Upper Ridge Road SB TSMR	39	38	37	38	38	46	44	46	42	45
Wolverine Way NB TSMR	44	51	49	42	47	61	58	56	55	58
Upper Ridge Road NB Conventional	50	41	46	52	47	55	53	47	49	51
Wolverine Way SB Conventional	49	43	40	41	43	49	50	49	49	49

Table E-3: Cover Depth Measurements

Bridge Location	Test Location	Cover Depth (in.)				
		North Transverse	South Transverse	East Longitudinal	West Longitudinal	Average
Upper Ridge Road SB TSMR	1	3.25	3.25	3.20	3.30	3.25
	2	3.15	3.20	3.25	3.25	3.21
	3	2.80	2.85	2.85	2.80	2.83
	4	3.25	3.25	3.20	3.20	3.23
Wolverine Way NB TSMR	1	2.75	3.35	2.95	3.00	3.01
	2	2.95	3.00	3.25	3.20	3.10
	3	2.65	3.25	3.35	3.20	3.11
	4	2.80	2.80	2.95	3.20	2.94
Upper Ridge Road NB Conventional	1	3.15	3.15	3.10	3.25	3.16
	2	2.65	2.65	2.75	2.75	2.70
	3	3.20	3.25	3.25	3.20	3.23
	4	2.75	2.75	2.65	2.95	2.78
Wolverine Way SB Conventional	1	2.90	2.85	3.60	3.55	3.23
	2	4.20	3.35	3.70	3.85	3.78
	3	2.95	2.95	3.25	3.15	3.08
	4	3.20	3.15	-	3.95	3.43

Table E-4: Chloride Concentrations at 3 Months

Bridge Location	Chloride Concentration (lb Cl^-/yd^3 Concrete)				
	Depth (in.)	1	2	3	4
Upper Ridge Road SB TSMR	0.0 to 0.5	0.3	0.2	0.6	0.4
	0.5 to 1.0	0.3	0.4	0.4	0.4
Wolverine Way NB TSMR	0.0 to 0.5	0.8	0.4	0.4	0.4
	0.5 to 1.0	0.2	0.2	0.3	0.2
Upper Ridge Road NB Conventional	0.0 to 0.5	0.4	0.4	0.4	0.3
	0.5 to 1.0	0.3	0.2	0.2	0.1
Wolverine Way SB Conventional	0.0 to 0.5	0.8	0.5	0.3	0.2
	0.5 to 1.0	0.3	0.5	0.4	0.2

Table E-5: Chloride Concentrations at 1 Year

Bridge Location	Depth (in.)	Chloride Concentration (lb Cl^-/yd^3 Concrete)							
		Non-Cracked Concrete				Cracked Concrete			
		1	2	3	4	1	2	3	4
Upper Ridge Road SB	0.0 to 0.5	-	14.6	-	8.1	-	11.3	13.2	-
TSMR	0.5 to 1.0	-	2.5	-	1.5	-	2.4	2.9	-
Wolverine Way NB	0.0 to 0.5	8.6	5.6	-	-	-	-	8.6	8.4
TSMR	0.5 to 1.0	1.5	1.4	-	-	-	-	2.7	1.5
Upper Ridge Road NB	0.0 to 0.5	7.2	-	-	9.9	-	28.8	8.6	-
Conventional	0.5 to 1.0	1.0	-	-	1.6	-	2.6	3.3	-
Wolverine Way SB	0.0 to 0.5	12.6	-	-	9.3	-	-	8.5	12.4
Conventional	0.5 to 1.0	0.9	-	-	1.8	-	-	2.8	2.7

Table E-6: Chloride Concentrations at 2 Years

Bridge Location	Depth (in.)	Chloride Concentration (lb Cl^-/yd^3 Concrete)							
		Non-Cracked Concrete				Cracked Concrete			
		1	2	3	4	1	2	3	4
Upper Ridge Road SB	0.0 to 0.5	11.3	11.1	12.2	14.1	13.5	11.8	15.6	12.7
TSMR	0.5 to 1.0	0.7	2.7	1.9	1.6	5.2	5.2	3.9	5.2
Wolverine Way NB	0.0 to 0.5	8.6	5.5	13.2	10.9	11.6	5.9	12.8	11.1
TSMR	0.5 to 1.0	0.5	1.4	1.5	1.6	4.2	2.8	4.2	3.0
Upper Ridge Road NB	0.0 to 0.5	12.6	10.4	12.9	12.4	11.1	11.0	13.2	12.8
Conventional	0.5 to 1.0	1.7	1.8	1.3	1.8	3.1	3.7	4.3	2.2
Wolverine Way SB	0.0 to 0.5	12.7	9.2	11.6	12.4	11.1	10.5	11.4	14.0
Conventional	0.5 to 1.0	2.3	1.2	1.9	1.7	6.2	4.7	4.5	7.8

Table E-7: Crack Properties at Chloride Concentration Testing Locations at 1 Year

Bridge Location	Test Location	Crack Width (in.)	Crack Depth (in.)
Upper Ridge Road SB	2	0.0039	Surface Crack
TSMR	3	0.0039	Surface Crack
Wolverine Way NB	2	0.0098	Surface Crack
TSMR	3	0.0059	0.25
Upper Ridge Road NB	2	0.0039	Surface Crack
Conventional	3	0.0157	Surface Crack
Wolverine Way SB	3	0.0118	Surface Crack
Conventional	4	0.0039	Surface Crack

Table E-8: Crack Properties at Chloride Concentration Testing Locations at 2 Years

Bridge Location	Test Location	Crack Width (in.)	Crack Depth (in.)
Upper Ridge Road SB TSMR	1	0.0059	Surface Crack
	2	0.0059	0.33
	3	0.0079	0.50
	4	0.0079	0.45
Wolverine Way NB TSMR	1	0.0157	0.25
	2	0.0059	Surface Crack
	3	0.0197	Surface Crack
	4	0.0236	0.50
Upper Ridge Road NB Conventional	1	0.0079	0.50
	2	0.0039	Surface Crack
	3	0.0098	0.50
	4	0.0059	Surface Crack
Wolverine Way SB Conventional	1	0.0059	Surface Crack
	2	0.0059	0.50
	3	0.0059	0.50
	4	0.0079	Surface Crack

APPENDIX F DISTRESS MAPS

Figures F-1 to F-12 provide distress maps of the bridge decks recorded after approximately 3 months, 1 year, and 2 years from the time of construction of the bridge decks.

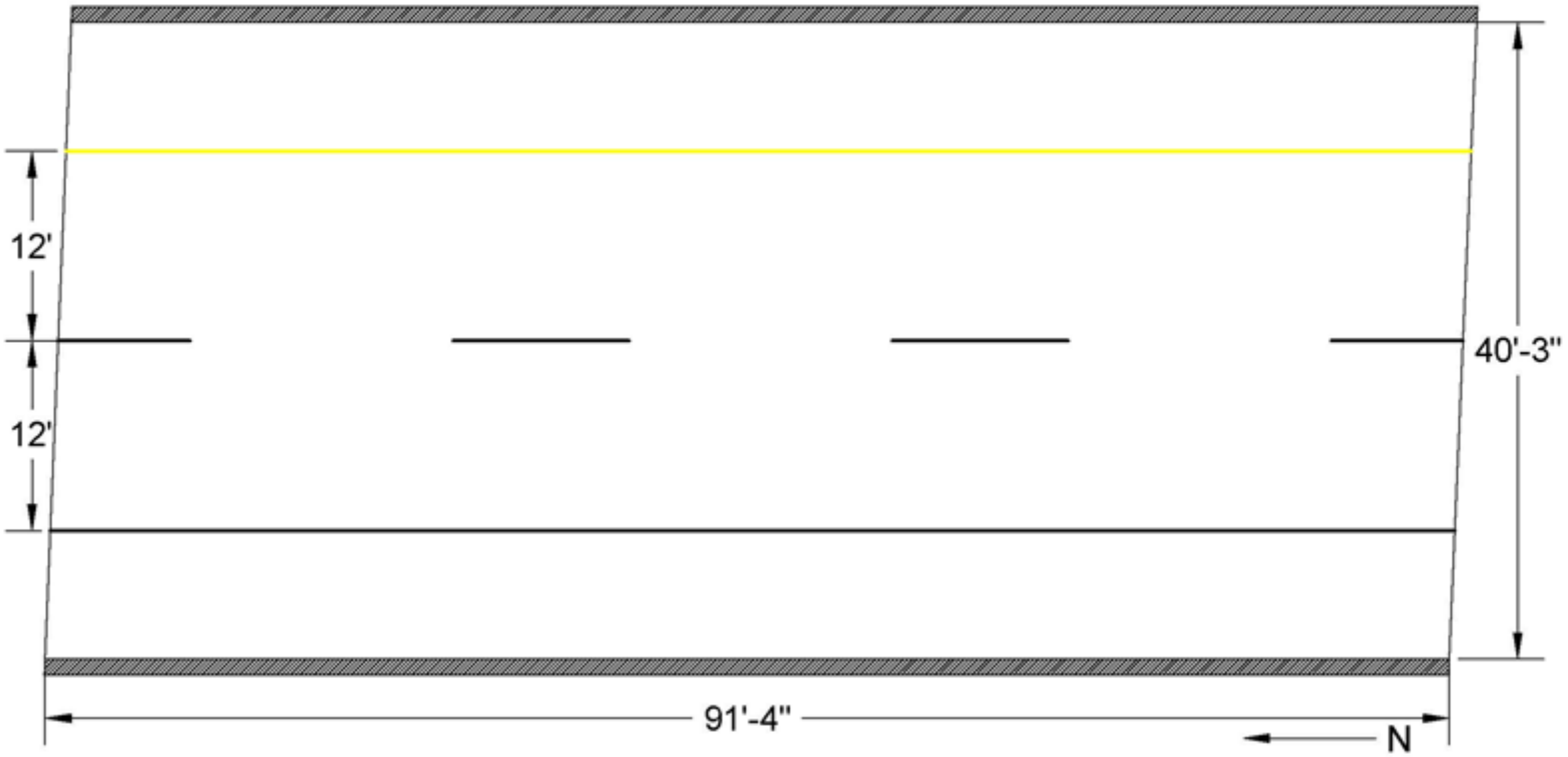

Figure F-1: Distress map for Upper Ridge Road SB TSMR deck at 3 months.

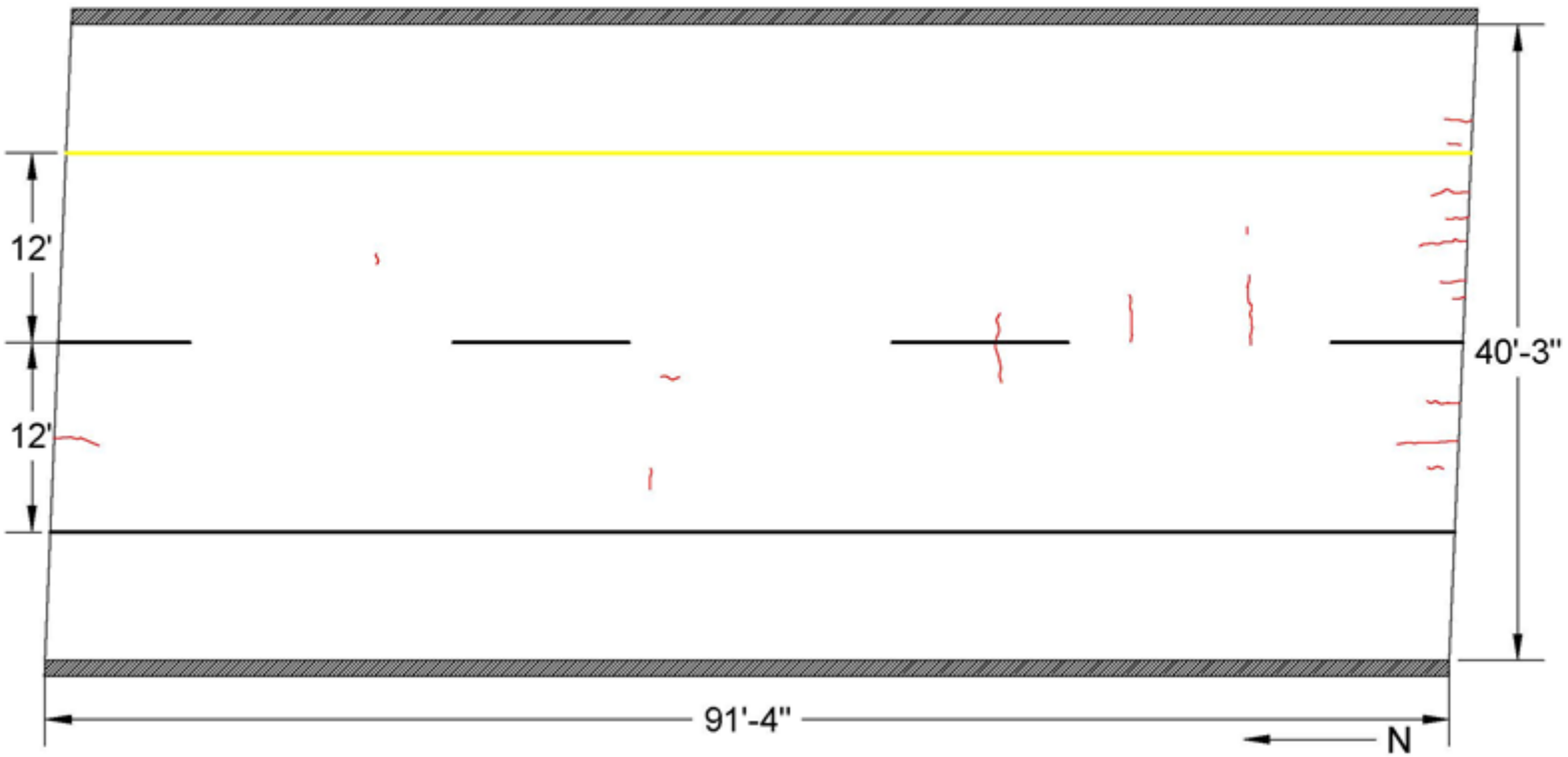

Figure F-2: Distress map for Upper Ridge Road SB TSMR deck at 1 year.

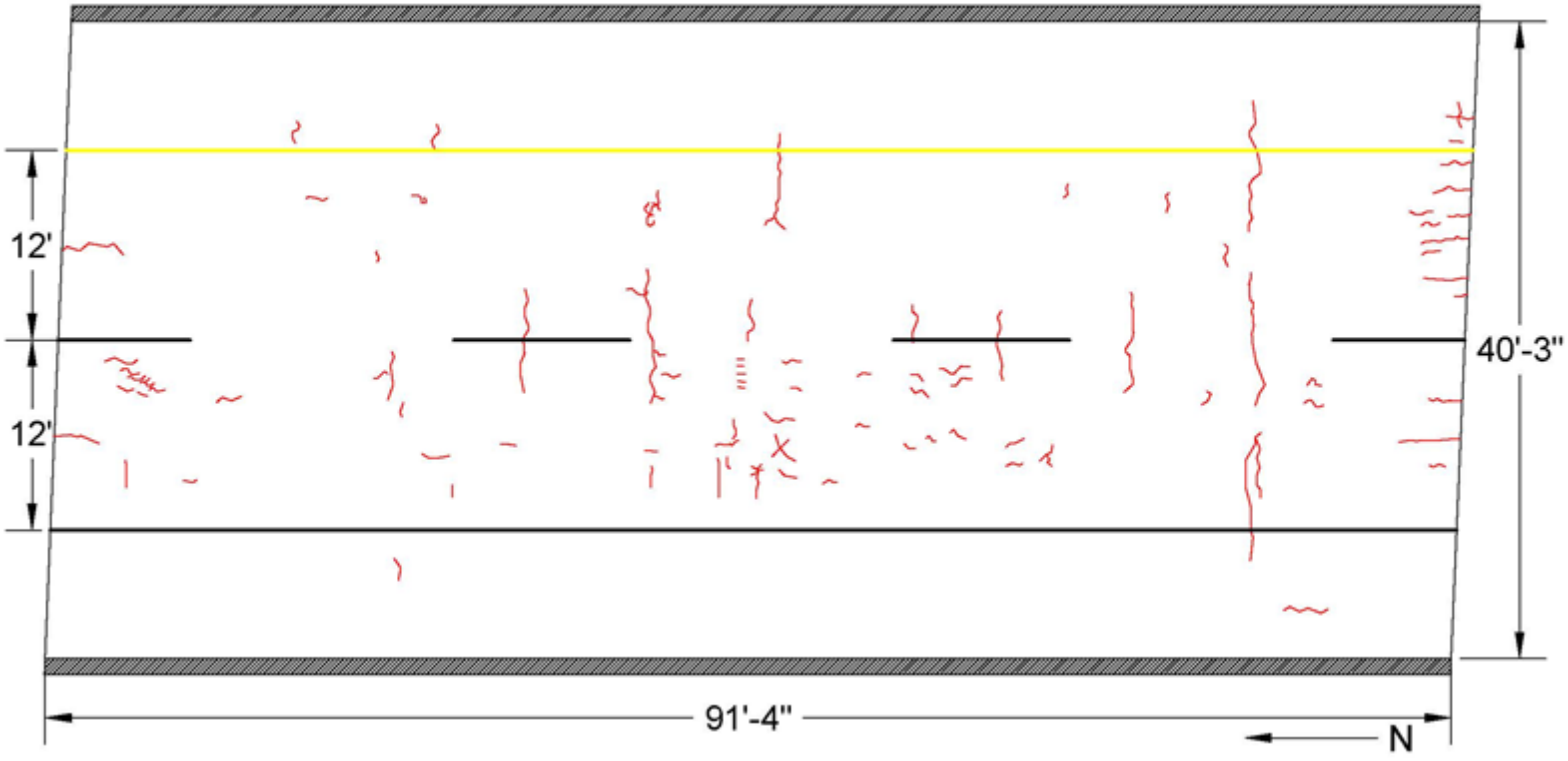

Figure F-3: Distress map for Upper Ridge Road SB TSMR deck at 2 years.

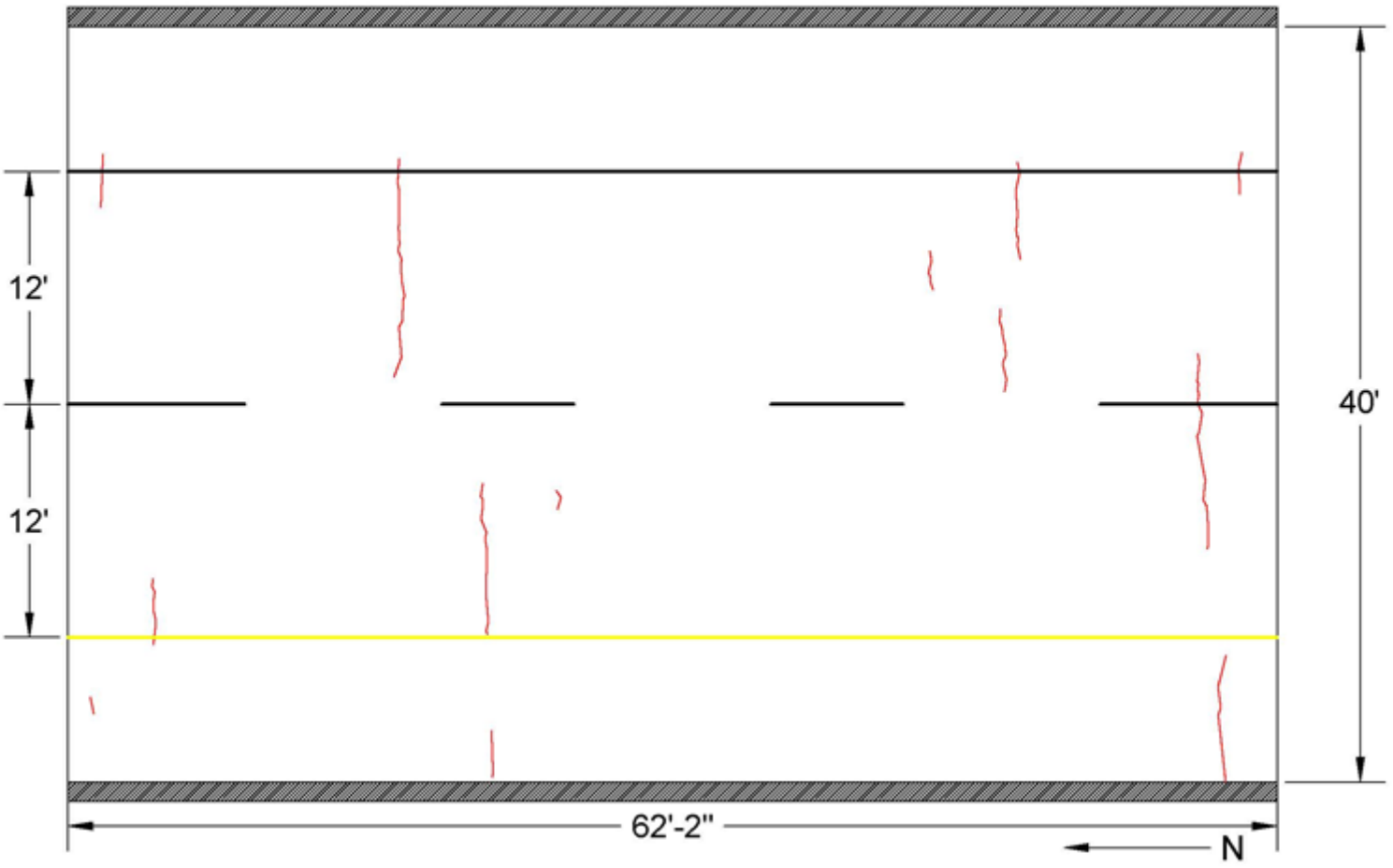

Figure F-4: Distress map for Wolverine Way NB TSMR deck at 3 months.

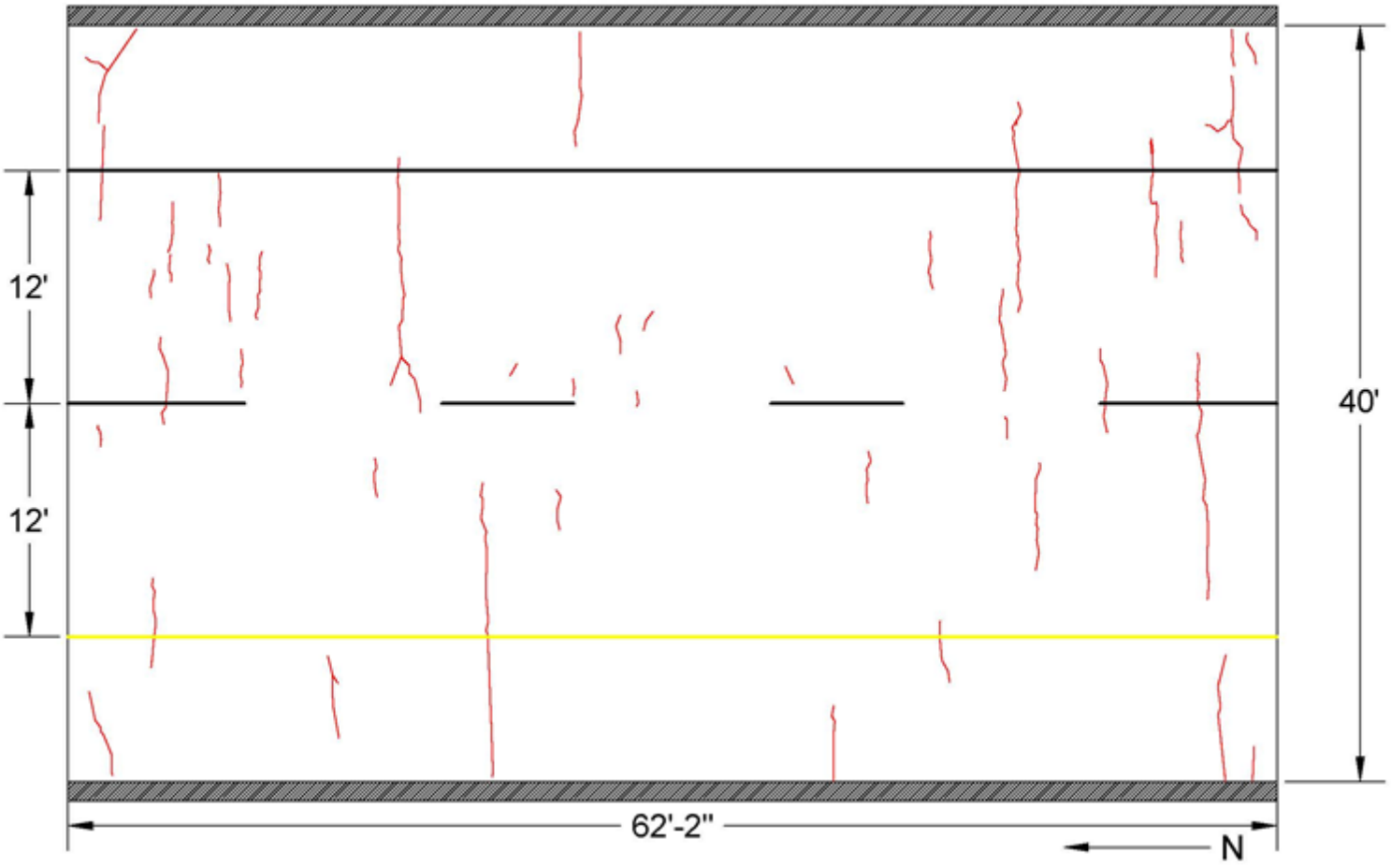

Figure F-5: Distress map for Wolverine Way NB TSMR deck at 1 year.

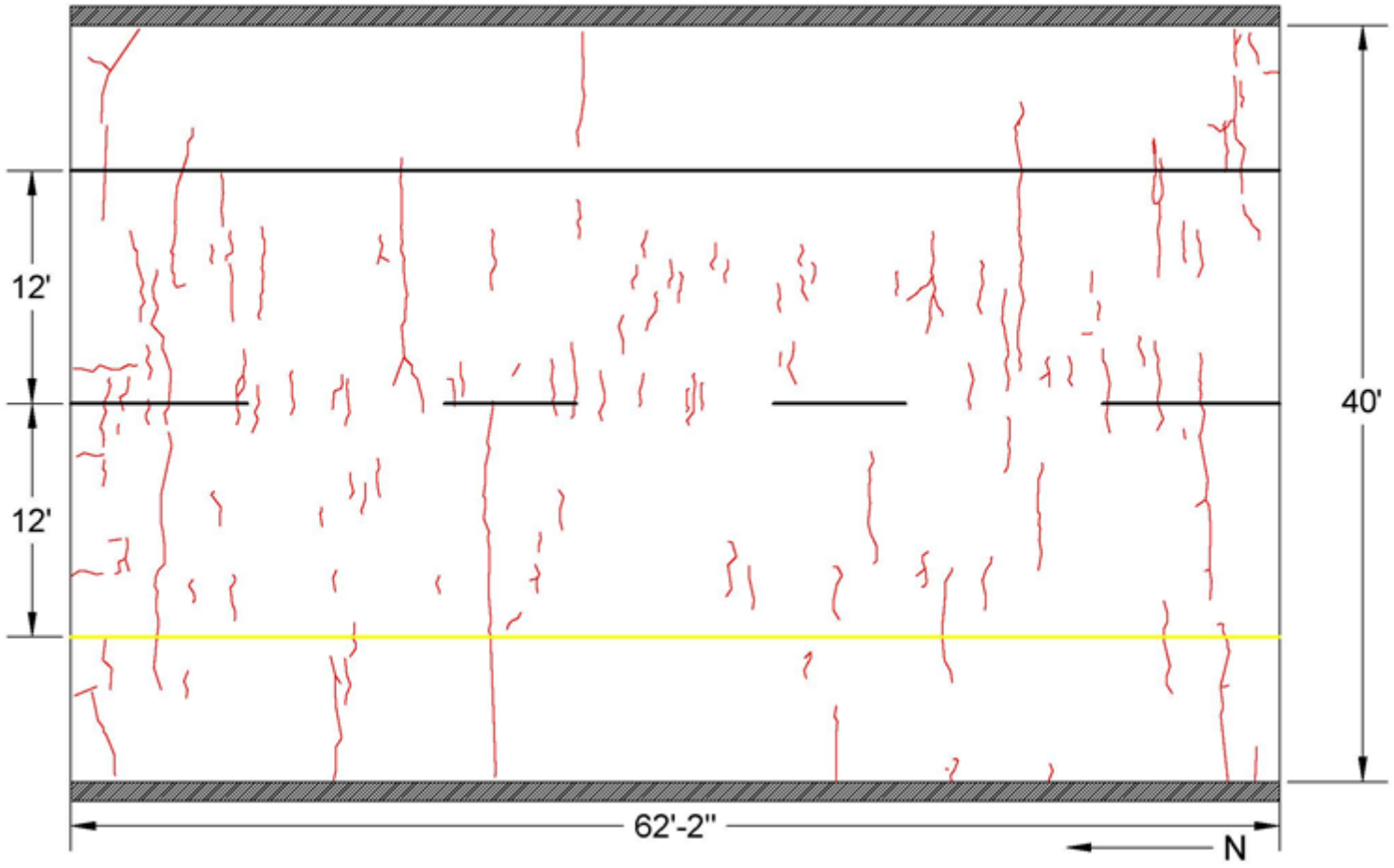

Figure F-6: Distress map for Wolverine Way NB TSMR deck at 2 years.

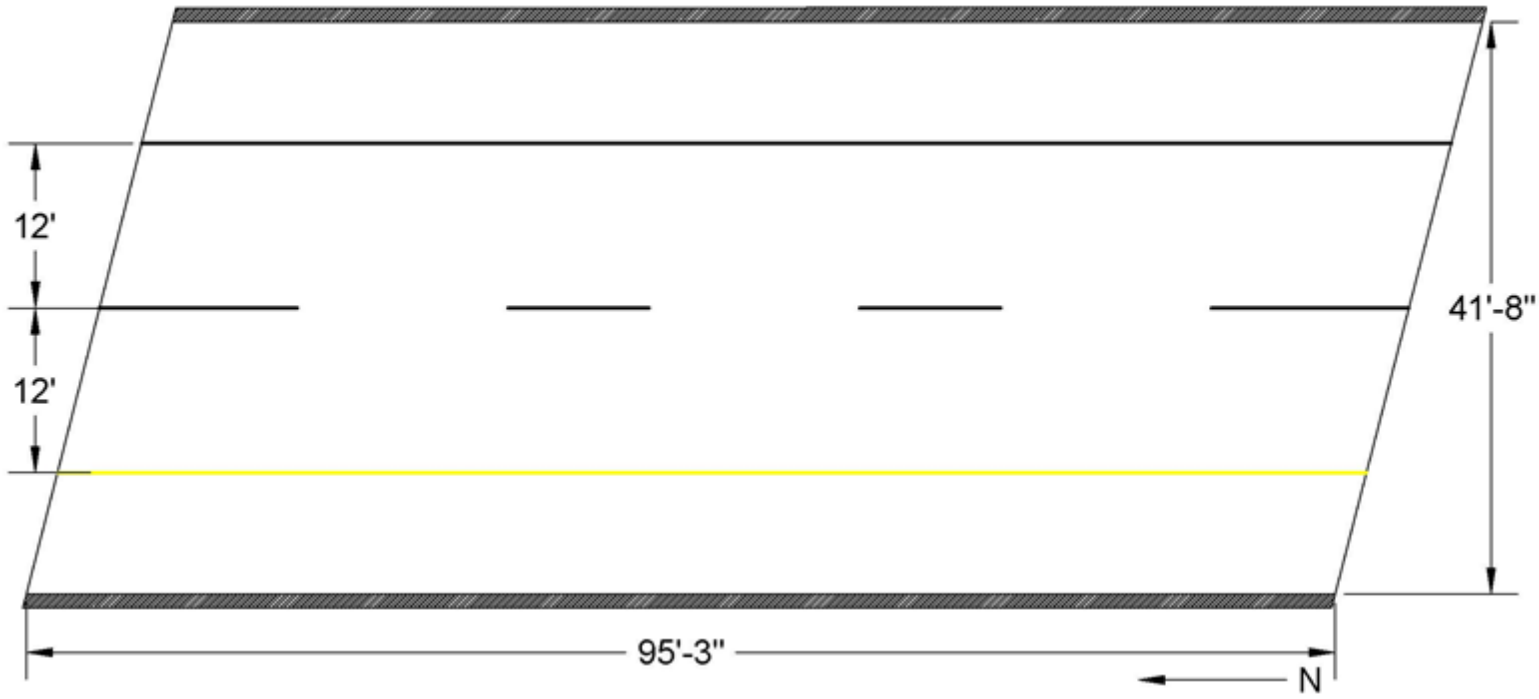

Figure F-7: Distress map for Upper Ridge Road NB conventional deck at 3 months.

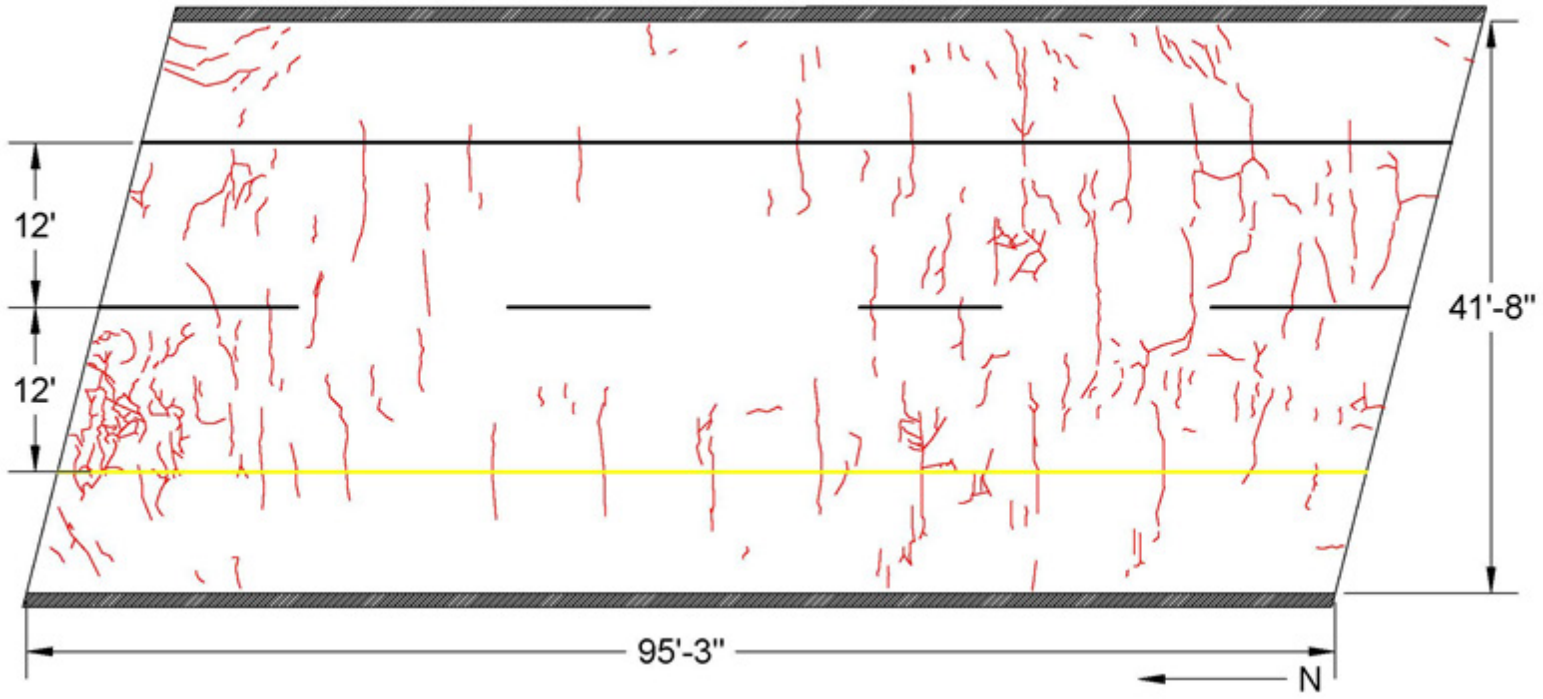

Figure F-8: Distress map for Upper Ridge Road NB conventional deck at 1 year.

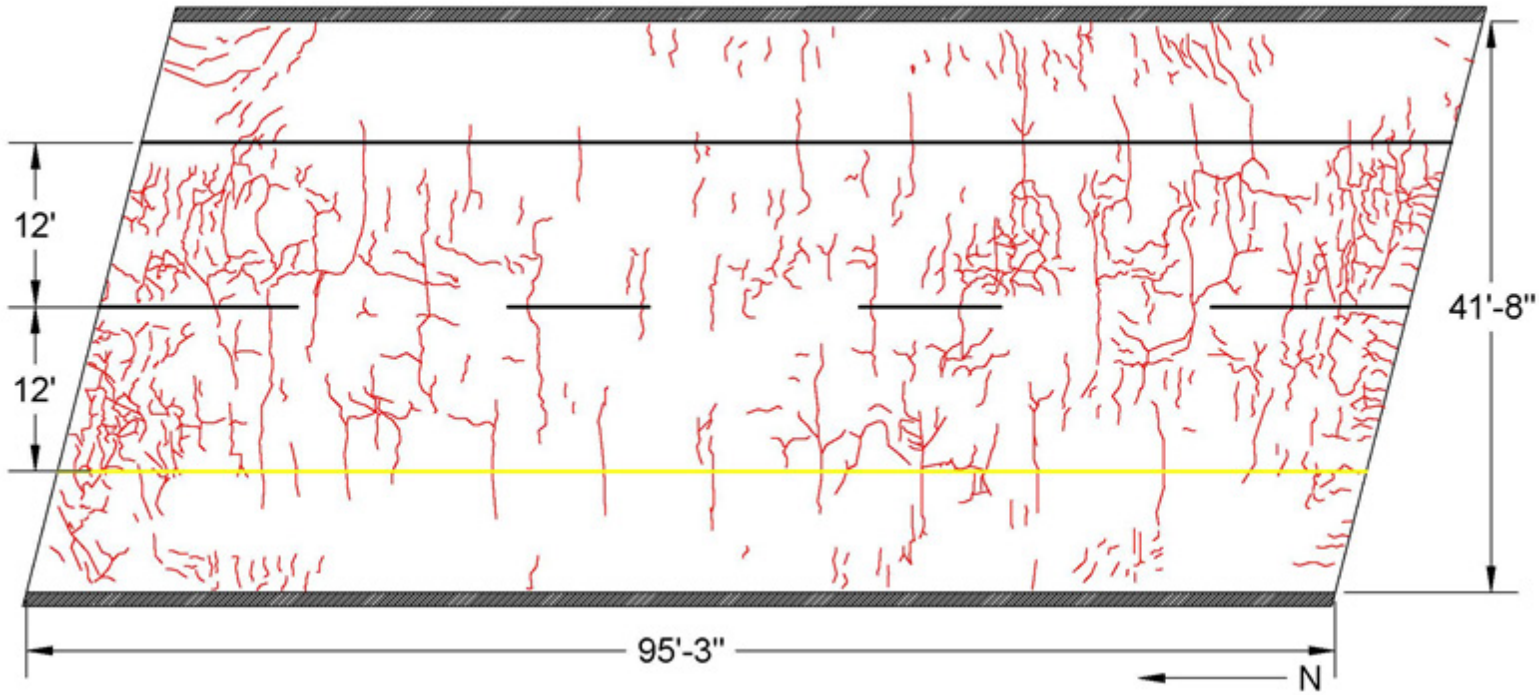

Figure F-9: Distress map for Upper Ridge Road NB conventional deck at 2 years.

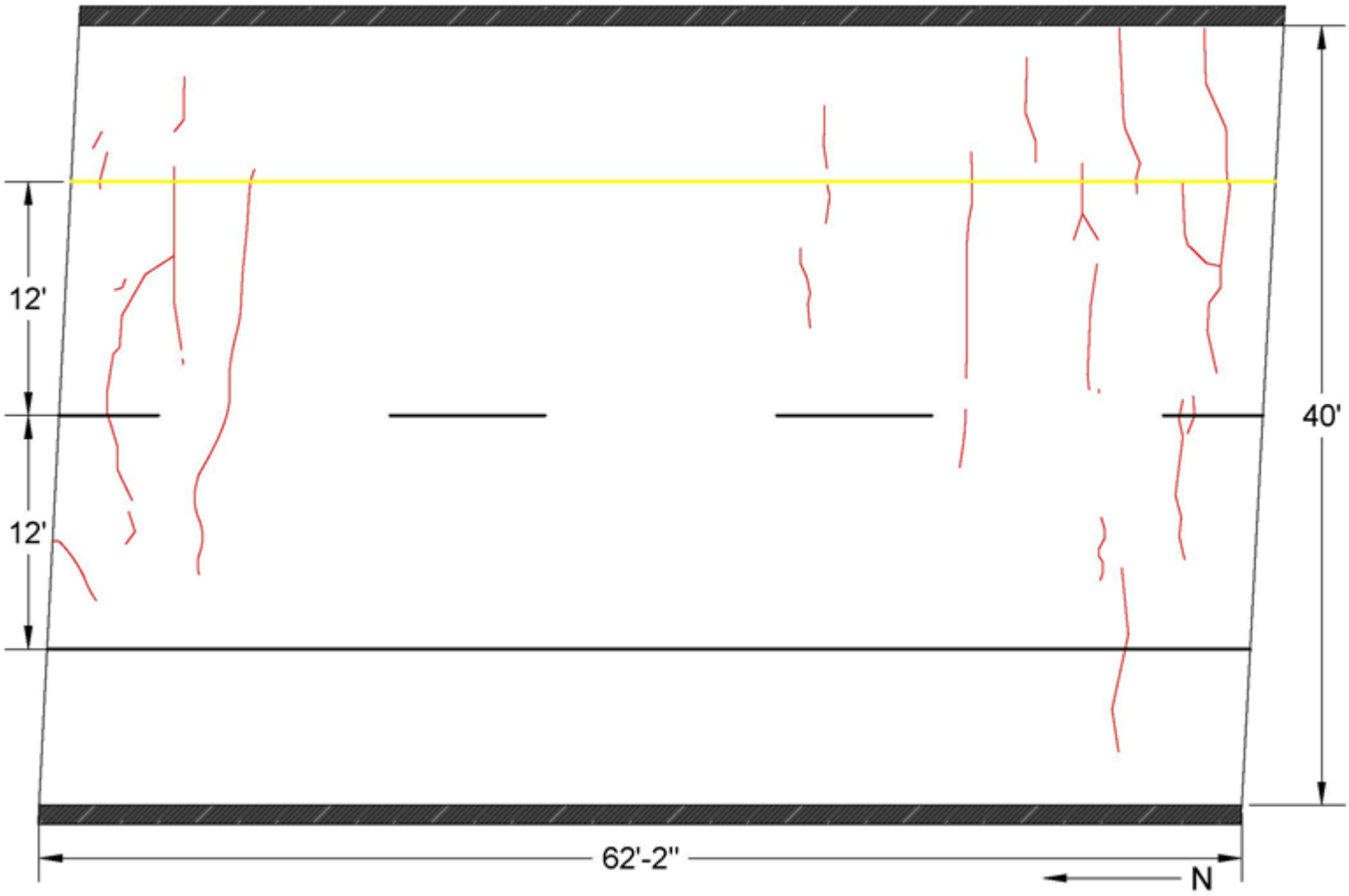

Figure F-10: Distress map for Wolverine Way SB conventional deck at 3 months.

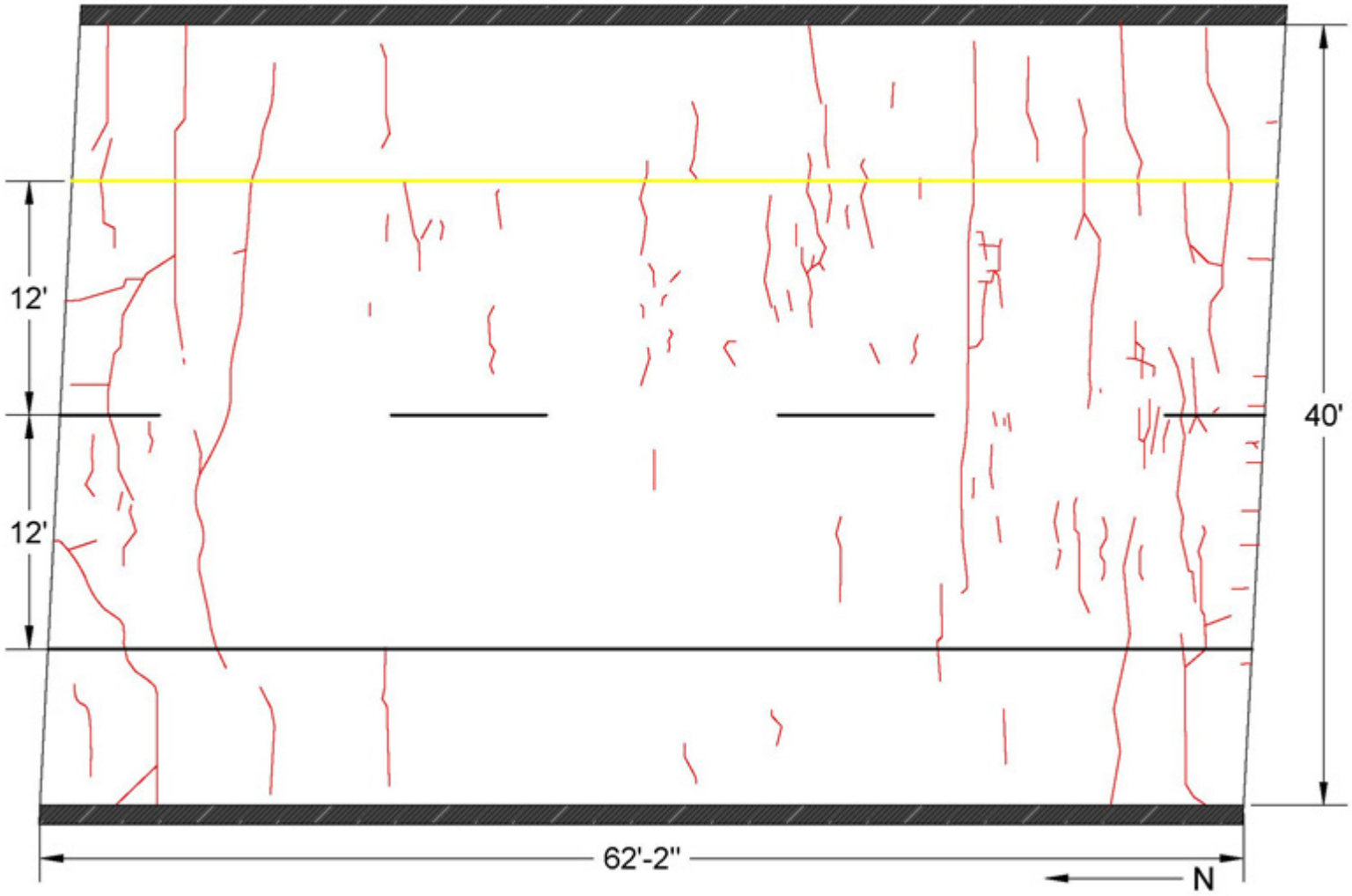

Figure F-11: Distress map for Wolverine Way SB conventional deck at 1 year.

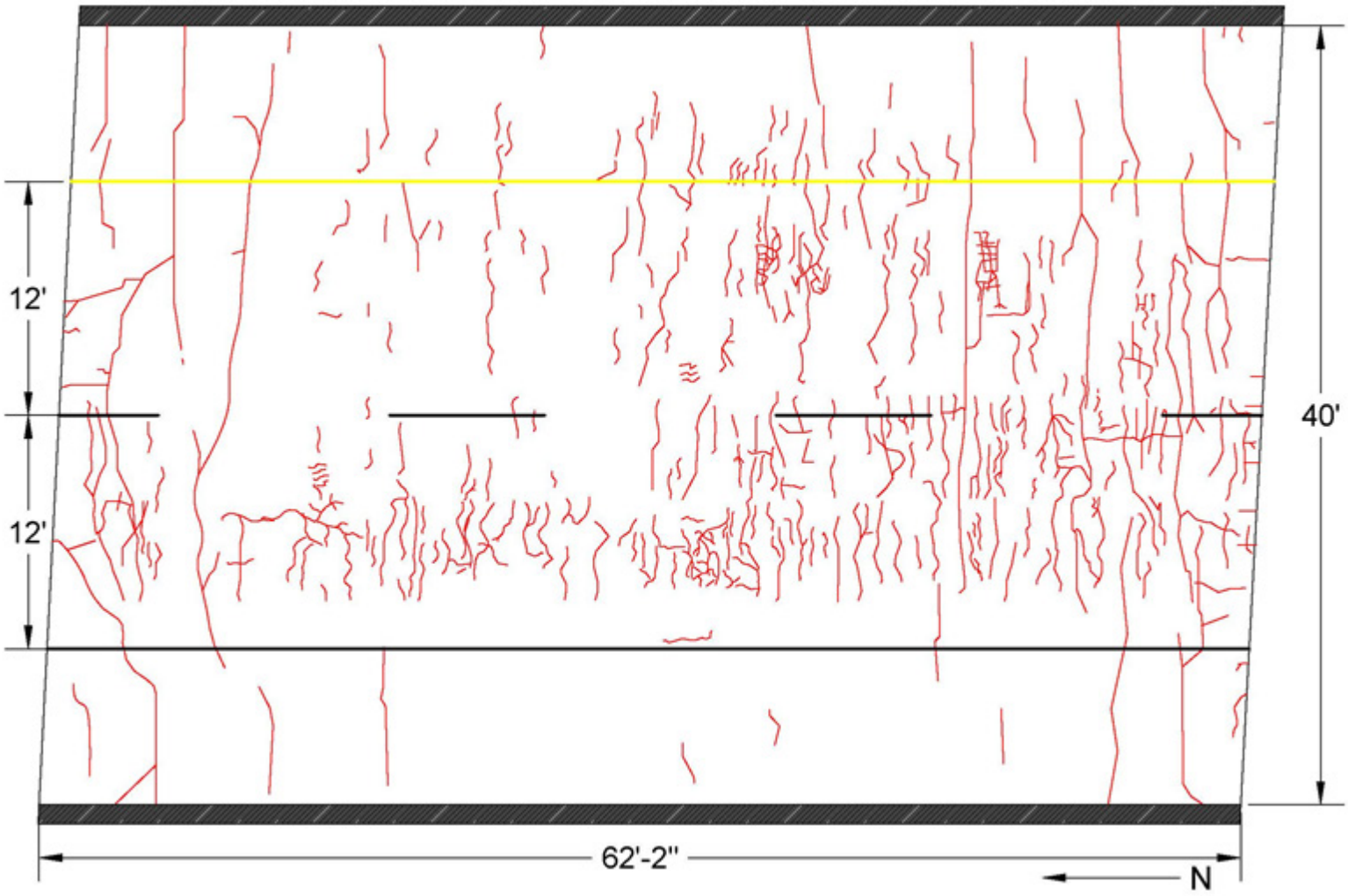

Figure F-12: Distress map for Wolverine Way SB conventional deck at 2 years.